INVESTIGATIONS ON THE CATION INDUCED LIQUID CRYSTALLINE PHASES OF HIGH MOLECULAR WEIGHT DNA

THESIS SUBMITTED TO

COCHIN UNIVERSITY OF SCIENCE AND TECHNOLOGY

IN PARTIAL FULFILLMENT OF THE REQUIREMENTS

FOR THE DEGREE OF

DOCTOR OF PHILOSOPHY

UNDER THE FACULTY OF TECHNOLOGY

BY

NEETHU SUNDARESAN

CHEMICAL SCIENCES AND TECHNOLOGY DIVISION
REGIONAL RESEARCH LABORATORY
THIRUVANANTHAPURAM-695019, INDIA

APRIL 2006

Dedicated to

My Parents

REGIONAL RESEARCH LABORATORY
Council of Scientific and Industrial Research
THIRUVANANTHAPURAM– 695 019
INDIA

Phone: 91-471-2493633/2515363 (O), 2491263 (R)
Fax: 91-471-2491712/2490186
Email: ckspillai@yahoo.com

Dr. C.K.S. Pillai,
Head, Chemical Sciences & Technology Division.

14.04.2006

CERTIFICATE

This is to certify that the thesis entitled **"INVESTIGATIONS ON CATION INDUCED LIQUID CRYSTALLINE PHASES OF HIGH MOLECULAR WEIGHT OF DNA"** is an authentic record of the research work carried out by Ms. Neethu Sundaresan, M.Sc., under my supervision in partial fulfillment of the requirements for the degree of **Doctor of Philosophy** of the **Cochin University of Science and Technology**, Kochi, and further that no part of this thesis, has been presented before, for any other degree.

Dr. C. K. S. Pillai,
(Thesis Supervisor)
Head, Chemical Sciences &Technology Division,
Regional Research Laboratory,
Thiruvananthapuram.

DECLARATION

I, Neethu Sundaresan, do hereby declare that this thesis entitled **"INVESTIGATIONS ON CATION INDUCED LIQUID CRYSTALLINE PHASES OF HIGH MOLECULAR WEIGHT OF DNA"** is a bonafide record of research work done by me, and that no part of this thesis has been submitted earlier for the award of any other Degree, Diploma, Title or Recognition.

Thiruvananthapuram Neethu Sundaresan

14.04.2006

ACKNOWLEDGEMENTS

It gives me great pleasure to express my profound gratitude to my research supervisor Dr. C. K. S. Pillai, for his guidance, constant inspiration and invaluable suggestions for carrying out this work. The enlightening discussions held with him throughout the tenure had motivated me to work with greater zeal and enthusiasm.

I am indebted to Dr. C.H. Suresh for his invaluable guidance and fruitful discussions on molecular modeling studies.

I am grateful to Prof. T. K. Chandrashekhar, Director, RRL for providing me the facilities to carry out the work.

I am thankful to Prof. T. J. Thomas, UMDNJ, USA, and Dr.M. Saminathan for their valuable discussions and encouragement.

I am thankful to Dr. T. Emilia Abraham, for her support at the earlier stages of my work.

I am highly obliged to Dr. Roschen Sasikumar, for providing facilities to carry out molecular modeling studies.

My sincere thanks are due to:
Prof. R. Varadarajan, Molecular Biophysics Unit, I.I.Sc Bangalore for his experimental support.

Dr.C.Pavithran,Dr.A.R.R.Menon,Dr.V.S.Prasad,Dr.J.D.Sudha,Mr.M.Brahmakumar Mr.P.Anandan, Dr. M.Jayakannan and Dr. S.K. Asha for their moral support and encouragement.

Dr .U. Shyamaprasad and Mr. P. Gurusamy for the experimental support.

Thanks are due to Dr. K.Y. Sandhya, Mrs. Gisha Kuncheria, Dr.K.C.Lakshmi, Ms. Priya Senan, Mr. S. V. Valsaraj, Mrs. Resmi Suresh, Dr. Jegan Roy, Ms.Sangeetha, Mrs.Nisha Chitrakumar, Ms. Sindhu Mathew, Ms. Viola B. Morris, Mr. I.O.Bakare, Ms.Jancy Baby, Ms. Amrutha Rajan, Ms .P. Smitha, Ms. T.S. Sasikala, Ms.Bindu.P.Nair, Ms.P.Deepa, Mr.Deepak.D.Vishnu, Mr.P.Anilkumar, Mr. Jijoy Joseph, Ms. Aswathy Mary Varghese and Ms. Archana Joseph for their friendship.

I also wish to express my sincere thanks to Mr. P. Alex Andrews for his help in documentation.

Financial support of CSIR is gratefully acknowledged.

I wish to acknowledge the staff and colleagues of RRL for their forbearance and mutual help, which was essential for the successful completion of this work.

Finally, I owe my heartfelt love to my beloved parents, grandmother, husband, brother and son for their constant support, encouragement and care which gave me the strength to complete the endeavor with success. Above all, I thank god for his continuous grace showered on me, without which nothing was possible.

Neethu Sundaresan.

PREFACE

Liquid Crystalline DNA is emerging as an active area of research, due to its potential applications in diverse fields, ranging from nanoelectronics to therapeutics. Since, counter ion neutralization is an essential requirement for the expression of LC DNA, and the present level of understanding on the LC phase behavior of high molecular weight DNA is inadequate, a thorough investigation is required to understand the nature and stability of these phases under the influence of various cationic species. The present study is, therefore, mainly focused on a comparative investigation of the effect of metal ions of varying charge, size, hydration and binding modes on the LC phase behavior of high molecular weight DNA.

The critical DNA concentration (C_D) required for the expression of LC phases, phase transitions and their stability varied considerably when the binding site of the metal ions changed from phosphate groups to the nitrogenous bases of DNA, with Li^+ giving the highest stability. Multiple LC phases with different textures, sometimes diffused and unstable or otherwise mainly distinct and clear, were observed on mixing metal ions with DNA solutions, which in turn depended on the charge, size, hydration factor, binding modes, concentration of the metal ions and time. Molecular modeling studies on binding of selected metal ions to DNA supported the experimental findings. The results of the present investigation have been published/communicated/ presented as described below:

Publications:

1. Lithium ion induced stabilization of Liquid Crystalline DNA.
   Sundaresan, N.; Thomas, T.; Thomas, T. J.; Pillai, C. K. S. Macromol Biosci 2006, 6, 27-32.

2. Investigations on the Liquid Crystalline Phases of cation induced condensed DNA.
   C.K.S. Pillai, **Neethu Sundaresan**, M. Radhakrishna Pillai, T. Thomas, T. J. Thomas. Pramana, Journal of Physics, 65, 4, 2005, 723-729.

3. Liquid Crystalline phase behavior of high molecular weight DNA: A comparative study of the condensation of DNA by metal ions of varying size, charge and binding modes using polarizing light microscopy.
   Neethu Sundaresan, C.K.S. Pillai, T. Thomas, T. J. Thomas.
   (Under revision- Biopolymers).

4. Investigations on the spermine induced liquid crystalline phase behavior of high molecular weight DNA in the presence of alkali and alkaline earth metal ions.
   Neethu Sundaresan, C.K.S. Pillai, T. Thomas, T. J. Thomas.
   (Accepted in International Journal of Biological Macromolecules).

5. A base-sugar-phosphate three layer ONIOM model for cation binding: Relative binding affinities of alkali and alkaline earth metals for phosphate anion in DNA.
   Neethu Sundaresan, C. K. S. Pillai, Cherumuttathu H. Suresh. (Communicated to *Journal of Physical Chemistry A*).

6. Role of Mg^{2+} in Inducing DNA Condensation: Evidence from ONIOM-based QM-MM Study of a DNA Fragment.
   Neethu Sundaresan, C. K. S. Pillai, Cherumuttathu H. Suresh. (Communicated to *Journal of Physical Chemistry A*).

Papers presented at Conferences:

1. Metal ion induced compaction of DNA: A Polarized Light Microscopic study of the effect of cations on its LC phase behavior.
   Neethu Sundaresan, C. K. S. Pillai, T. Thomas , T. J. Thomas. Published in the Proceedings of the Macro-2002.

2. A Polarized Light Microscopic study on the effect of alkaline earth metal ions on the LC behavior of DNA.
   Neethu Sundaresan, C. K. S. Pillai, T. Thomas, T. J. Thomas. Published in the Proceedings of the Macro-2004.

CONTENTS

CHAPTER 1

INTRODUCTION

CHAPTER 2A

INDUCTION AND STABILIZATION OF LIQUID CRYSTALLINE PHASES OF DNA BY ALKALI METAL IONS: STUDIES ON LC BEHAVIOR USING POLARIZED LIGHT MICROSCOPY.

CHAPTER 2B

A BASE-SUGAR-PHOSPHATE THREE- LAYER ONIOM MODEL FOR CATION BINDING: BINDING AFFINITIES OF ALKALI METAL IONS FOR PHOSPHATE GROUP IN DNA

CHAPTER 3A

INDUCTION AND STABILIZATION OF LIQUID CRYSTALLINE PHASES OF DNA BY ALKALINE EARTH METAL IONS: STUDIES ON LC BEHAVIOR USING POLARIZED LIGHT MICROSCOPY

CHAPTER 3B

A BASE-SUGAR-PHOSPHATE THREE-LAYER ONIOM MODEL FOR CATION BINDING: BINDING AFFINITIES OF ALKALINE EARTH METAL IONS FOR PHOSPHATE GROUP IN DNA

CHAPTER 4

THE EFFECTS OF MULTIVALENT, TRANSITION AND HEAVY METAL IONS ON THE LIQUID CRYSTALLINE PHASES OF DNA

CHAPTER 5

SPERMINE INDUCED LIQUID CRYSTALLINE PHASES OF DNA IN THE PRESENCE OF ALKALI AND ALKALINE EARTH METAL IONS.

CHAPTER 6

CHAPTER 1

INTRODUCTION

1.1. DNA in the Cell Nucleus

Liquid Crystalline (LC) DNA has gained considerable interest over the last few decades, mainly due to its role in understanding the *supramolecular organization* of DNA in the condensed state, and also its potential applications in the fields of therapeutics (eg. gene delivery),[1] in designing biosensing units,[2] DNA chips[3] etc. The DNA molecule is known to exist (densely packed), in the LC states in *chromosomes, bacterial nucleoids, sperm heads,* and *viruses*[4-9]. Recent investigations *in vitro* also showed that DNA exhibits LC phases, in the concentration range similar to that in the cell under controlled environment. Genetic processes such as DNA *replication* and *genetic recombination*, instead of being inhibited are known to be stimulated by DNA condensation[4]. To understand how DNA functions in the condensed state, it is essential to know the *supramolecular organization* of DNA in the condensed state. DNA, because of its polyanionic nature is always associated with counter-ions; therefore, understanding of DNA packaging (in living organisms) requires the knowledge of DNA-counter ion and DNA-DNA interactions in the condensed states. Studies on the LC domains can be hence used as a probe to obtain vital information on the *supramolecular organization* of DNA. The present level of understanding on the LC phase behavior of DNA is inadequate, and a thorough

investigation is required to understand the nature, texture and stability of these phases under the influence of various environmental conditions. It is now well established that, counter ion neutralization is an essential step in the induction and stabilization of the LC phases of DNA. The present work is an attempt towards understanding the LC phase behavior of high molecular weight DNA provoked by selected cations of varying size, charge, hydration and binding modes.

1.2. The Structure of DNA

Deoxyribonucleic acid (DNA), the ultimate genetic material of living systems, is a double helical polymeric molecule consisting of nucleotide units (monomers), each comprising a phosphate group, a sugar (deoxyribose) and a nitrogenous base (two purines- adenine -A and guanine -G and two pyrimidines – cytosine-C and Thymidine-T). It has two chains of right handed helices, with the nitrogenous bases arranged within the interior of the helix, and the negatively charged phosphate groups projected towards the exterior of the helix, which are usually neutralized with counter ions such as metal ions, cationic proteins and polyamines. The nitrogenous bases are so neatly stacked inside the double helix that an adenine of one chain is always hydrogen bonded to thymine of the other chain, and a guanine of one chain is hydrogen bonded to a cytosine of the other chain, i.e. a purine faces a pyrimidine base. Thus, the ratio of A and T and G and C, are maintained as 1:1 (See Fig.1.1). In this arrangement, the sequences of one chain are automatically fixed, if the sequences of the other chain are known[10]. The diameter of the DNA molecule

is about 22 A^0 while the length can exceed several meters in some organisms[4]. One of the major problems of molecular biology is how this giant molecule can be packaged into a cell or virus that is far smaller than the length of the DNA molecule. In addition, it is important to the cell to access the DNA molecule for the purposes of genetic control, routine cellular maintenance, and reproduction[11,12].

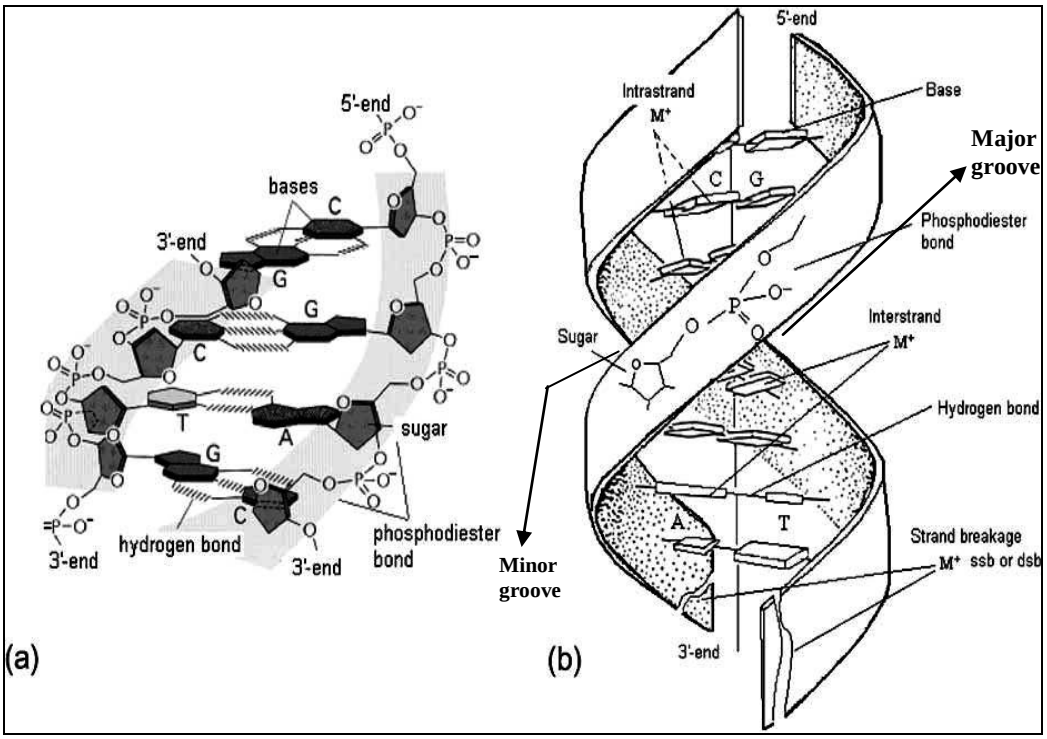

Fig.1.1. The DNA double helix (a) The complementary A-T and G-C bases are linked through hydrogen bonds (b) Metal ions can bind to one or two sites of the same strand (intra-strand) or of opposite strands (inter-strand)[13].

The most common DNA structure in solution is the B-DNA[4]. Under conditions of applied force or twists in the DNA, or under low hydration conditions, it can adopt several helical conformations, referred to as A-DNA, Z-DNA etc. A and B forms exist in right handed helical structure, whereas the Z form exists in a left handed helical conformation, and differs in their sugar

puckering mode, base pair tilt, axial rise per residue etc[10]. B-DNA possessing higher phosphate hydration, has less exposed sugar residues and smaller hydrophobic surface, is stabilized at high water activity, whereas A-DNA, with its shared inter-phosphate water bridges, is more stable at low water activity[12].

The phosphate-sugar strand backbones of DNA are closer together on one side of the helix than on the other. The **major groove** occurs, where the backbones are far apart, and the **minor groove** occurs, where they are close together. The grooves twist around the molecule on opposite sides. Certain proteins bind to DNA to alter its structure or to regulate transcription (copying DNA to RNA) or replication (copying DNA to DNA). It is easier for these **DNA binding proteins** to interact with the bases (the internal parts of the DNA molecule) on the major groove side because the backbones are not in the way[10].

1.3. Metal ion -DNA Interactions

Metal ions play a crucial role in the stabilization and functioning of DNA. They are essential for several cell reactions and varied metabolic and physiological functions[14-19]. As DNA is a supercoiled negatively charged polyelectrolyte, the positively charged metal ions interact directly or indirectly with the sites characterized by high electron density or negatively charged residues of DNA. Such sites on DNA could be the negatively charged phosphates of the backbone of both strands and the electron donor atoms of the bases, such as N and O. The possible ways of metal binding are shown in Fig.1.1. Metal ions can bind tightly to DNA, as partially dehydrated or fully hydrated and this binding can be direct or indirect (through water molecules)

with DNA[17]. Metal ions exist as ‘free’ or ‘bound’ in the body. They are hydrated and can move freely around in the body liquids and are ‘bound’ when they form complexes with the covalently bonded regions of DNA[13]. The predominant mode of metal binding depends on the type of metal ions. For example, alkali and alkaline earth metal ions predominantly bind to the phosphate moieties, whereas heavy metal ions such as mercury bind to the bases, at the N7 and O6 of guanine, N7 and N1 of adenine and the N3 of pyrimidines.

Metal ions binding to the bases (atoms of bases engaged in hydrogen bonding with the complementary base) will usually disrupt the hydrogen bonding between them and destabilizes the double helix[20-33]. On the other hand metal ions that neutralize the excess negatively charged phosphate groups stabilizes the helix[34-39]. The binding of metal ions to nucleotides or poly-nucleotides does influence the sugar conformation[40]. As a result of this change in sugar puckering, helical conformation can change from B-DNA to A-DNA or Z-DNA. The conformation of nucleic acids depends on the kind of metal ion that binds to DNA[41-46]. Furthermore, cations localize preferentially at AT-rich sequences in the minor groove, while in the major groove the preferential sites are the GC-rich sequences. The binding of metal ions to DNA is also sequence dependent[1,13,39,47-70]. The DNA binding sites accessible for metal binding and affinities of some of the metal ions for different sites of DNA are listed in Table 1.1

Table 1.1. Metal ions and the binding sites of DNA[19,71].

Binding sites	**Metal ions**
Phosphate group	Li^{+}, Na^{+}, K^{+}, Rb^{+}, Cs^{+}, Mg^{2+}, Ca^{2+}, Ba^{2+}, Sr^{2+}, Cr^{3+}, Fe^{3+}, Al^{3+}
Phosphate and base	Co^{2+}, Ni^{2+}, Mn^{2+}, Cd^{2+}, Pb^{2+}, Cu^{2+}, Fe^{2+}, Mg^{2+}, Fe^{3+}, Cd^{2+}
Base	Au^{3+} Ag^{+}, Hg^{+}, Pt^{2+}, Pt^{4+}, Pd^{2+}

The transition metal ions interact with one or two different sites[72] and their interactions with DNA are more complicated[73-79]. The transition metal ions lose their water molecules very easily and give inner sphere (direct contact to DNA) co-ordinated complexes[77].

They usually bind directly to the bases, and indirectly to the phosphate groups. Most of the transition metal ions react chemically with the N7 atom of purine or N3 of pyrimidine and perturb the double helix. The binding of transition metal particularly at G–C sites of DNA leads to its damage through radical generation from oxidation by H_2O_2[74-76]. Most of the earlier studies on metal ion-DNA interactions, were conducted in dilute DNA solutions, however, DNA exists ***in vivo*** in domains where the localized concentrations are very high[4]. Later, it was shown that double stranded DNA could exhibit LC phases, ***in vitro*** in concentrated solutions, which has become very interesting due to the fact that similar structures existed in cells as well[4-9]. Binding of metal ion will disrupt the ordered water structure around DNA strands

(dehydration), thereby facilitates the ordering of DNA strands required for exhibiting LC behavior.

Counter ion neutralization, an essential requirement for the induction of LC phases[4], which in turn is known to be dependent on the type, size and concentration of the counter ion associated with the polyanionic molecule[80]. Those metal ions that bind primarily to the phosphates stabilize the helix by reducing the intermolecular repulsion, which provokes LC ordering, whereas a distortion of the double helix by base binding metal ions might result in the loss of rigid rod like shape of the DNA molecule, which is the determinant factor of its LC behavior.

1.4. Origin of LC Behavior in DNA

The possibility of rod like and semi-rigid polymers to form ordered LC phases above a critical concentration was first described by Onsager[81] and later elaborated by Flory[82] and others. This behavior has been studied and well established for synthetic polymers,[83] but the behavior of many natural polymers has not been properly investigated. Natural polymers such as DNA are also expected, and recently shown to exhibit LC behavior, due to the same excluded volume effects.

The hypothesis that double stranded DNA molecules are able to exist in the LC phase *in vitro* in concentrated solution, was first put forward in 1961, by Luzzati and his coworkers[84]. Robinson, at the same time obtained unequivocal evidence, for the formation of cholesteric phases by concentrated calf thymus DNA solution[85]. Later, Iizuka *et al.*[86,87] and Potaman *et al.*[88] attempted to

reproduce the observations of Robinson. The first attempt to prepare LC phases from synthetic polyribonucleotide, was also made by Iizuka and his coworkers[89].

The LC transformation of DNA was then observed with fragmented DNA of 150 bp length, at concentrations >200 mg/ml[90-92]. The LC behavior of DNA is complicated by the necessity of the requirements of counter ion shielding. A strong polyelectrolyte is surrounded by a counter ion layer, which determines the effective particle radius and hence the effective axial ratio and excluded volume. So, the phase behavior is largely influenced by the counter ion type and ionic strength[82]. A basic requirement for the exhibition of LC phase in DNA is a critical local DNA concentration (C_D)[93]. Critical DNA concentration is achieved due to the cation-DNA and DNA-DNA interactions. Merchant and Rill studied the chain length dependence on C_D, and found a dramatic reduction in C_D as the size of the DNA increased. For example, the C_D values for 147 and 8000 bp DNA samples were 135 and 13 mg/ml, respectively[94]. In a series of experiments, Livolant and colleagues, demonstrated that spermidine and spermine are capable of provoking multiple LC forms of fragmented DNA[95-100]. DNA condensation by multivalent ions, including the natural polyamines, results in a significant increase in the local concentration of DNA. Recent reports indicate that some synthetic polyamine analogues are also capable of inducing and stabilizing LC phases of DNA[101]. It would be appropriate here, to discuss briefly about LC polymers.

1.4.1. Liquid Crystalline Polymers

LC polymers (LCP's) are unique polymeric materials, with high performance and functional applications, in diverse fields like ultra high strength fibers, non-linear optical and information storage systems[102-107]. They rose into prominence because (a) the orientational order of the LC phase can be retained in the polymer, even after processing, hence the performance properties underwent a quantum jump to values close to those of theoretical predictions, thereby obtaining extremely high modulus, high strength, high heat resistance etc. which were not imaginable in earlier situations and (b) that the LC phase can be trapped or stabilised in the glassy phase of the polymer, so that the electro-optical and magnetic properties can be conveniently manipulated for applications in areas such as imaging technology, non-linear optics, telecommunications etc[108-111]. Moreover, they have excellent dimensional stability, thermal stability, and flame resistance coupled with the absence of creep and shrinkage, these properties make them ideal candidates, for high performance applications[112-119].

The LC state, also called as the fourth state of matter, represents a number of different stages, whose degree of order lies between that of a perfect crystal and an isotropic liquid. Order and mobility are the two basic principles of nature, which govern the structure of the condensed phase. Crystalline, amorphous and liquid are the conventional limiting states of the condensed phase. Crystals, on melting completely lose their long-range positional and

long-range orientational orders. Liquid crystals on melting do not completely lose their long-range orders. They retain partially the ordering of the crystals, while maintaining the mobility of the liquid phase[102,113,120].

The discovery of liquid crystals was credited to an Austrian Botanist, Friedrich Reinitzer[121] in 1888, who noticed the formation of a cloudy fluid on melting cholesteryl benzoate at 146.6^{O}C, which when further heated suddenly clarified at 180.6^{O}C. The turbid liquid was named liquid crystals by Lehman[122]. The liquid crystals are usually identified through their phases (as described below), under crossed polarizers[120,123] and confirmed through their thermal behavior in DSC[124] and X-ray diffraction patterns[125].

LCP's and small molar liquid crystals are characterised by the presence of a '*mesogen'*, the structural entity that is responsible for the LC behavior. A mesogen, in general, is a rigid rod or a disc-like or lathe-like molecule, the presence of which produces a pronounced anisotropy in shape[113]. The asymmetry in molecular shape allows the thermodynamically stable orientational order in preferred direction of the molecular axis. These orientationally ordered liquids or positionally disordered solids are widely known as liquid crystals[113]. The name liquid crystal was given because of the obvious liquid like flow of these materials. The molecules with sufficient rigidity and linearity can form LC phases either on melting (thermotropic) or on dissolution (lyotropic)[126,127]. There are *amphotropic* systems also which show liquid crystallinity, both in melt and in solution[128,129].

1.4.2. Thermotropic Liquid Crystals

In thermotropic liquid crystals, the mesophase transitions are brought about by the influence of temperature. These phases are strongly anisotropic though the phases themselves may be as mobile as water[130]. The first order transition points are used to distinguish these thermotropic liquid crystals from the normal liquids.

1.4.3. Lyotropic Liquid Crystals

In lyotropic systems, mesophases are induced by the influence of solvents[131-133]. DNA falls under this category of liquid crystal systems. The lyotropic liquid crystals are formed when a certain classes of organic compounds and polymers are dissolved in suitable solvents. The solvent strength, concentration of the solution and temperature are the three important variables that are to be optimized. The solvents widely used are water, sulphuric acid, trichloroacetic acid etc.

The first report on mesogenic character of macromolecules, came in biological systems, in 1937, when Bawden and Pirie[134] observed birefringent mesophase in a solution of tobacco mosaic virus. Later, Elliot and Ambrose[135] observed lyotropic behavior in a chloroform solution of a polypeptide, poly(γ-benzyl L-glutamate). Robinson[136,137] later proved it as a cholesteric phase. An important feature of the solutions of lyotropic LCP's is their sudden change in viscosity with increasing polymer concentrations at the point where LC order begins[138].

1.4.4. Liquid Crystalline Phases

Depending on the structure of the phases, liquid crystal systems can be classified into the following types.

1.4.4.1. Nematic Liquid Crystals (NLC's)

One of the most common and frequently observed LC phases is the nematic, where the molecules have no positional order, but they do have long-range orientational order. Thus, the molecules can flow, and are randomly distributed as in a liquid, but they all point on an average to the same direction (within each domain). Most of the nematics are uniaxial; they have one axis that is longer and preferred, with the other two being equivalent. Some liquid crystals are biaxial nematics, where, in addition to their long axis, they also orient along a secondary axis[113] (Fig.1.2).

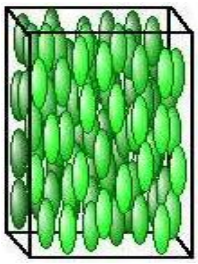

Fig.1.2. Nematic alignment of mesogens

1.4.4.2. Cholesteric Liquid Crystals (Chiral nematic liquid crystals)

Thermodynamically equivalent phase to nematic phase is the cholesteric phase, which results if the mesogen is chiral, or if a chiral molecule is dissolved in a nematic liquid crystal. The name cholesteric is obviously due to the observation of cholesteric phase in cholesterol derivatives at early times.

Cholesteric is very similar to nematics, with a spontaneous twist about an axis perpendicular to the molecular axis or the director resulting in a helical structure (Fig.1.3)[113].

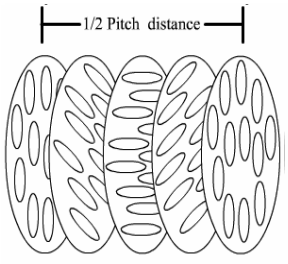

Fig.1.3. Cholesteric arrangement of mesogens

1.4.4.3. Smectic Liquid Crystals (SLC's)

The smectic phase is one where in addition to the orientation order, the mesogens are also grouped into layers, enforcing long-range positional order in one direction. The smectic phase shows a layered structure. The layers in SLC's are liquid like, with molecules upright on the average and negligible in-plane and inter layer positional correlations. The layers can slide past one another (Fig.1.4).

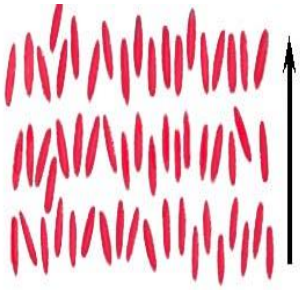

Fig.1.4. Smectic alignment of mesogens

Smectics are more ordered than nematics. The Smectic liquid crystals show polymorphism, in which the layer structure is the common feature. Due to the layered structure, the large-scale movement in any direction other than

tangential to the layer surface is difficult. Therefore, smectic phase is quite viscous. The smectics are classified into seven different polymorphs according to their intra molecular arrangements[113].

1.4.4.4. Columnar or Discotic Liquid Crystals

In 1977 Chandrasekhar[138] was able to show that not only rod like molecules, but compounds with disc like molecular shape, are also able to form LC phases. The term discotic is often used to describe both the shape of the mesogen as well as the type of the mesophase formed by it, though the phase is sometimes referred as columnar. Disc shaped mesogens form partially ordered mesophase, in which they are organized in vertical stacks like coin or poker chips (Fig.1.5). Two different types of discotic phases have been identified: a *columnar* mesophase and a *columnar nematic* phase. The columnar phases are characterised by stacked phases of mesogens with columns being packed together to form three-dimensional crystalline-like array.

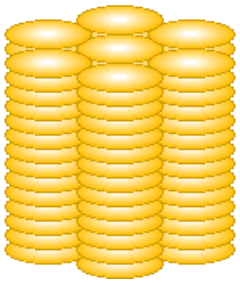

Fig.1.5. Columnar arrangement of mesogens

Within the column, the positions of the mesogens may have short or long-range order, but the columns register in, along their axes, and are not three dimensionally ordered like a crystal. As in conventional nematics, the nematic discotic phase is an anisotropic fluid with a single order parameter, which in

this case is associated with the tendency of the disc to align parallel. The disc normal thus tends to point along a common direction, the director $\hat{n}$.

1.5. Liquid Crystalline DNA

The cellular DNA is in a macromolecular crowded environment, surrounded by proteins and cationic molecules, including the polyamines[139]. These crowded conditions cannot be neglected in understanding the functional properties of DNA molecules, such as replication and transcription. DNA condensation, is however known to stimulate the functions of DNA rather than inhibiting them[140].

DNA *in vivo*, exists in domains, where the localized concentrations are very high, often exceeding 400-600 mg/ml or 70 percent weight/volume[141]. It has been shown that DNA exists in the LC state *in vivo* in bacteria, viruses etc. and similar conditions can be obtained *in vitro* under controlled conditions[5-8]. The existence of distinct states of DNA compaction, is vital to the functions of viruses, bacteria, and eukaryotic cells[1]. The more compact states lead to the efficient packing of colossal genomic DNA molecules within the small confines of the cell nucleus, the bacterial cytoplasm, and viral capsids. Equally important are the less compact states of DNA required during much of the cell life cycle to allow proteins to access the DNA template for a multitude of biological tasks (e.g. gene regulation, transcription, replication). The biologically relevant DNA condensing agents, *in vivo* include cationic proteins (eg. Histones) and polyamine molecules, such as spermidine and spermine, and are known to be critical for DNA compaction[142]. Polyamines are also required

in DNA catenation (interlocking) by topoisomerases, presumably for locally condensing neighboring DNA segments[142,143].

Condensed DNA can be obtained *in vitro* by numerous methods: simply by preparing concentrated solutions of DNA in water, in the presence of monovalent ions, as first realized by Robinson,[85,144] Luzzati and Nicolaieff, [145,146] or by addition of neutral polymer to dilute solutions of DNA, in the presence of monovalent ions[147-149]. It can also be obtained by precipitation of DNA with ethanol,[150,151] multivalent cations (polyamines, cobalt hexamine),[152] polypeptides or proteins[153,154] and by interaction with detergents, either cationic or anionic[155,156] and their nature depends largely on polymer concentration. However, much remains to be understood on the nature of the ionic environment (size, charge, complexation, state of hydration etc.) DNA undergoes a series of LC phase transitions when it is compressed *in vivo* into chromosome-sized packages. *In vitro* studies have shown that as the DNA concentration is varied, various phases appear as shown below:

Isotropic → blue phases → cholesteric spherulites → cholesteric → columnar hexagonal → crystalline.

In dilute solutions (<1mg/ml), DNA exists in random coils, or is randomly oriented, and the solution is a classical isotropic liquid. Under the polarized light, the DNA solution will be totally dark. As the DNA concentration is increased slowly (100-200 mg/ml), a weakly birefringent, dynamic, "precholesteric" mesophase occurs with microscopic textures intermediate between those of a nematic liquid crystal and a true cholesteric

phase first. At slightly higher DNA concentrations (200-300 mg/ml), a second mesophase forms that is a strongly birefringent, well-ordered cholesteric LC phase with a concentration-dependent pitch varying from 2 to 10 micrometers. In cholesteric phase, the molecules are aligned in parallel and their orientation rotates continuously along a direction called the cholesteric axis. Cholesteric liquid crystals, in which the long axes of the molecules lie in pseudoplanes that are slightly twisted with respect to each other, have periodic variations in refractive index and fringe patterns with spacings of P/2 where P is the cholesteric pitch (Fig.1.6).

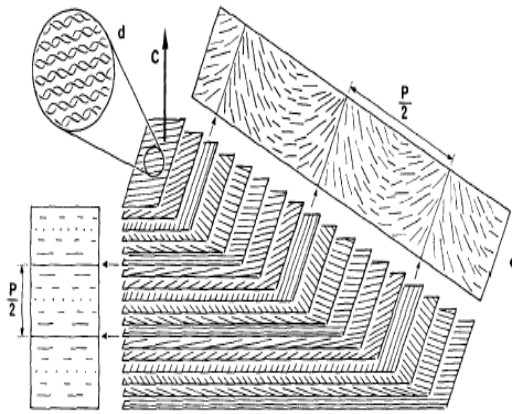

Fig.1.6. Schematic diagram showing cholesteric alignment of DNA molecules[32].

At DNA concentrations higher than 350mg/ml, a two-dimensionally ordered, columnar hexatic phase is formed, which exhibits a characteristic focal conic texture, similar to those seen in both lyotropic and thermotropic LC phases with small molecules[90-92,140]. This is due to the natural tendency of semi-rigid polymers to form LC phases in concentrated solutions.

Columnar hexagonal phase is two-dimensional; the molecules are longitudinally aligned with a lateral hexagonal order (Fig.1.7). They are,

however, not true crystals. The molecules present some disorder around their position in the hexagonal array. While the cholesteric phase has a twist, columnar hexagonal phase does not. A series of textures are obtained with increase in concentration till true crystals appear above C_D 447 mg/ml.

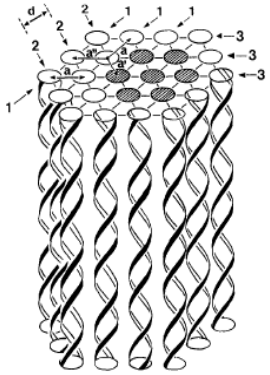

Fig.1.7. Schematic diagram showing columnar alignment of DNA molecules[32].

Rill and coworkers by using in parallel ^{31}P NMR spectroscopy and polarizing microscopy, showed that with monodisperse 50 nm DNA fragments, C_D varies moderately with the ionic environment of the molecule: from about 130 mg/ml in 0.01M Na solution to 170 mg/ml at 1M Na^+ (at 25^0C). The effective diameter D_{eff} of DNA molecule was calculated from these data, and were found to decrease from 4.2 nm in 0.1 M Na^+ to 3.4 nm for 1M Na^+ [91,93,157,158]. Discrepancies are observed in many of these values possibly because the molecules in crowded conditions do not necessarily follow the same rules as in dilute solutions.

Besides, counter ion type and ionic strength, C_D also depends on various factors such as persistence length of the mesogen, polydispersity, temperature, dielectric constant of the medium, polymer-solvent interaction parameter

(including influence of secondary forces such as hydrogen bonding) etc.

As DNA is believed to be condensed into LC states *in vivo*, because of the various condensing factors, present in the cell nucleus, a discussion on DNA condensation would be interesting.

1.6. DNA Condensation

DNA condensation has become a lively area for research, in diverse areas of science. In biochemistry, biophysics, and molecular biology it represents a process by which the genetic information is packaged and protected. In polymer physics, and condensed matter physics, it presents intriguing problems of phase transitions, liquid crystal behavior and polyelectrolytes. And in biotechnology and medicine, it provides a promising means, whereby DNA containing genes of therapeutic interest can be prepared for transfer from solution to target cells, for gene therapy applications.

DNA condensation is the collapse of extended DNA chains into compact, orderly particles containing only one or a few molecules. In aqueous solutions, condensation normally requires cations of charge +3 or greater. Those most commonly used in condensation studies are, the naturally occurring polyamines spermidine^{3+} spermine^{4+} and the inorganic cation $[Co(NH_3)_6]^{3+}$ [159].

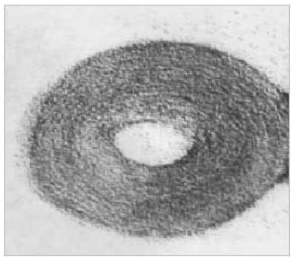

Fig.1.8. A DNA Toroid

Polyamines have been shown to induce DNA condensation, and to stabilize compact forms of DNA. The binding of polyamines to DNA results in duplex and triplex DNA stabilization and condensation of dilute solutions to toroids (Fig.1.8) and spheroids, as well as the aggregation and resolubilization of DNA[98,160-166].

Toroidal condensates are a highly organized form of DNA, and a recent study indicates the organization of DNA, in a columnar hexagonal array, in toroids[167-170]. The organization of DNA in these structures, composed of one or only a limited number of DNA molecules, has attracted much attention recently because of the technological importance of these 'artificial virus' particles as gene delivery vehicles[171-173]. Most of these transfection agents are composed of multivalent cations, cationic lipids, polyethylenimine, polylysine, polyamines or their derivatives. A recent report indicates that the columnar hexagonal packing of DNA facilitates the cellular transport of DNA[174]. The hexagonal packing of DNA has been found in many cases of DNA crystallization; however, the finding of such an arrangement in a toroid composed of two molecules of DNA is very interesting[167].

Much attention has been paid recently to the condensation of DNA with cationic liposomes, since the complex can be an efficient agent for transfection of eukaryotic cells. This is presumably because the condensed state of the DNA protects it from nucleases and allows it to pass more easily through small openings, while the lipid coating on the DNA increases its permeability through cell membranes[175-178]. The existence of the LC phase of DNA has also

been shown in complexes of cationic lipids and DNA, used as gene delivery vehicles[1].

Recent attention has been focused largely on counter ion fluctuations and hydration forces. Because at close range, both hydration and ionic forces, appear to depend on the effect of apposing surface lattices, on the fluctuating correlations of ions and water molecules between them, the two types of force may prove difficult to disentangle[179]. The counter-ions not only screen coulombic repulsions between the DNA phosphates, they also produce attraction through correlated fluctuations of the ion atmosphere. Rau and Parsegian proposed that polyvalent ligands bound to DNA double helices, appear to act by reconfiguring the water between macromolecular surfaces to create attractive long-range hydration forces[180,181]. As hydration of DNA is an important parameter, which governs the formation and stabilization of DNA mesophases, a short discussion on the importance of water molecules on DNA structure appears relevant.

1.7. Nucleic Acid Hydration

It is well known that the conformation and functions of nucleic acids are largely dependent on the hydration forces. Because of the regular structure of DNA, hydrating water is held in a cooperative manner along the double helix in both the major and minor grooves. The cooperative nature of this hydration, aids both the zipping (annealing) and unzipping (unwinding) of the double helix. In DNA, even though the bases are involved in hydrogen bonded pairing they are capable of one further hydrogen bonding link to water within the

major or minor grooves except for the hydrogen bonded ring nitrogen atoms (pyrimidine N3 and purine N1).

Hydration of phosphate groups in the major groove is thermodynamically stronger, but exchanges faster. There are six (from crystal structures)[182] or seven (from molecular dynamics)[183] hydration sites per phosphate,[184] not including hydration of the linking oxygen atoms to the deoxyribose or ribose residues. All deoxyribose oxygen atoms (O3' phosphoester, ring O4' and O5' phosphoester) hydrogen bond to one water molecule whereas the free 2'-OH in ribose is much more capable of hydration and may hold on to about 2.5 water molecules. The total for all these hydrations, in a G-C duplex, would be about 26-27, but about 14 of these water molecules are shared. There are a number of ways in which these water molecules can be arranged with B-DNA, possessing 22 possible primary hydration sites per base pair in a G-C duplex, but only occupying 19 of them[183]. The DNA structure depends on how these sites are occupied; water providing the zip, holding the two strands together. It should be noted that about 2% of the hydrating water molecule sites might be transiently replaced by cations.

The B-DNA possessing higher phosphate hydration, is stabilized at high water activity whereas A-DNA, with its shared inter-phosphate water bridges, is more stable at low water activity. Thus, if the relative humidity is kept constant, there will tend to be a transformation from B-DNA to A-DNA with increasing temperature[12].As nucleic acids as well as cations, are heavily and specifically hydrated, any interaction between them is accompanied by an

overlapping of their hydration shells and the release of water molecules to bulk state. The magnitude of these hydration changes is determined by the actual position of the cation relative to the atomic groups at the surface of DNA and can characterize the structure of the complexes. Binding of metal ion will disrupt the ordered water structure around DNA strands thereby facilitating the LC ordering.

1.8. Applications of Liquid Crystalline DNA

Biopolymers attract much attention as building blocks for innovative materials[185-187]. The application of synthetic or natural nucleic acids in this field is based on the wide spectrum of chemical and physical properties exhibited by these biopolymers.

First, the intrinsic molecular recognition elements of nitrogen bases inducing the self assembling of nucleic acids, allows to build complex molecular structures or to functionalize pre-formed structures. Second, it is possible to modulate the properties of the above structures not only by changing their nitrogen base sequence, but also by modifying the properties of the solvent in which they are formed. Third, structures arising from biopolymeric molecules and inorganic current-conducting components as additional building elements would be relevant not only to the field of nanoelectronics, but also in terms of obtaining sensing units for analytical devices like biosensors[192-193]. Liquid crystals formed from linear double stranded DNA, can be used for creating biosensing units for detection of coloured biologically active compounds, which can form strong complexes

with DNA nitrogen bases, for testing water, food, soil, and plant samples for the presence of analytes (carcinogens, drugs, mutagenic pollutants, etc.). Presently, double stranded nucleic acids (dsDNA), forming lyotropic liquid crystals, are used for supramolecular design of advanced materials[188,189].

The condensed phase of DNA chains tethered by divalent counter ions in 2D may have interesting potential applications. The hybrid DNA-lipid-metal ion phase, with trapped metal ions forming a 1D liquid between the DNA chains at a density of 0.63 ions/DNA base pair can be a precursor to novel organometallic materials. Different reaction routes may lead to the simultaneous large-scale synthesis of nanoscale wires. The extreme packing state for the DNA chains attached to surfaces within these lamellar complexes renders these materials ideal for high-density storage and straightforward retrieval of genetic information[190].

It has been proved that endogenous molecules like polyamines are capable of provoking LC phases *in vitro*, which is important to understand the nature and organization of DNA in the cell[90,95,96,98-101]. Synthetic polyamines and oligoamines are under development as chemotherapeutic agents for different forms of cancer[191-193].

The dilute solutions of DNA are condensed by polyamines into toroids[160-166]. Toroidal condensates are highly organized form of DNA, and a recent study indicates the organization of DNA in a columnar hexagonal array in toroids[49,168-170]. The existence of the LC phase has also been shown in complexes of cationic lipids and DNA, which are used as gene delivery

vehicles[1] (Fig.1.9). A recent report indicates that the columnar hexagonal packing of DNA facilitates the cellular transport of DNA[1].

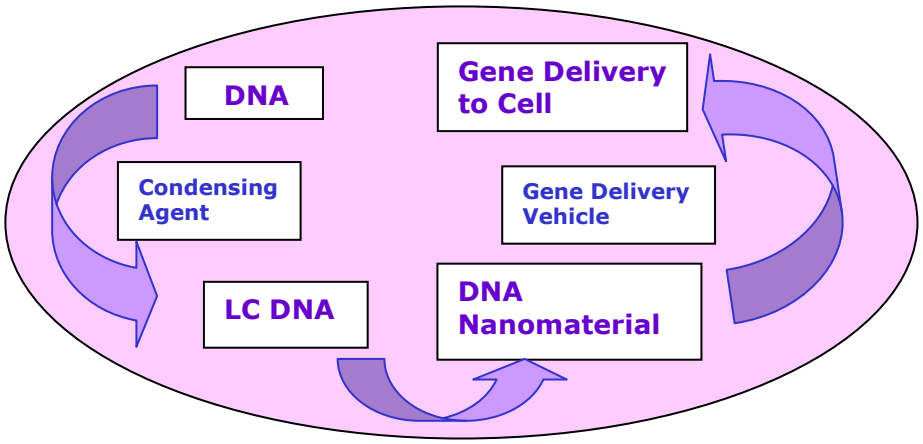

Fig.1.9. Schematic diagram showing the application of LC DNA in gene delivery

Since liquid crystals (LC's) are highly birefringent and the molecular alignment is greatly affected by the delicate change of surface conditions, it is suitable for detecting hybridization results in DNA chips[3]. Studies on the possibility of the DNA detection in DNA chips using liquid crystal alignment shows that the surface morphologies as well as chemical properties are totally changed by reaction of complementary DNA with oligonucleotide. Since the change alters LC alignment, and the light passing through the chip is greatly enhanced by the alignment, we can easily observe the reaction results by naked eye. It was found that the LC alignment depends on the packing ratio, and ordering of the oligonucleotide on the glass.

1.9. Scope and Objectives of the Present Work

As discussed in the preceding section, condensation of DNA into LC domains has become a lively area of research due to its potential applications in

the fields of therapeutics (eg. gene delivery),[1,2,194-202] design of biosensing units,[3] DNA chips[90-92,140] etc. However, from the literature data, it has become evident that the present level of understanding on the LC phase behavior of DNA is inadequate, and a thorough investigation is required to understand the nature and stability of these phases under the influence of varying environmental conditions. Earlier studies on the induction and characterization of LC DNA, were mostly focused on low molecular weight fragmented DNA which is known to exhibit a complex and polymorphic behavior, in the presence of few biologically important counter ions[82,91]. Since, DNA molecules in the cell nucleus are quite long, and are known to exist in the condensed states in vivo[4-9] it would be interesting to study the LC behavior of the high molecular weight DNA. The LC phase behavior of DNA, however is known to be largely influenced by the counter ion type and concentration because the effective particle radius and hence the effective axial ratio and excluded volume of DNA are determined by the counter ion shielding[203]. Understanding of DNA packaging in living organisms therefore, requires the knowledge of DNA-counter ion and DNA-DNA interactions in condensed states. Metal ions in general, have been divided into three main categories, according to their binding mode to DNA molecule, as phosphate binders, phosphate cum base binders and pure base binders[204]. Metal ions with different binding modes, when interacts with the DNA macromolecule, are known to alter the secondary structure of DNA, which in turn could affect rigid rod like behavior of the DNA molecule responsible for the LC properties of DNA. Those metal ions

that bind primarily to the phosphates stabilize the helix, by reducing the intermolecular repulsion, which provokes LC ordering, whereas a distortion of the double helix by base binding metal ions might result in the loss of rigid rod like shape of the DNA molecule, which is the determinant factor of its LC behavior.

Some of the metal ions such as sodium, potassium, magnesium, calcium etc. are involved in a variety of cellular functions[205] (enzymatic activities related to replication, transcription, recombination etc.) including DNA condensation,[206] whereas certain metal ions such as cadmium,[207] aluminium,[208] vanadium[209,210] etc. are known for their genotoxic effects. An investigation of the interaction between the metal ions of different binding modes with high molecular weight DNA, might be useful to correlate the supramolecular organization of DNA with its biological functions, and pave the way for understanding, metal ion induced genotoxic effects. A detailed investigation on the LC properties of DNA, would also be beneficial to improve upon the performance of DNA based devices, under investigation in the fields of nanoelectronics,[211,212] and biosensors[162,179,213].

Polyamines have been shown to induce DNA condensation, and to stabilize compact forms of DNA[214]. Moreover, polyamines and polyamine derivatives such as polyaminolipids, are under development as DNA delivery vehicles for gene therapy[215]. The stability and character of complexes with polyamines and fragments of nucleic acids is known to depend mainly on the type of metal ion bound to DNA[97]. Eventhough, the spermine induced LC

organization of fragmented DNA is known in the presence of few biologically important metal ions; it remains unclear with high molecular weight DNA. Hence, the investigations on the induction and stabilization of LC phases of high molecular weight DNA by spermine, in the presence of alkali and alkaline earth metal ions, would be useful in understanding the organization of DNA *in vivo*, and could be an aid, in the field of gene delivery research. Among the polyamines, spermine is of higher valence state, and spermine-based drugs have become chemotherapeutically important.

Thus, a comparative investigation of the expression of LC phases of DNA, by its interaction with metal ions of varying charge, size and binding modes, might give an understanding on the supramolecular organization of DNA. This study might lead to elucidate the role played by the condensed state of DNA (fiber, gel, liquid crystal), on the cellular and molecular basis of normal cell expressions, metal toxicity and pave way for better therapeutics.

Therefore, the objectives of the present work are:

1) Investigations on the induction and stabilization of LC phases of high molecular weight DNA by alkali metal ions.
2) Investigations on the induction and stabilization of LC phases of high molecular weight DNA by alkaline earth metal ions.
3) Effects of multivalent, transition and heavy metal ions on the LC phase behavior of high molecular weight DNA.
4) Investigations on spermine induced LC behavior of high molecular weight DNA in the presence of alkali and alkaline earth metal ions.

1.10. References

1. Koltover, I.; Salditt, T.; Radler, J. O.; Safinya, C. R., *Science* **1998,** 281, 78.
2. Yevdokimov, Y. M.; Salyanov, V. I., *Biosensors & Bioelectronics* **1996,** 11, 889.
3. Cognard, J., *Mol. Cryst. Liq. Cryst. Suppl.* **1982**, 1.
4. Livolant, F., *J. Mol. Biol.* **1991,** 218, 165.
5. Bouligand, Y.; Soyer, M. O.; Puiseux-Dao, *Chromosoma* **1968,** 24, 251.
6. Livolant, F., *Eur. J. Cell. Biol.* **1984,** 33, 300.
7. Rill, R. L.; Livolant, F.; Aldrich, H. C.; Davidson, M. W., *Chromosoma* **1989,** 98, 280.
8. Gourett, J. P., *Biol. Cell* **1978,** 32, 299.
9. Lepault, J.; Dubochet, W.; Baschong, W.; Kellenberger, E., *EMBO J.* **1987,** 6, 1507.
10. Kunjappu, J. T.; Venkatachalam, S. R.; Nair, C. K. K., *J. Sci.& Ind. Res.* **1995,** 54, 717.
11. Simmerman, S. B., *Biochim. Biophys. Acta,* **1993,** 175, 1216.
12. Albiser, G.; Lamiri, A.; Premilat, S., *Int. J. Biol. Macromol.* **2001,** 28, 199.
13. Anastassopoulou, J., *J. Mol. Str.* **2003,** 19, 651.
14. Manning, G. S., *Q. Rev. Biophys.* **1978,** 11, 179.
15. Lohman, T. M.; Mascotti, D. P., *Methods Enzymol* **1992,** 212, 400.
16. Anderson, C. F.; M.T., R. J., *Annu. Rev. Phys. Chem.* **1995,** 46, 657.
17. Duguid, J. G.; Bloomfield, V. A.; Benevides, J. M.; Thomas Jr, G. J., *Biophys. J.* **1995,** 69, 2623.
18. Sigel, H. *Metal-DNA Chemistry*; American Chemical Society: Washington, DC, 1989
19. Saenger, W., *Principles of Nucleic Acid Structure*. ed.; Springer-Verlag: New York, 1994.
20. Yangs, D.; Wang, A. H., *J. Prog. Biophys. Mole. Biol.* **1996,** 66, 81.
21. Theophanides, T., *Appl. Spectrosc.* **1981,** 35, 461.

22. Katz, S., *Nature* **1962,** 194, 569.
23. Katz, S., *Biochem. Biophys. Acta* **1963,** 68, 240.
24. Luck, G.; Zimmer, Ch, *Eur. J. Biochem* **1971,** 18, 140.
25. Mansy, S.; Rosenberg, B.; Thomson, A. J., *J. Amer. Chem. Soc.* **1973,** 92, 1633.
26. Pillai, C. K. S.; Nandi, U. S. *Indian J Phys* **1976**, Commemorative Volume, 277.
27. Pillai, C. K. S.; Nandi, U. S., *Biochim. Biophys. Acta* **1977,** 474, 11.
28. Pillai, C. K. S.; Nandi, U. S.; Levinson, W., *Bio-inorganic Chem.* **1977,** 7, 151.
29. Robins, A. B., *Ibid* **1973,** 6, 135.
30. Rosenberg, B., *Platinum Rev* **1971,** 15, 42.
31. Shooter, K. V.; Howse, R.; Merrifield, R. K.; Robins, A. B., *Chem. Biol. Inter*. **1972,** 5, 289.
32. Yamane, T.; Davidson, N., *J. Amer. Chem. Soc.* **1961,** 83, 2599.
33. Zhakharenko, E. T.; Moshkovskii, Y. S., *Biofizika*, **1972,** 17, 373.
34. Anastassopoulou, J., *Magnesium Res.* **1992,** 5, 97.
35. Manfait, M.; Theophanides, T., *Magnesium.* **1983,** 2, 323.
36. Tajmir-Riahi, H. A.; Theophanides, T., *Can. J. Chem.* **1983,** 61, 1813.
37. Tajmir-Riahi, H. A.; Theophanides, T., *Inorg. Chim. Acta* **1983,** 80, 223.
38. Tajmir-Riahi, H. A.; Theophanides, T., *Can. J. Chem.* **1985,** 63, 2065.
39. Theophanides, T., *Int. J. Quantum Chem.* **1984,** 26, 933.
40. Tajmir-Riahi, H. A.; Theophanides, T., *Can. J. Chem.* **1984,** 62, 266.
41. Polissiou, M.; Theophanides, T., *Metal based anti-tumor drugs.*; Freund Publishing House Ltd: London, 1991.
42. Theophanides, T.; Anastassopoulou, J., *in Equilibri in soluzione, Aspeti teorici, sperimentali ed applicaviti*. ed.; Italy, 1988.
43. Theophanides, T.; Anastassopoulou, J.; Schmid, E. D., *Spectroscopy of BiologicalMolecules-New Advances*. Willey: Chichester, 1987 .

44. Theophanides, T.; Bal, W.; Jezierski, A., *Proceedings in Second Symposium on Inorganic Biochemistry and Molecular Biophysics*. ed.; Wroclaw, 1989, 114.

45. Hossain, Z.; Huq, F., *J. Inorg. Biochem* **2002,** 90, 97.

46. Zacharias, W.; Klysik, J. E.; Stirdivant, S. M.; Wells, R. D., *J. Biol. Chem.* **1982,** 257, 2775.

47. Egli, M., *Chem. Biol.* **2002,** 9, 277.

48. Low, L. Y.; Hernandez, H.; Robinson, C. V.; Obrien, R.; Grossmann, J. G.; Ladbury, J. E.; Luisi, L., *J. Mol. Biol.* **2002,** 100, 87.

49. Hud, N. V.; Polak, M., *Curr. Struct. Biol.* **2001,** 11, 293.

50. Nordenskiold, L.; Chang, D.; Anderson, C.; Record, T. J., *Biochemistry* **1998,** 37, 16877.

51. Woods, K. K.; McFail-Ison, L.; Sines, C. C.; Stephens, R. K.; Williams, L. D., *J. Am. Chem. Soc.* **2000,** 122, 1546.

52. Stelwagen, N. C.; Magnusdottir, S.; Gelfi, C.; Righeti, P. G., *J. Mol. Biol.* **2001,** 305, 1025.

53. Tereshko, V.; Wilds, C. J.; Minasov, G.; Prakash, T. P.; Maier, M. A.; Howard, A.; Wawrzak, Z.; Manoharan, M.; Egli, M., *Nucleic Acids Res.* **2001,** 29, 1208.

54. Danisov, V. P.; Halle, B., *Proc. Natl Acad. Sci.USA* **2000,** 97, 629.

55. Gruenwedel, D. W.; Hsu, C. H.; Lu, D. S., *Biopolymers* **1971,** 10, 47.

56. Koltover, I.; Wagner, K.; Safinya, C. R., *Proc. Natl. Acad. Sci* **2000,** 97, 14046.

57. Korolev, N. *Biomacromolecules* **2000,** 1, 648.

58. Korolev, N. I. *Ph.D Thesis* 1985, Moscow.

59. Korolev, N. I.; Vlasov, A.P.; Kuznetsov, I.A, *Biopolymers* **1994,** 34, 1275.

60. Kuznetsov, I. A.; Gorshkov, V. I.; Ivanov, V. A.; Kargov, S. I.; Korolev, N. I.; Filipov, S. M.; Khamisov, R. K., *Reactive Polym.* **1984,** 3, 37.

61. Kuznetsov, I. A.; Kargov, S. I.; Khamisov, R. K.; Gorshkov, V. I., *Molek. Biolog.* **1983,** 18, 1569.

62. Kuznetsov, I. A.; Meznetsev, A. I.; Gurunovich, A. K., *Biofizik,* **1968,** 13, 20.

63. Kuznetsov, I. A.; Meznetsev, A. I.; Moshkovskii, Y. S.; Lukanin, A. S., *Biofizika* **1967,** 12, 373.

64. Kuznetsov, I. A.; Yachmenyov, V. V.; Belousov, P. S.; Pishonkov, A. G.; Shagalov, L. B.; Vsynberg, Yu. P., *Molek. Biolog,* **1976,** 10, 270.

65. Ivanov, V. I.; Minchenkova, L. E.; Schyolkina, A. K.; Poletaev, A. I., *Bioploymers* **1973,** 12, 89.

66. Manning, G. S., *Biopolymers* **1981,** 20, 2337.

67. Record, M. T.; Woodburry, C. P.; Lohman, T. M., *Biopolymers,* **1976,** 15, 893.

68. Anastassopoulou, J.; Theophanides, T., *Critical Reviews in Oncology/Hematology* **2002,** 42, 79.

69. Barbarossou, K.; Aliev, A.; Gerothanassis, I. P.; Anastassopoulou, J.; Theophanides, T., *Inorg. Biochem.* **2001,** 40, 3626.

70. Marcus, Y., *Biophys. Chem.* **1994,** 51, 111.

71. Pillai, C. K. S., *Ph.D Thesis,* **1974**.

72. Cejudo, R.; Alzuet, G.; González-Álvarez, M.; García-Gimenez, J. L.; Borrás, J.; Liu-González, M., *J. Inorg. Biochem.* **2006**, 70.

73. Anastassopoulou, J.; Barbarossou, K.; Korbaki, V.; Theophanides, T.; Legrand, P., *Spectroscopy of Biological Molecules,* Kluwer Academic Publishers. Dodrecht, 1997.

74. Geierstanger, B. H.; Kagawa, T. F.; Chen, S. L.; Quigley, G. L.; Ho, P. S., *J. Biol. Chem.* **1991,** 266, 20185.

75. Kruszewski, M.; Green, M.; Lowe, J.; Szumiel, I., *Mut. Res.* **1994,** 308, 233.

76. Kruszewski, M.; Iwanenko, T.; Bouzyk, E.; Szumiel, I., *Mut. Res.* **1999,** 53, 434.

77. Lu, X.; Zhu, K.; Zhang, M.; Liu, H.; Kang, J., *J. Biochem.Biophys. Methods* **2002,** 52, 189.

78. Mrevlishvili, G. M.; Sottomayor, M. J.; Manuel, A. V.; Da Silva, R., *Thermochimica Acta.* **2002,** 394, 83.
79. Munno, G. D.; Medaglia, M.; Armentano, D.; Anastassopoulou, J.; Theophanides, T., *Chem. Soc., Dalton Trans.* **2000,** 10, 1625.
80. Davidson, M. W.; Strzelecka, T. E.; Rill, R. L., *Nature* **1988,** 331, 457.
81. Onsager, L., *Ann. NY Acad. Sci.* **1949,** 51, 627.
82. Flory, P. J., *Proc. R. Soc. Lond. Ser. A* **1956,** 234, 73.
83. Vorlander, D., *Kristallinisch- flussige Substanzen*. ed.; Enke Verlag: 1908.
84. Luzzati, V.; Nicolaieff, A.; Masson, F., *J. Molec. Biol.* **1961,** 3, 185.
85. Robinson, C., *Tetrahedron* **1961,** 13, 219.
86. Iizuka, E., *Polym. J.* **1977,** 9, 173.
87. Iizuka, E., *Polym. J.* **1983,** 15, 525.
88. Potaman, V. N.; Alexeev, D. C.; Skuratovsky, I. Y.; Rabinovich, A. Z.; Shlyakhtenko, L. S., *Nucl. Acids. Res.* **1981,** 9, 55.
89. Iizuka, E.; Yang, J. T., *Liquid crystals and Ordered Fluids*. ed.; Plenum Press: 1977.
90. Rill, R. L.; Hilliard, P. R. J.; Levy, G. C., *J. Biol. Chem.* **1983,** 258, 250.
91. Strzelecka, T. E.; Davidson, M. W.; Rill, R. L., *Nature* **1988,** 331, 457.
92. Livolant, F.; Levelut, A. M.; Doucet, J.; Benoit, J. P., *Nature* **1986,** 339, 724.
93. Strzelecka, T. E.; Rill, R. L., *Biopolymers* **1990,** 30, 57.
94. Merchant, K.; Rill, R. L., *Biophys. J* **1997,** 73, 3154.
95. Leforestier, A.; Fudaley, S.; Livolant, F., *J. Mol. Biol.* **1999,** 290, 481.
96. Leforestier, A.; Livolant, F., *Biophys. J.* **1993,** 65, 56.
97. Pelta, J., Jr; Durand, D.; Doucet, J.; Livolant, F., *Biophys. J.* **1996,** 71, 48.
98. Pelta, J.; Livolant, F.; Sikorav, J. L., *J. Biol. Chem.* **1996,** 271, 5656.
99. Raspaud, E.; Olvera de la Cruz, M.; Sikorav, J. L.; Livolant, F., *Biophys. J.* **1998,** 74, 381.
100. Sikorav, J. L.; Pelta, J.; Livolant, F., *Biophys. J.* **1994,** 67, 1387.

101. Saminathan, M.; T., T.; Shirahata, A.; Pillai, C. K. S.; Thomas, T. J., *Nucl. Acids. Res* **2002,** 30, 3722.

102. Demus, D.; Goodby, J.; Gray, G. W.; Spiess, H. W.; Vill, V., *High Mol.Weight Liquid Crystals*. ed.; Wiley VCH: London, 1998.

103. Isayev, A. I.; Kyu, T.; Cheng, S. Z. D., *Liqiuid Crystalline Polymer Systems; Technological Advances*. ed.; ACS Symp. Ser.: Washington, DC, 1996.

104. Noel, C.; Navard, P., *Prog. Polym. Sci,* **1991,** 16, 55.

105. Tukruk, V. V.; Wendorff, J. H., *Supramolecular Polymers and Assemblies-Beyond Mesomorphism,* TRIP,3, 1995.

106. Pillai, C. K. S., *Pure & Appl. Chem.* **1998,** 70, 1249.

107. Cowie, J. M. G., *Polymers: Chemistry and Physics of Modern Materials;* 2 ed.; Blackie Academic& Professional: 1991.

108. Sutherland, R. L., *Handbook of Nonlinear Optics*. ed.; Marcer Dekker: New York, 1996.

109. Economy, J.; Goranov, K., *High Performance Polymers*. ed.; Springer Verlag: Berlin, 1994.

110. Sandhya, K. Y.; Pillai, C. K. S.; Sree Kumar, K., *J. Polym. Sci: Part B: Polym. Physics* **2004,** 42, 1289.

111. Sandhya, K. Y.; Pillai, C. K. S.; Sato, M.; Tsutsumi, N., *J. Polym. Sci.; Polym. Chem.* **2003,** 1257.

112. Chung, T. S.; Calundann, G, W.; East, A. J., *Liquid Crystalline Polymers and their Applications*. ed.; Marcel Dekker: NY, 1989.

113. Chandrasekhar, S., *Liquid Crystals*.; Cambridge University Press: London, **1977**.

114. Sudha, J. D.; Pillai, C. K. S., *Polymer* **2005,** 46, 6986.

115. Prasad, V. S.; Pillai, C. K. S., *J. Polym. Sci.; Polym. Chem.* **2002,** 40, 1845.

116. Prasad, V. S.; Pillai, C. K. S.; Kricheldorf, H. R., *J. Polym. Sci. Polym. Chem. Edn.* **2001,** 39, 2430.

117. Saminathan, M.; Pillai, C. K. S., *Polymer* **2000,** 41, 3103.

118. Pillai, C. K. S., *Pure Appl. Chem.*, **1998,** 70, 1249.
119. Pillai, C. K. S.; Sherrington, D. C.; Sneddon, A., *Polymer* **1992,** 33, 3968.
120. Demus, D.; Diele, S.; Grande, S.; Sackmann, H., *Polymorphism in liquid crystals*. ed.; Academic Press: New York, 1983.
121. Reinitzer, F., *Monatsh Chem.* **1888,** 9, 421.
122. Lehmann, O., *Z. Phys.Chem.* **1989,** 4, 462.
123. Demus, D.; Richter, L., *Textures in liquid crystals*. ed.; Verlag Chemie: Weinheim, 1978.
124. Noel, C.; Laupretre, F.; Friedrich, C.; Fayolle, B.; Bosio, L., *Polymer* **1984,** 25, 808.
125. Noel, C.; Billard, J.; Bosio, L.; Friedrich, C.; Laupretre, F.; Strazielle, C., *Polymer* **1984,** 25, 263.
126. Blumstein, A.; Maret, G.; Vilasagar, S., *Macromolecules* **1981,** 14, 1543.
127. Percec, V.; Tsuda, Y., *Pol. Bull.* **1990,** 23, 225.
128. Tseng, S. L.; Valente, A.; Gray, D. G., *Macromolecules* **1981,** 14, 715.
129. Aharoni, S. M., *Macromolecules* **1979,** 12, 94.
130. Jin, J. I.; Kang, C. S., *Prog. Polym. Sci.* **1997,** 22, 937.
131. Tsvetkov, V. N.; Shtennikova, I. N., *Macromolecules* **1978,** 11, 479.
132. Hummel, J. P.; Flory, P. J., *Macromolecules,* **1980,** 13, 479.
133. Laupretre, F.; Monnerie, L., *Eur.Polym.J.* **1978,** 14, 415.
134. Bawden, F. C.; Pirie, N. W., 123, 1274, *Proc. R. Soc., Ser.B* **1937,** 123, 1274.
135. Elliot, A.; Ambrose, E. J., *Discuss. Faraday Soc.* **1950,** 9, 246.
136. Robinson, C., *Trans. Faraday Soc.* **1956,** 571.
137. Robinson, C.; Ward, J. C., *Nature* **1957,** 180, 1183.
138. Chandrasekhar, S.; Sadashiva, B. K.; Suresh, K. A., *Pramana* **1977,** 9, 471.
139. Minton, A. P., *Biopolymers* **1981,** 20, 209.
140. Livolant, F.; Leforestier, A., *Prog. Polymer Sci.* **1996,** 21, 1115.

141. Torbet, J.; DiCapua, E., *EMBO J.* **1989,** 8, 4351.
142. Lewin, B., *Genes VII*. ed.; Oxford Univ. Press, London: 1999.
143. Krasnow, M. A.; Cozzarelli, N. R., *J. Biol. Chem.* **1982,** 257, 2687.
144. Robinson, C., *Mol. Cryst,* **1966,** 1, 467.
145. Luzzati, V.; Nicolaieff, A., *J. Mol. Biol.* **1959,** 1, 127.
146. Luzzati, V.; Nicolaieff, A., *J. Mol. Biol.* **1963,** 7, 142.
147. Jordan, C. F.; Lerman, L. S.; Venable, J. H., *Nature New Biology* **1972,** 67, 236.
148. Lerman, L. S., *Cold Spring Harb. Symp. Quant. Biol.* **1974,** 38, 59.
149. Maniatis, T.; Venable, J. H.; Lerman, L. S., *J. Mol. Biol.* **1974,** 84, 37.
150. Cheng, S. M.; Mohr, S. C., *Biopolymers* **1975,** 14, 663.
151. Huey, R.; Mohr. S. C., *Biopolymers* **1981,** 20, 2533.
152. Bloomfield, V. A., *Biopolymers* **1991,** 31, 1471.
153. Shapiro, J. T.; Leng, M .; Felsenfeld, G., *Biochemistry* **1969,** 8, 3219.
154. Zlatanova, J.; Yaneva, J, *DNA and Cell Biol.* **1991,** 10, 239.
155. Battisel, E.; Imre, E. V.; Luisi, P. L., *Controlled release of Drugs and aggregates Systems*.; VCH: New York, 1989.
156. Ghirlando, R.; Wachtel, E. J.; Arad, T.; Minsky, A., *Biochemistry* **1992,** 31, 7110.
157. Rill, R. L.; Strzelecka, T. E.; Davidson, M. W.; Van Winkle, D. H., *Physica A* **1991,** 176, 87.
158. Van Winkle, D. H.; Davidson, M. W.; Chen. W, X.; Rill, R. L., *Macromolecules* **1990,** 23, 4140.
159. Bloomfiled, V. A., *Current Opinion in Structural Biology* **1996,** 6, 334.
160. Thomas, T. J.; Bloomfield, V. A., *Biopolymers* **1984,** 23, 1295.
161. Thomas, T.; Thomas, T. J., *Biochemistry* **1993,** 32, 14068.
162. Gosule, L. C.; Schellman, J. A., *J. Mol. Biol.* **1978,** 121, 311.
163. Wilson, R. W.; Bloomfield, V. A., *Biochemistry* **1979,** 18, 2192.
164. Marx, K. A.; Ruben, G. C., *J. Biomol. Struct. Dyn.* **1984,** 1, 1109.
165. Saminathan, M.; Antony, T.; Shirahata, A.; Sigal, L. H.; Thomas, T.; Thomas, T. J., *Biochemistry* **1999,** 38, 3821.

166. Vijayanathan, V.; Thomas, T.; Shirahata, A.; Thomas, T. J., *Biochemistry* **2001,** 40, 13644.
167. Hud, N. V.; Downing, K. H., *Proc. Natl Acad. Sci. USA* **2001,** 98.
168. Golan, R.; Pietrasanta, L. I.; Hsieh, W.; Hansma, H. G., *Biochemistry* **1999,** 38, 14069.
169. Lin, Z.; Wang, C.; Feng, X.; Liu, M.; Li, J.; Bai, C., *Nucleic Acids Res.* **1998,** 26, 3228.
170. Ubbink, J.; Odijk, T., *Biophys. J.* **1995,** 68, 54.
171. Remy, J. S.; Kichler, A.; Mordvinov, V.; Schuber, F.; Behr, J. P., *Proc. Natl Acad. Sci. USA* **1995,** 92, 1744.
172. Wagner, E.; Cotton, M.; Foisner, R.; Birnstiel, M. L., *Proc. Natl Acad. Sci. USA* **1991,** 88, 4255.
173. Zuber, G.; Dauty, E.; Nothisen, M.; Belguise, P.; Behr, J. P., *Adv. Drug Delivery Rev.* **2001,** 52, 245.
174. Pitard, B.; Aguerre, O.; Airiau, M.; Lachage, A. M.; Boukhnikachvili, T.; Byk, G.; Dubertret, C.; Herviou, C.; Scherman, D.; Mayaux, J. F.; Crouzet, J., *Proc. Natl Acad. Sci. USA* **1997,** 94, 14412.
175. Feigner, P. L.; Gadek, T. R.; Holm, M.; Roman, R.; Chan, H, W.; Wenz, M .; Northrop , J.P.; Ringold G. M.; Danielsen M., *Proc Nat/Acad Sci USA* **1987,** 84, 7413.
176. Liu, G.; Molas, M.; Grossmann, G. A.; Pasumarthy, M.; Perales, J. C.; Cooper, M. J.; Hanson, R. W., *J. Biol. Chem.* **2001,** 276, 34379.
177. Farhood, H. G.; Son, K.; Yang, Y.; Lazo, J.; Huang, L.; Barsourn, J.; Bottega, R.; Epand, R., *Ann NY Acad Sci* **1994,** 23, 716.
178. Gustafsson, J.; Arvidson, G.; Karlsson, G.; Alrngren, M., *BBA-Biomembranes* **1995,** 305, 1325.
179. Bloomfield, V. A., *Biopolymers* **1992,** 31, 1471.
180. Leikin, S.; Rau, D. C.; Parsegian, V. A., *Phys Rev A,* **1991,** 44, 5272.
181. Rau, D. C.; Parsegian, V. A., *Biophys J* **1992,** 61, 246.
182. Schneider, B.; K., P.; Berman, H. M., *Biophys. J.* **1998,** 75, 2422.
183. Auffinger, P.; Westhof, E., *J. Mol. Biol.* **2000,** 300, 1113.

184. Cho, H.; Singh, S.; Robinson, G. W., *Faraday Discuss.* **1996,** 103, 19.
185. Bethel, D.; Schiffrin, D. J., *Nature* **1996,** 382, 581.
186. Service, R. F., *Science* **1997,** 277, 1036.
187. Seeman, N. C., *Acc. Chem. Res.* **1997,** 30, 357.
188. Seeman, N. C., *Ann.Rev. Biomol. Struct.* **1998,** 27, 225.
189. Yevdokimov, Y. M.; Skuridin, S. G.; Lortkipanidze, G. B., *Liquid crystals* **1992,** 12, 1.
190. Koltover, I.; Wagner, K.; Safinya, C. R., *Proc. Natl. Acad. Sci* **2000,** 97, (26), 14046.
191. Thomas, T.; Thomas, T. J., *Cell. Mol. Life Sci.* **2001,** 58, 244.
192. Casero, R. A., Jr; Woster, P. M., *J. Med. Chem.* **2001,** 44, 1.
193. Marton, L. J.; Pegg, A. E., *Annu. Rev. Pharmacol. Toxicol.* **1995,** 35, 55.
194. Zimmerman, S. B.; Murphy, L. D., *FEBS Lett* **1996,** 390, 245.
195. Tabor, C. W.; Tabor, H., *Annu Rev Biochem* **1976,** 45, 285.
196. Canellakis, E. S.; Viceps-Madore, D.; Kyriakidis, D. A.; Heller, J. S., *Curr Top Cell Regul* **1979,** 15, 155.
197. Thomas, T.; Thomas, T. J., *Cell Mol Life Sci* **2001,** 58, 244.
198. Dam, L. V.; Korolev, N.; Nordenskiöld., L., *Nucleic Acids Research* **2002,** 30, 419.
199. Santhakumaran, L. M.; Chen, A.; Pillai, C. K. S.; Thomas, T.; He, H. X.; Thomas, T. J., *Nanotechnology in Non-Viral Gene Delivery, book chapter in "Nanofabrication for Biomedical Applications*. ed.; Wiley-VCH: 2004.
200. Vijayanathan, V.; Thomas, T.; Thomas, T. J., *Biochemistry* **2002,** 41, 14085.
201. Vijayanathan, V.; Thomas, T.; Sigal, L. H.; Thomas, T. J., *Antisense Nucleic Acid Drug Dev* **2002,** 12, 225.
202. Vijayanathan, V.; Thomas, T.; Shirahata, A.; Thomas, T. J., *Biochemistry* **2001,** 40, 9387.
203. Hackl, E. V.; Kornilova, S. V.; Blagoi, Y. P., *International Journal of Biological Macromolecules* **2005,** 35, 175.

204. Sigel, A., Sigel, H., *Metal Ions in Biological Systems*, Eds.; Marcel Dekker: New York, ed.; 1996.

205. Widom, J., *J. Mol. Biol.* **1986**, 190, 411.

206. Beyersmann, D.; Hechtenberg, S., *Toxicol.Appl. Pharmacol.* **1997,** 144, 247.

207. Delhaize, E.; Ryan, P. R.; Hebb, D. M.; Yamamoto, Y.; Sasaki, T.; Matsumoto, H., *Proc. Natl. Acad. Sci. USA* **2004**, 15249.

208. Chasteen, N. D., *The biochemistry of vanadium, Struct. Bonding.* **1983,** 53, 107.

209. Keen, R. E. *U.S.Patent No.6,060,327* **2000.**

210. Keen, R. E. *U.S.Patent No 6,326,215* **2001.**

211. Keen, R. E. *U.S.Patent No.6,699,667* **2004.**

212. Evdokimov; Mikhailovich, J.; Skuridin; Gennadievich, S.; Chernukha; Alexandrovich, B.; Mikhailov; Leonidovich, E.; Kompanets; Nikolaevich, O.; Romanov; Nikolaevich. S.; Kolosov; Vasilievich. *U. S. Patent No.*6,246, 470 **2001**.

213. Raspaud, E.; Chaperon, I.; Leforestier, A.; Livolant, F., *Biophys. J.* **1999,** 77, 1547.

214. Remy, J. S.; Kichler, A.; Mordvinov, V.; Schuber, F.; Behr, J. P., *Proc. Natl Acad. Sci. USA* **1995,** 92, 1744.

215. Lomozik, L.; Lastrzab, R.; Gasowska, A., *Polyhedron* **2000,** 19, 1145.

CHAPTER 2

INDUCTION AND STABILIZATION OF LIQUID CRYSTALLINE PHASES OF DNA BY ALKALI METAL IONS:

A. STUDIES ON LC BEHAVIOR USING POLARIZED LIGHT MICROSCOPY.

B. STUDIES ON BINDING BEHAVIOR OF ALKALI METAL IONS USING MOLECULAR MODELING.

CHAPTER 2 A

INDUCTION AND STABILIZATION OF LIQUID CRYSTALLINE PHASES OF DNA BY ALKALI METAL IONS: STUDIES ON LC BEHAVIOR USING POLARIZED LIGHT MICROSCOPY

2.A.1. Abstract

A comparative study of the effects of alkali metal ions, such as Li^+, Na^+, K^+, Rb^+ and Cs^+, on the LC organization of high molecular weight calf thymus DNA, using polarized light microscopy, indicated major differences in the presence of Li^+ ions. Critical DNA concentration (C_D) required to exhibit anisotropic behavior was same for all the alkali metal ions, except Li^+ ion. Multiple LC phases of high molecular weight DNA could be generated at concentrations (7.14 mg/ml) that are far less than that required for low molecular weight DNA fragments (200 mg/ml). DNA initially showed cholesteric textures, which later on turned to a more ordered columnar phase, but the cholesteric-columnar transition was facilitated by increased size of the ion. In the presence of Li^+ ion, a nematic Schlieren like texture was formed initially, which after a few days changed to a higher ordered and highly stable (for more than two months) biphasic cholesteric-columnar arrangement. The observed differences between Li^+ and other alkali metal ions could be understood on the basis of its higher hydration factor and also of its outer

sphere binding mechanism. Hence, lithium can be used as a counter ion to prepare highly stable DNA mesophases which may find applications in the field of nanolectronics, in designing biosensing units, and in DNA chips.

2.A.2. Introduction

DNA liquid crystals represent the simplest model systems for DNA packing in nature, as observed in cell nuclei and bacteriophage heads[1-4]. The highly ordered and condensed LC textures of nucleic acids in *vivo* are largely due to their interaction with basic proteins, charged aliphatic amines and metal ions. These condensed LC states are important to allow proteins to access the DNA template for a multitude of biological tasks, including replication and transcription[5]. Studies on the DNA LC domains can therefore be used as a probe, to obtain vital information on its supramolecular organization *in vivo*, and also on the functioning of DNA in the condensed states. In a condensed state of DNA, the mean concentration of counter ion is very high (1-2 M)[6]. Understanding of DNA packaging (in living organisms) requires the knowledge of DNA-counter ion and DNA-DNA interactions in the condensed states. In monovalent salt solutions, DNA is known to exhibit the following sequence of LC phases, with decreasing DNA concentration: crystalline (hexagonal, orthorhombic), hexagonal, line hexatic, cholesteric, blue phase and isotropic[7]. Counter ion neutralization is essentially required for the generation of LC phases.

Both metal ions and nucleic acids are specifically hydrated in an aqueous solution, and an overlapping of their hydration spheres and the release

of water accompany any interaction between them[8]. The affinity of a cation for a specific site on a polynucleotide is a general function of its charge, hydration-free energy, coordination geometry, and coordinate bond-forming capacity[9,10]. The hydration-free energy is particularly important in distinguishing monovalent from divalent cation binding. Monovalent cations are generally less strongly solvated than divalent cations and therefore tend to interact with DNA purely electrostatically without making hydrogen bonds from metal-coordinated water molecules[11]. As a consequence, DNA-associated monovalent cations are generally not clearly identified in x-ray crystallographic studies of duplex DNA[12,13]. Among the alkali metal ions, Na^+ and K^+ are widely distributed in most of the biological systems and are involved in a variety of cellular functions. Na^+ and K^+ are the major extracellular and intracellular cations respectively in the body fluids of animals including the human beings[14]. Their concentrations are maintained inside and outside the cell by a Na^+ -K^+ pump with the help of a carrier protein. Depending on their electronic structure, the alkali metal ions can produce electrostatic or ionic binding. Molecular dynamic (MD) simulations, solution NMR and crystallographic results agree that the monovalent cations Na^+, K^+, Rb^+, Cs^+ and NH_4^+ prefer direct binding (inner sphere) at the ApT step in A-track of DNA minor groove[15,16]. Li^+ is reported to interact with minor groove via water bridge[17]. In an attempt to understand the binding nature of few biologically important metal ions with a DNA fragment using molecular modeling, we could observe that Li^+, Na^+ and

K^+ ions, can interact both in an outer and inner sphere manner, which in turn depends on the charge of the DNA fragment (see Chapter 2B for the details).

A recent study carried out by Wilson and co-workers on MD simulations of 10 ns and longer on DDD (Dickerson-Drew dodecamer with sequence CGCGAATTCGCG)[18], and by Feig and Pettitt on the DNA duplex (A5G5)•(C5T5)[19], with Na^+ as the counter ion observed a correlation between the entrance of Na^+ into the minor groove and groove narrowing. It was also noted that the geometry of Na^+ coordination in the minor groove could vary significantly depending upon the exact position of the cation. Wilson and co-workers also observed that Na^+ does not have to penetrate deep inside the minor groove in order to cause groove narrowing, as previously believed[20]. The minor groove may actually be narrowest when Na^+ is at the outer edge of the groove, where it makes direct contact (inner sphere coordination) with phosphate oxygens[21].

The LC phase behavior of DNA, however, is known to be largely influenced by the counter ion type and concentration because the effective particle radius and hence the effective axial ratio and excluded volume of DNA are determined by the counter ion shielding. It has been shown that DNA gets transformed from an isotropic to anisotropic LC phase after a critical concentration (C_D) of DNA and counter ion. According to Flory, C_D depends on the axial ratio of the molecule, (axial ratio = L/d)[22]. Dielectric constant of the medium, polymer-solvent interaction parameter (including influence of secondary forces such as hydrogen bonding), molecular parameters such as

persistence length and effective diameter of the molecule are shown to influence the phase behavior[23]. There are, however, a large number of closely related parameters yet to be studied to understand the nature, stability, texture and the influence of various environmental factors on the structure and stability of the LC phase(s) of DNA. Currently, the effects of ionic size, ionic charge, and complexation conditions of the counter ions on phase formation of high molecular weight of DNA are not known. In addition, solvation conditions, rate of evaporation, surface properties of solids, and polydispersity of DNA are expected to influence the phase behavior of LC DNA. In an attempt to understand some of these parameters on the induction and stabilization of LC DNA, in the presence of alkali metal ions, the behavior of DNA in the presence of Li^+ ion, was quite interesting. Li^+ ions stabilize the LC phases of DNA, especially the biphasic cholesteric-columnar arrangement. Highly stable DNA mesophases may find applications in the field of nanoelctronics[24], in designing units[25] and in DNA chips[26]. This chapter deals with the effects of alkali metal ions such as Li^+, Na^+, K^+, Rb^+ and Cs^+, on the LC organization of high molecular weight DNA.

2.A.3. Experimental Section

A) ***Preparation of Samples****:* Calf Thymus DNA was purchased from Worthington Biochemical Corporation, Freehold, NJ, USA, and has been used without further purification. The weight average molecular weight of DNA was 6×10^6. Autoclaved millipore water was used as the medium in all the experiments. DNA was dissolved in 0.1M NaCl (pH 7). The dissolved DNA

was then dialysed against NaCl (0.1M) 3-4 times. The observed A_{260}/A_{280} ratio of the DNA solution was 1.88, indicating that the DNA was free of protein contamination. The concentration of calf thymus DNA was determined by measuring the absorbance at 260 nm, using the molar extinction coefficient (Є) of 6900 per M/cm. The final concentration of DNA was 7.143 mg/ml. LiCl, NaCl, KCl, RbCl and CsCl of analytical grade were used for our experiments.

The LC behavior of Calf Thymus DNA was studied under the following conditions: (1) Varying DNA concentration, keeping the concentrations of metal ions constant, to arrive at the critical DNA concentration in the presence of each ions; and (2) Varying the metal ion concentration, while keeping the DNA concentration fixed, to examine the effect of different metal ion concentrations on the LC organization of DNA.

B) ***Polarized Light Microscopy***: Microscopic glass slides and coverslips were soaked in chromic acid and further rinsed with deionised water and dried using analar acetone prior to use. Desired concentrations of metal ion and DNA solutions were mixed in an eppendorf tube, and vortexed for 15 minutes and were then allowed to equilibrate at room temperature (26 °C) for two hours. 20 µL of each metal ion DNA solution was sandwiched between a clean microscopic glass slide and a cover slip, and the cover slips were then sealed with DPX mountant (a neutral solution of polystyrene and plasticizers in xylene used in microscopy work, M/s Nice Chemicals Ltd., Mumbai) to prevent the dehydration of the sample[27,28]. The preparations were then incubated at 37°C for extended time periods to observe the phase changes until

crystallization or complete darkening (isotropization) occurred. The preparations were monitored periodically for phase changes under a Nikon Optiphot Polarized Light Microscope equipped with a Nikon camera and photographs were taken when the phases became prominent and distinct. The phases and granular boundaries were clear and sharp when the sample was incubated at 37°C. A triplicate of each sample was made to ensure the reproducibility of the phase changes. The results were reproducible in three sets of separate experiments. The following parameters were noted: (a) C_D – critical DNA concentration required to exhibit anisotropy, (b) T_{tr}- Time required for cholesteric to columnar phase transition (c) T_{iso}- Time required for the LC phases to darken and disappear ie isotropization.

C) ***FTIR Spectra:*** DNA-metal complexes were precipitated using ethanol, and the precipitates were centrifuged and dried, for recording the IR spectra[29,30]. IR spectra were recorded in a Shimadzu IR spectrophotometer, using the KBr pellet technique.

D) ***Circular Dichroism Measurements:*** Circular Dichroism (CD) spectra[31] of dilute DNA solutions were obtained with a Jasco-715 spectropolarimeter using a quartz cuvette of 1 cm path length.

Also, several attempts were made to obtain X-ray diffraction data, which faced problems in obtaining the required birefringence (even after keeping the sample filled in the capillary in an oven set at 37^0C for long periods) for the instrument to make measurements. Probably, it must be the difficulty with the high molecular weight DNA system in anchoring/ordering of the long DNA

molecules when sandwiched between the glass slide and cover slip and within the capillary where the sample is filled.

2.A.4. Results and Discussion

It has been shown that low molecular weight DNA, exhibits a complex and polymorphic behavior, in the presence of monovalent counter ions such as sodium and potassium[28,32-34]. At low concentrations (<1mg/ml), DNA molecules are randomly oriented and the solution is a classical *isotropic liquid*. As the concentration gets higher (>1mg/ml), the molecules order in the liquid and transform into a liquid crystal of the "*cholesteric type"*. At still higher concentrations (160mg/ml), the DNA turns itself into a "*columnar hexagonal"* phase[28,32-34]. Similar effects have been reported on neutralization of DNA with certain organic cations[35-38]. The role of other alkali metal ions on the induction and stabilization of LC phase of high molecular weight DNA is not well understood. One of the earlier report on high molecular weight DNA and polyamines, showed that LC phases of DNA can be obtained at a lower concentration than that required for low molecular weight DNA[36].

Table 2.A.1 shows the effect of alkali metal ions on the induction of LC phase behavior of DNA. It can be noted that all of the alkali metal ions, except Li^+, induced LC phase at a critical DNA concentration of 0.89 mg/ml (Fig.2. A.1)[39]. However, LC textures of DNA occurred only at a concentration of 3.75 mg/ml in the presence of 1 M of Li^+ ion concentration ($C_D\ Li^+ > C_D\ Na^+ = C_D\ K^+ = C_D\ Rb^+ = C_D\ Cs^+$). It appears that up to a concentration of 3.75 mg/ml of DNA, liquid crystallinity of DNA is blocked by the Li^+ ion.

Table 2.A.1. LC textures obtained when DNA concentration was varied keeping metal ion concentrations fixed (1M).

DNA Concn. Mg/ml	LiCl (1M)	NaCl (1M)	KCl (1M)	RbCl (1M)	CsCl (1M)
7.14	Nematic Schleiren Textures.	Cholesteric planar	Cholesteric and columnar hexagonal	Cholesteric and herring bone like texture	Iridiscent Cholesteric Texture
3.57	Isotropic	Cholesteric	Cholesteric Oily streak and finger print pattern	Columnar hexagonal turning to crystal phase.	Cholesteric, columnar hexagonal
1.79	Isotropic	Cholesteric	Cholesteric	Columnar hexagonal turning to crystal phase.	Cholesteric
0.89	Isotropic	Isotropic	Isotropic	Isotropic	Isotropic
0.45	Isotropic	Isotropic	Isotropic	Isotropic	Isotropic
0.22	Isotropic	Isotropic	Isotropic	Isotropic	Isotropic

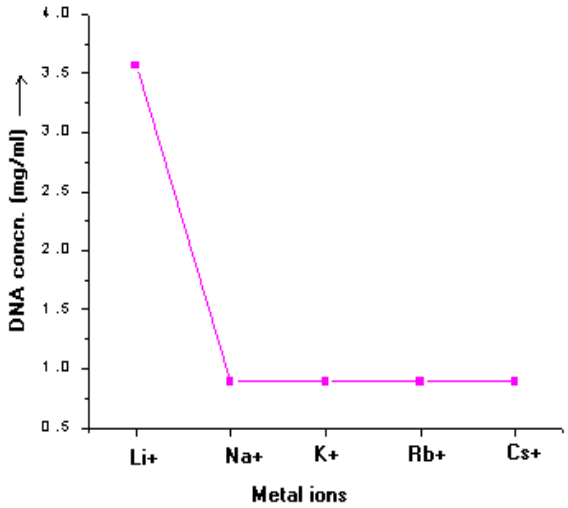

Fig.2.A.1. Critical DNA concentration required for anisotropy in the presence of alkali metal ions

At higher DNA concentration, a fluidic and birefringent cholesteric like phase (Fig.2.A.2.a) was formed initially on which periodic nematic schlieren

like texture with two pointed black brushes appeared slowly (Fig.2.A.2.b). Nematic textures revealed by the presence of two branch brush defects are quite rare and probably correspond to the cholesteric phase, in which the twist is prevented by anchoring defect on the glass slides. On prolonged incubation at room temperature (26°C), the same phase transformed into an iridescent cholesteric phase with finger print pattern, embedded with the undulations typical of the columnar hexagonal phase[36](Fig.2.A.2.d). These phases coexisted and remained stable for more than two months (T_{iso}> 2 months). In most of the earlier studies, LC phase transitions were observed as a function of concentration, but in the present study, sample evaporation is prevented by sealing it with a neutral solution of plasticisers and xylene. It should be noted here that the changes observed in the LC textures in the present investigation is a consequence of time-dependent reorganization of the DNA strands in the presence of metal ions. The unusual stability of the mesophase of DNA observed in the presence of Li^+, might be due to the fact that Li^+ ion can help the DNA molecules in the LC phase to maintain the moisture content around it, as it has a higher hydration energy (Table.2.A.2)[40]. Earlier studies indicate that the induction of LC phase and the state of hydration of DNA are inter-related. Thus, counter ion binding to DNA is associated with the removal of water molecules[8] from neighboring DNA strands, which brings ordered alignment of DNA molecules.

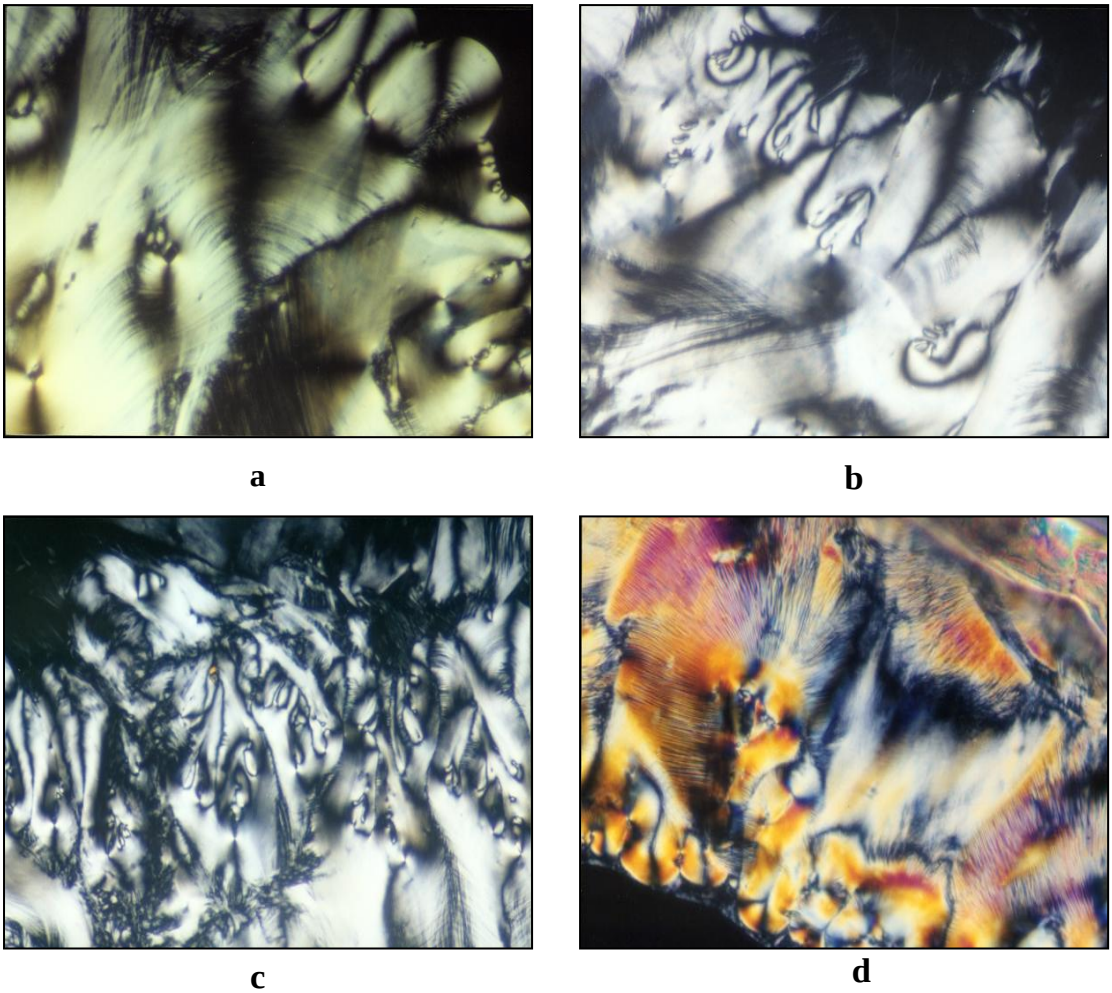

a **b**

c **d**

Fig.2.A.2. LC phases of high molecular weight DNA obtained in the presence of alkali metal ions. a) Cholesteric phase formed in presence of Li^+ ion (1M) after 2 hours of incubation at 37^{o}C. b) Nematic schleiren like texture obtained in presence of Li^+ ion after 5 hours of incubation at 37^{o}C. c) Two brush defects of the nematic texture increased after 24 hours of incubation at 37^{o}C. d) The same phase after 2 days changed to a biphasic texture with cholesteric finger print pattern and undulations typical of columnar phase. This remained stable for more than two months. Mag.10X. Concentration of DNA dissolved in 0.1 M NaCl (pH 7) is ~4 mg/ml.

Table 2.A.2. Hydration energies of alkali metal ions[40].

Metal ion	Enthalpy of hydration (kJ/mol)
Li^+	-519
Na^+	-406
K^+	-323
Rb^+	-293
Cs^+	-264

Different textures of the LC phase arise, due to such packing or alignment of DNA molecules in space. Numerous indirect and direct experimental data on the interaction between DNA and Li^+ in aqueous solution show that Li^+ has some specific binding mode in its interaction with DNA[41-52]. It is reported that specific binding of Li^+ to the DNA double helix is followed by partial Li^+ dehydration. Li^+ ions bind to the phosphate groups of DNA, and complexation of Li^+ with N7 of guanine, accessible from the major groove of B-form DNA also may takes place[44]. The higher stability of B form of Li-DNA, in comparison to the other forms of DNA, in the B-A transition of the polynucleotides, supports this hypothesis.

According to recent molecular dynamic studies, Li^+ ions bind predominantly to DNA phosphate oxygen atoms and are capable of making stable ion pairs without disrupting water spine around DNA which contribute significantly to the stabilization of the B-form[53]. However, it is well known that dehydration is essential for the induction of LC phases in DNA. Li^+ is also

reported to bind DNA through a water bridge and our molecular modeling studies (See Chapter 2B) also indicated that Li^+ ion binds to DNA in an outer sphere mechanism, which does not favor the dehydration of DNA strands. However the reports regarding Na^+, K^+ Rb^+ and Cs^+ ions; and our molecular modeling studies (See Chapter 2 B) indicate that these ions bind to DNA in an inner sphere manner, which could be due to their large difference in hydration energy compared to those of Li^+ ions (see Table 2.A.2). Inner sphere binding mode can facilitate the dehydration of DNA, which explains the reason for higher C_D in the presence of Li^+ ions, compared to that with Na^+, K^+, Rb^+ and Cs^+ ions. It should also be pointed out here that Li^+ has the highest affinity for DNA in aqueous solutions, in terms of counter ion interactions[54].

Table 2.A.3 presents the LC behavior of high molecular weight DNA in the presence of varying alkali metal ion concentration. DNA showed cholesteric textures (Fig.2.A.3.a and b) initially, irrespective of the metal ion concentrations, which later on turned to a more ordered columnar phase, but the rate of phase transition from lower ordered cholesteric to higher ordered columnar (T_{tr}) differed from ion to ion (Fig.2.A.4.a-e). The spontaneous flow and finger print patterns of the LC phase, are characteristic of cholesteric arrangement[55-57], whereas the herring bone texture with restricted fluidity, is typical of columnar hexagonal phase[57](Fig.2.A.3). In some cases, cholesteric phase with characteristic tear shaped defects[58] were also observed (Photograph not shown).

Table 2.A.3. LC phases obtained when metal ion concentration was varied keeping DNA concentration (7.143 mg/ml) fixed.

Metal ion concn.	LiCl	NaCl	KCl	RbCl	CsCl
1M	Nematic Schleiren Textures	Cholesteric	Cholesteric and two brush like defects at some regions	Cholesteric+ Columnar hexagonal	Cholesteric+ Columnar hexagonal
0.75 M	Nematic Schleiren Textures.	Cholesteric	Cholesteric	Cholesteric+ Columnar hexagonal	Cholesteric+ Columnar hexagonal
0.5M	Iridescent Cholesteric With Banded patterns	Cholesteric	Cholesteric	Cholesteric+ Columnar hexagonal	Cholesteric+ Columnar Hexagonal
0.13M	Iridescent Cholesteric With Banded Patterns	Cholesteric	Cholesteric	Cholesteric Banded like	Cholesteric+ Columnar hexagonal
0.03M	Iridescent Cholesteric With Banded Patterns	Cholesteric	Cholesteric	Cholesteric	Cholesteric+ Columnar hexagonal

Fig.2.A.4 shows the time dependent phase transitions of DNA in the presence of alkali metal ions. It can be seen from Fig.2.A.4 that the transition from cholesteric to columnar phase is dependent on the size of the ion ($T_{tr}\ Li^+ < T_{tr}\ Na^+ < T_{tr}\ K^+ < T_{tr}\ Rb^+ < T_{tr}\ Cs^+$). The transition is faster at high metal ion concentrations, and when the size of the ion is larger. Thus, in the cases of Rb^+ and Cs^+, the transition occurred within few hours (after ~ 3 hrs.) giving rise to textures typical of columnar hexagonal phase (Fig.2.A.3.c) and the phases remained stable for 2-3 days (Fig.2.A.4). A behavior similar to this phase

transition was reported in the case of DNA condensation in the presence of spermine, spermidine and its N^4-methyl spermidine[36]. As the charge density increased in the cases of spermine, spermidine and its N^4-methyl derivative, the phase transition from cholesteric to columnar phase took only few hours for spermidine, whereas in the case of spermine and its N^1-acetyl derivative the time taken for transformation was around 12-48 h[36].

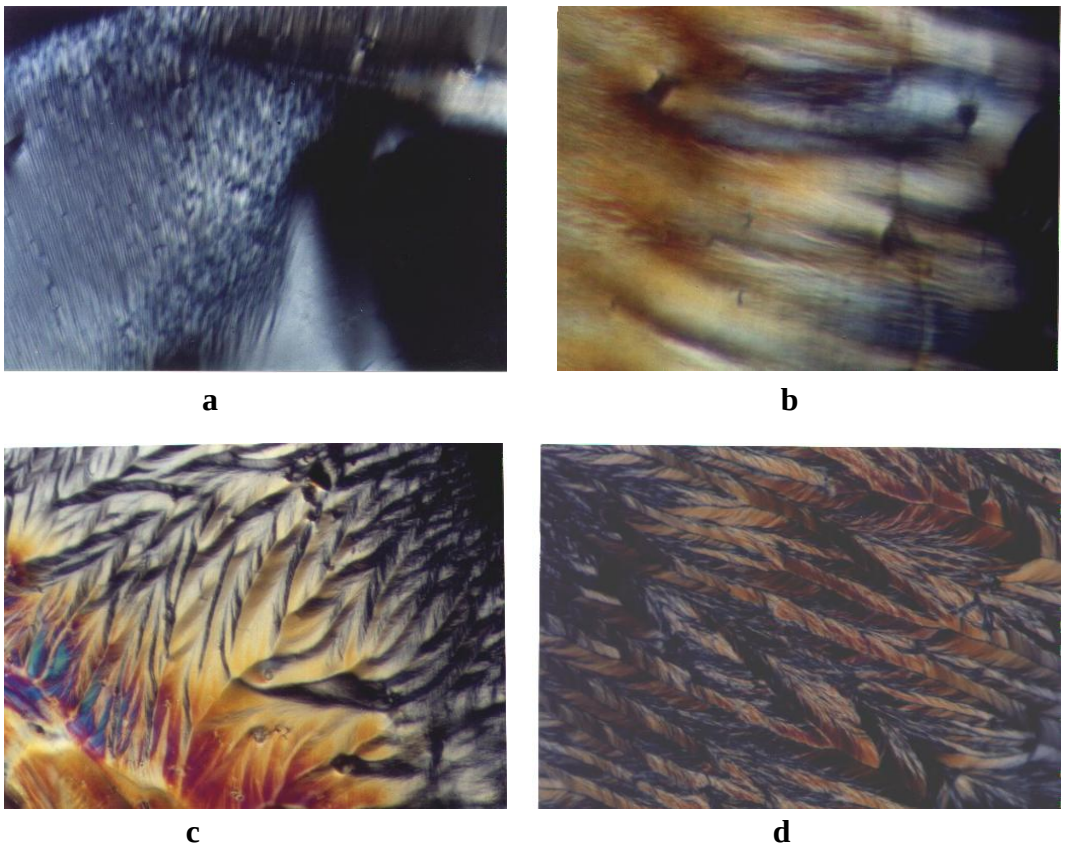

a **b**

c **d**

Fig.2.A.3. LC phases of high molecular weight DNA obtained in the presence of alkali metal ions. a and **b** shows the cholesteric blue phase and cholesteric finger print pattern of DNA in the presence of Na^+ and K^+ (0.5M) obtained after 3 hours of incubation at 37^{o}C. **c** and **d** shows the herring bone pattern of the columnar hexagonal phase of DNA in presence of Cs^+ and Na^+ (1M) respectively. Concentration of DNA dissolved in 0.1 M NaCl (pH 7) is ~4 mg/ml. Mag.10X. All the phases were obtained under controlled conditions.

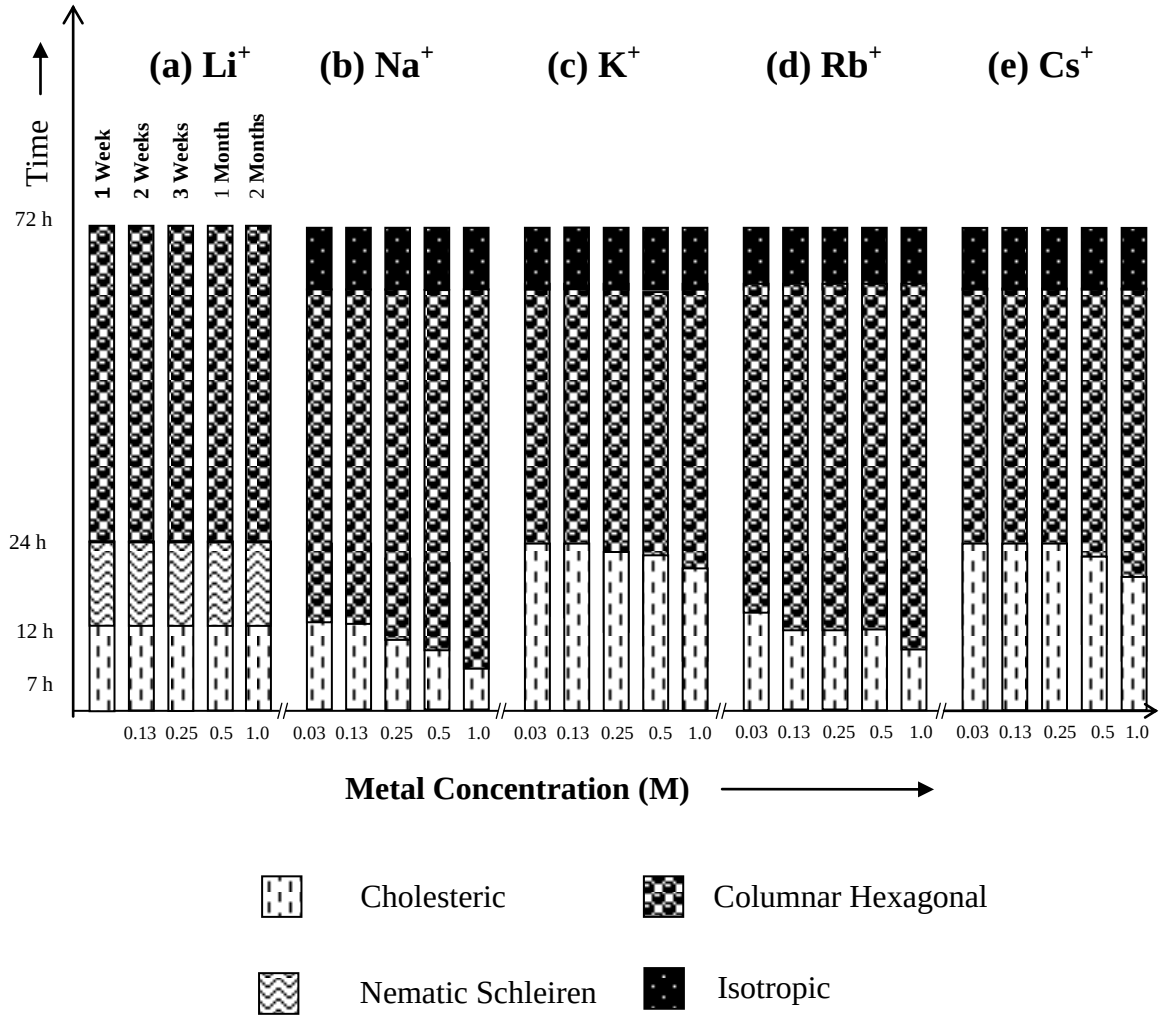

Fig.2.A.4. Time dependent phase transitions of LC DNA (7.14 mg/ml) in the presence of alkali metal ions [(a) Li^+, (b) Na^+, (c) K^+, (d) Rb^+ and (e) Cs^+] (Y-axis Scales are not fixed arbitrary units).

Table 2.A.2 shows that the level of hydration decreases as the size of the ion increases, hence the least hydrated ions dehydrates DNA favoring rapid phase transition from less ordered cholesteric to higher ordered columnar hexagonal phase.

The alkali metal ions are known to stabilize the DNA by interacting with the negatively charged phosphate moieties[59]. The binding sites of the alkaline

earth metal ions on DNA were probed using IR spectra and CD measurements. CD profiles of DNA after adding the alkali metal ions are given in Appendix Fig.2. Absence of shift in absorbance indicates that the binding of the metal ions were purely to phosphates and not to bases. CD experiments could be carried out only with the dilute solutions of DNA and there was no significant deviation from the B-conformation. It should be noted that the LC phases occur only at higher DNA concentrations, which could not be done due to the instrumental limitations. The IR spectra obtained for alkali metal-DNA complexes were similar to that of DNA without metal ions, except a slight shift of 1-2 cm^{-1}, and an increase in intensity in the phosphate region 1223 cm^{-1} [60] which supports the phosphate binding nature of alkali metal ions (The IR spectra are given in the appendix, Fig.1 A).

2.A.5. Conclusions

In summary, the results of the present study indicate that the overall phase behavior of DNA is polymorphous, exhibiting highly birefringent domains, indicating a supramolecular ordering of DNA. LC phases of DNA are generated at concentrations that are far less than that required for low molecular weight (150 bp length) DNA fragments. Alkali metal ions, except Li^+, exhibit similar effects in terms of critical DNA concentration. The observed differences between Li^+ and other alkali metal ions, can be explained on the basis of its outer sphere binding to DNA and higher hydration factor. An unusual stability was observed for the LC phases of DNA in presence of Li^+, which could be due to higher water retaining capability of Li^+ ions. DNA

initially showed cholesteric textures in the presence of all alkali metal ions, which later on turned to a higher ordered columnar phase, but the cholesteric-columnar transition, was facilitated by increased size of the ion. The higher stability imparted by Li^+ ions to LC DNA may find applications, in the field of nanolectronics, in designing biosensing units, and in DNA chips.

2.A.6. References

1. Robinson, C., *Tetrahedron,* **1961,** 13, 219.
2. Livolant, F., *Eur. J. Cell Biol.* **1984,** 33, 300.
3. Bouligand, Y.; Soyer, M. O.; Dao, P., *Chromosoma* **1968,** 24, 251.
4. Rill, R. L.; Livolant, F.; Aldrich, H. C.; Davidson, M. W., *Chromosoma* **1989,** 98, 280.
5. Koltover, I.; Wagner, K.; Safinya, C. R., *Proc. Natl. Acad. Sci.* **2000,** 97, 14046.
6. Minton, A. P., *Biopolymers* **1981,** 20, 2093.
7. Livolant, F.; Leforestier, A., *Prog. Polymer Sci.* **1996,** 21,1115.
8. Anastassopoulou, J., *J. Mol. Str.* **2003,** 19, 651.
9. Glusker, J. P., *Adv. Protein Chem.* **1991,** 42, 1.
10. Misra, V. K.; Draper, D. E., *Biopolymers,* **1998,** 48, 113.
11. Chiu, T. K.; Dickerson, R. E., *J. Mol. Biol.* **2000,** 301, 915.
12. Howerton, S. B.; Sines, C. C.; VanDerveer, D.; Williams, L. D., *Biochemistry* **2001,** 40, 10023.
13. Tereshko, V.; Wilds, C. J.; Minasov, G.; Prakash, T. P.; Maier, M. A.; Howard, A.; Wawrzak, Z.; Manoharan, M.; Egli, M., *Nucleic Acids Res.* **2001,** 29, 1208.
14. Sigel, H., *Metal-DNA Chemistry*. T.D. Tullius (Ed.) ed.; American Chemical Society: Washington, DC, 1989.
15. Tereshko, V.; Wilds, C. J.; Minasov, G.; Prakash, T. P.; Maier, M. A.; Howard, A.; Wawrzak, Z.; Manoharan, M.; Egli, M., *Nucleic Acids Res.* **2001,** 29, 1208.
16. Stelwagen, N. C.; Magnusdottir, S.; Gelfi, C.; Righeti, P. G., *J. Mol. Biol.* **2001,** 305, 1025.
17. Zheng, J.; Li, Z.; Wu, A.; Zhou, H., *Biophysical Chemistry* **2003,** 104, 37.
18. Hamelberg, D.; McFail-Isom, L.; Williams, L. D.; Wilson, W. D., *J Am Chem Soc* **2000,** 122, 10513.
19. Feig, M.; Pettitt., B. M., *Biophys. J* **1999,** 77, 1769.

20. Shui, X. Q.; Sines, C; McFail-Isom, L; VanDerveer, D; Williams, L. D., *Biochemistry* **1998,** 37, 1677.
21. Hud, N. V.; Polak, M., *Current Opinion in Structural Biology* **2001,** 11, 293.
22. Flory, P. J., *Proc. R. Soc. Lond. Ser. A,* **1956,** 234, 73.
23. Davidson, M. W.; Strzelecka, T. E.; Rill, R. L., *Nature* **1988,** 331, 457.
24. Tabata, H.; Cai, L. T.; Gu, J. H.; Tanaka, S.; Otsuka, Y.; Sacho, Y.; Taniguchi, M.; Kawai, T., *Synthetic metals* **2003,** 133-134, 469.
25. Yevdokimov, Y. M.; Salyanov, V. I., *Biosensors & Bioelectronics* **1996,** 11, (9), 889.
26. Cognard, J., *Mol. Cryst. Liq. Cryst. Suppl.* **1982**, 1.
27. Pelta, J., Jr; Durand, D.; Doucet, J.; Livolant, F., *Biophys. J.* **1996,** 71, 48.
28. Strzelecka, T. E.; Rill, R. L., *Biopolymers* **1990,** 30, 57.
29. Tu, A. T.; Reinosa, J. A., *Biochemistry* **1966,** 5, 3375.
30. Sutherland, G. B. B. M.; Tsuboi, M., *Proc. Royal Soc. London* **1957,** 239, Ser.A., 446.
31. Besik, K. I., *Biophysical Chemistry* **2000,** 84, 227.
32. Livolant, F.; Leforestier, A., *Prog. Polymer Sci.* **1996,** 21, 1115.
33. Leforestier, A.; Livolant, F., *Biophys. J.* **1993,** 65, 56.
34. Rill, R. L.; Hilliard, P. R.; Jr; Levy, G. C., *J. Biol. Chem* **1983,** 258, 250.
35. Leforestier, A.; Fudaley, S.; Livolant, F., *J. Mol. Biol.* **1999,** 290, 481.
36. Saminathan, M.; Thomas, T.; Shirahata, A.; Pillai, C. K. S.; Thomas, T. J., *Nucl. Acids. Res* **2002,** 30, 3722.
37. Raspaud, E.; Olvera de la Cruz, M.; Sikorav, J. L.; Livolant, F., *Biophys. J.* **1998,** 74, 381.
38. Raspaud, E.; Chaperon, I.; Leforestier, A.; Livolant, F., *Biophys J* **1999**, 1547.
39. Sundaresan, N.; Thomas, T.; Thomas, T. J.; Pillai, C. K. S., *Macromol. Biosci.* **2006,** 6, 27.

40. Cotton, A.; Wilkinson, G. *Advanced Inorganic Chemistry*; Wiley Interscience: Canada, 1996.
41. Gruenwedel, D. W.; Hsu, C. H.; Lu, D. S., *Biopolymers* **1971,** 10, 47.
42. Ivanov, V. I.; Minchenkova, L. E.; Schyolkina, A. K.; Poletaev, A. I., *Bioploymers* **1973,** 12, 89.
43. Korolev, N. I. *Ph.D Thesis* Moscow, 1985.
44. Korolev, N. I.; Vlasov, A.P.; Kuznetsov, I.A, *Biopolymers* **1994,** 34, 1275.
45. Kuznetsov, I. A.; Gorshkov, V. I.; Ivanov, V. A.; Kargov, S. I.; Korolev, N. I.; Filipov, S. M.; Khamisov, R. K., *Reactive Polym.* **1984,** 3, 37.
46. Kuznetsov, I. A.; Kargov, S. I.; Khamisov, R. K.; Gorshkov, V. I., *Molek. Biolog.* **1983,** 18, 1569.
47. Kuznetsov, I. A.; Meznetsev, A. I.; Gurunovich, A. K., *Biofizika,* **1968,** 13, 20.
48. Kuznetsov, I. A.; Meznetsev, A. I.; Moshkovskii, Y. S.; Lukanin, A. S., *Biofizika,* **1967,** 12, 373.
49. Kuznetsov, I. A.; Yachmenyov, V. V.; Belousov, P. S.; Pishonkov, A. G.; Shagalov, L. B.; P., V. Y., *Molek. Biolog*, **1976,** 10, 270.
50. Manning, G. S., *Biopolymers* **1981,** 20, 2337.
51. Manning, G. S., *J. Phys. Chem.* **1984,** 88, 6654.
52. Record, M. T.; Woodburry, C. P.; Lohman, T. M., *Biopolymers,* **1976,** 15, 893.
53. Korolev, N. *Biomacromolecules* **2000**, 1, 648.
54. Lyubartsev, A. P.; Laaksonen, A. J., *Biomol. Struct. Dyn.* **1998,** 16, 579.
55. Pelta, J.; Livolant, F.; Sikorav, J. L., *J. Biol. Chem.* **1996,** 271, 5656.
56. Hud, N. V.; Downing, K. H., *Proc. Natl Acad. Sci. USA,* **2001,** 98, 14925.
57. Livolant, F.; Leforestier, A., *Prog.Polym.Sci.* **1996,** 21, 1115.
58. Pelta, J.; Jr; Durand, D.; Doucet, J.; Livolant, F., *Biophys. J.* **1996,** 71, 48.
59. Anastassopoulou, J., *J. Mol. Str.* **2003,** 651-653, 19.

60. Andrushchenko, V. V.; Kornilova, S. V.; Kapinos, L. E.; Hackl, E. V.; Galkin, V. L.; Grigoriev, D. N.; Blagoi, Y. P., *J. Mol. Str.* **1997,** 408-409, (1), 225.

CHAPTER 2B

A BASE-SUGAR-PHOSPHATE THREE- LAYER ONIOM MODEL FOR CATION BINDING: BINDING AFFINITIES OF ALKALI METAL IONS FOR PHOSPHATE GROUP IN DNA

2.B.1. Abstract

The binding of hydrated Li^+, Na^+ and K^+ ions with a DNA fragment containing two phosphate groups, three sugar units and a G⎯C base pair was modeled in the anion (one negative charge) and dianion states (two negative charges) using a three layer ONIOM approach. Among the three metal binding combinations (outer sphere, inner sphere mono- and bi-dentate) studied, an outer sphere binding mode was the most stable structure observed for Li^+ ions in the anion model, and inner sphere bi- and mono-dentate binding modes for the Na^+ and K^+ ions respectively. However, in the dianion model, Li^+ and Na^+ and K^+ preferred inner sphere monodentate and outer sphere structures respectively. The present data on the binding behavior of Li^+, Na^+ and K^+ ions to the anion model of DNA and the higher affinity of Li^+ ions for DNA compared to Na^+ and K^+ ions were in good agreement with the experimental findings. The anion model, hence revealed a more realistic picture about DNA-alkali metal ion interactions, compared to the dianion model where the net charge on the system is not neutral. The charge of the DNA fragment appeared

to be crucial in deciding the binding strength and binding mechanisms of the metal ions. The outer sphere binding of Li^+ ion to the anion model of DNA is a point of support to the unique LC behavior of DNA in the presence of Li^+ ion. The inner sphere-binding mode of Na^+ and K^+ dehydrates DNA by establishing direct contact with it, which explains the lower C_D in the presence of Na^+ and K^+ compared to those with Li^+ ions.

2.B.2. Introduction

DNA, a highly anionic polyelectrolyte, is always stabilized in the cell nucleus by an array of cationic species, including metal ions. Metal cations are known to play a crucial role in both stabilizing and destabilizing the DNA double helix[1-4]. They can coordinate DNA at several sites of which the major sites are the phosphate groups, the sugar moiety, the base keto oxygens (O2 of thymine and O6 of guanine on the interior of the double helix), and the ring nitrogens (N7 of adenine and guanine on the exterior, N3 of adenine and guanine (see Fig.2.B.1). The affinity of a cation for a specific site on a polynucleotide is a general function of its charge, hydration-free energy, coordination geometry and coordinate bond-forming capacity[5,6]. Both the alkali and alkaline earth metal ions stabilize the DNA predominantly by neutralizing the negatively charged sugar-phosphate backbone[7-9]. Coordination of phosphate moieties by cations is essential for catalytic enzymatic reactions, the processes involving the transfer of genetic information, the synthesis of oligonucleotides etc.[10,11] and it can also stabilize the LC phases of DNA.

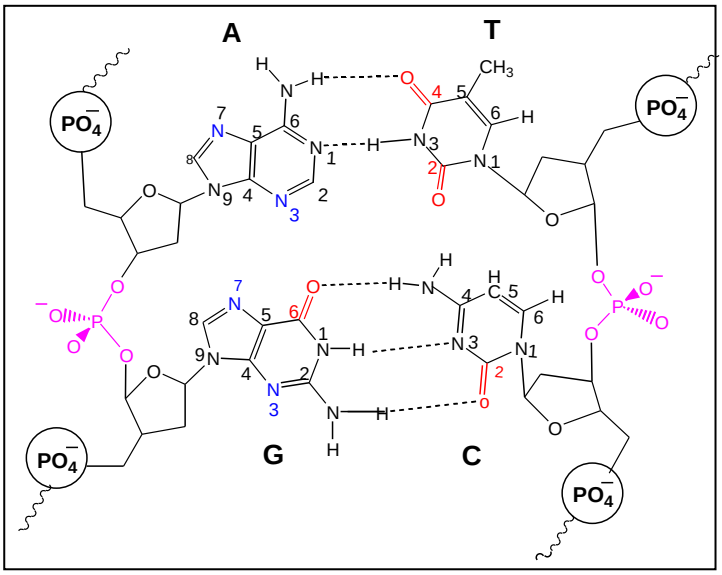

Fig.2.B.1. Schematic diagram of A-T and G-C base pairs of DNA linked by phosphate groups.

The DNA-metal ion interactions are governed by several parameters such as the nature of the metal, its size and charge which influence the conformation of DNA, by direct or indirect interaction through the water molecules with the basic sites of the nucleotides[12]. As monovalent cations are generally less strongly solvated than divalent cations, they tend to interact with DNA purely electrostatically, without making hydrogen bonds from metal-coordinated water molecules[13].

Theoretical studies performed by Sponer et al.[14-19] on small model systems such as isolated bases, base pairs, nucleotides with solvated metal ions and by Petrov and co-workers[20-22] on dimethyl phosphate anion with solvated metal ions, and by other groups[23-30] have shed new insights into metal binding to nucleic acids. In native DNA, the electronegative oxygen atoms of the

phosphate group are projected towards the exterior of the double helix, and the small models are largely ineffective in replicating such geometrical constraints.

So, it was thought worthwhile to study a model system, where negative oxygen atoms of the phosphate group project towards the exterior, which would be more comparable to the native DNA structure. In the present study, the selected model is a guanine-cytosine base pair region (G-C region), which also contains the related two sugar units (one connected to the guanine fragment and the other connected to cytosine fragment) and the associated two phosphate groups (one free anionic phosphate group at the cytosine end, which is the anion model). Because of the structural restrictions imposed by the sugar units, we hope that in the present model, the phosphate geometry will be maintained as in native DNA. As DNA is a highly anionic polyelectrolyte, the negative charge is in excess on DNA segments and all the theoretical studies reported so far are based on anion models only, which cannot adequately represent this excess negative charge effect. In fact in such models, the interaction of a mono cation with a dimethyl phosphate anion model would give a neutral system. To compare the effect of excess charge on DNA fragment on the interactions of alkali metal ion to DNA, besides the anion model, a dianionic model possessing two negative phosphate ends were also selected for the present study. Thus, the selected model systems (the anion and dianion models) appear to be more comparable to DNA structure than that of dimethyl phosphate anion and other models used so far in theoretical studies, and hence are expected to give a more realistic picture of metal-DNA

phosphate binding. As negatively charged phosphate groups are the major contributors to the polyanionic nature of DNA macromolecule, the present chapter is mainly focused on the interaction of metal ions such as Li^+, Na^+ and K^+ ions with the phosphate groups of a DNA fragment, using a three-layer ONIOM method.

2.B.3. Computational Details and Models

2.B.3.1. *A three- layer ONIOM Model*

In this work, a three layer ONIOM (Our Own N-Layered Integrated Molecular Orbital) method, developed by Morokuma and co-workers[31-33] was utilized to study the metal ion interactions with the DNA segment. The ONIOM method, allows the partitioning of a large chemical system into layers, and each layer can be treated at a different computational level. The underlying idea is that each of the various parts of the system plays its own role in the process under investigation, and therefore requires different accuracies. By this method, very accurate calculations can be carried out at a reasonable computational cost. ONIOM is a general hybrid method, which can combine any number of molecular orbital as well as molecular mechanics methods, and it is reported to be an efficient tool for accurately calculating chemical interactions in large systems[34,35]. In the ONIOM calculations, the molecular system, which is divided into layers or parts, is called the *real system*. The most important part of the molecule (reaction center) is called the *model system*, and is described at the highest level of theory.

In the present study, a typical system used for ONIOM calculation is given in Fig.2.B.2. According to the ONIOM terminology, the model HPSG_CSP$^-$_M_{hyd} is divided in to three layers, viz. (i) a high layer, (ii) medium layer and (iii) low layer, which are illustrated in Fig.2.B.2. Its high-level model system includes the anionic phosphate group and the hydrated metal. Base pairs, the phosphate and the sugar groups at the guanine end are treated at the medium level of theory and the two sugar moieties attached to the metal linked phosphate group are treated at the low level of theory. For the high layer, the hybrid density functional B3LYP (Becke-Lee-Yang-Paar) method[36,37] in conjunction with the standard 6-31G(d) basis set, was employed[38]. The medium layer was treated with the semi-empirical PM3 (Parameterized Order Number 3) method[39]. The low layer of the system is treated using the UFF (Universal Force Field) method of MM (Molecular Mechanics)[40]. We name this model as the anion model; HPSG**…**CSP$^-$**…**M_{hyd}, where HP stands for the protonated phosphate group at the guanine end, SG for the sugar and the connected guanine, the doted line indicates the hydrogen bond interaction between the guanine and cytosine, CSP$^-$ for the cytosine and the connected sugar units and the phosphate anion, and M_{hyd} indicates the interaction of the hydrated metal with the phosphate anion moiety. If we use this anion model, in the case of alkali metals, the total charge on the interacting system will be zero. To study the effect of excess charge of DNA fragment on the alkali metal-DNA interactions, a dianion model was also selected, which is designated as $(H_2O)_2$**…**$^-$PSG**…**CSP$^-$. Here also an ONIOM approach similar

to the one in Fig.2.B.2 was used, wherein the P^- at the cytosine end is in the high level and the P^- at the guanine end is in the medium level. In order to have a realistic picture, the guanine end is micro solvated with a water dimer, which is also in the medium layer.

All the geometries were optimized, using this three-layer ONIOM method. For interaction energy calculations, structures of hydrated metal ions were also fully optimized at B3LYP/6-31G (d) level of theory. A bare anion $HPSG\_CSP^-$ and a bare dianion $^-PSG\_CSP^-$ structures without the hexahydrated metal ions were also located.

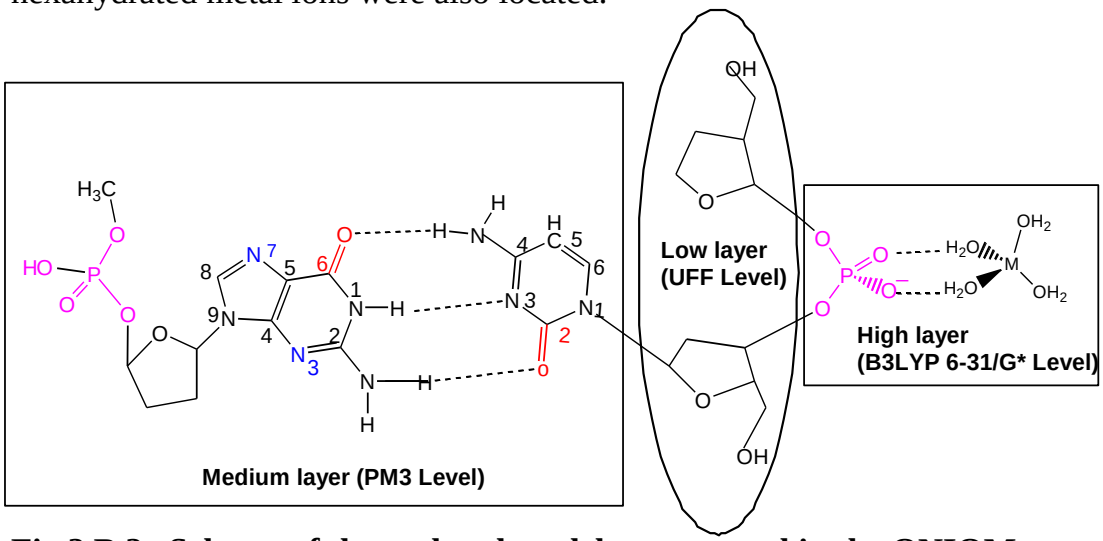

Fig.2.B.2. Scheme of the real and model system used in the ONIOM calculations for DNA-hydrated metal (outer sphere) interaction.

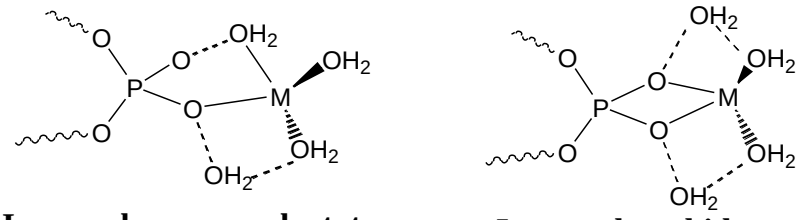

Inner sphere monodentate **Inner sphere bidentate**

Fig.2.B.3. Scheme of the different binding modes selected to study hydrated alkali metal ions and phosphate anion interactions.

In addition to the outer sphere-binding mode, given in Fig.2.B.2, the inner sphere mono- and bi-dentate binding modes (Fig.2.B.3) were also studied. In these models, one or two water molecules move(s) out from the tetra-hydrated shell of alkali metal ions (one for mono- and two for bi-dentate) to make room for the direct metal-phosphate oxygen bonds. Because of the computational limitations, we could not extend our studies with the other alkali metal ions.

2.B.3.2. *Interaction Energy Calculations*

In the present calculations, the following four geometry types were optimized, with a three-layer ONIOM method, viz.

(i) The bare anion HPSG…CSP^{-},

(ii) The bare dianion $(H_2O)_2$...$^{-}$PSG…CSP^{-}

(iii) Metal-Anion system, HPSG…CSP^{-}…$M(H_2O)_n$, and

(iv) Metal-Dianion system $(H_2O)_2$...$^{-}$PSG…CSP^{-}…$M(H_2O)_n$.

In type (i) and type (ii) geometries, the main interaction is between the bases G and C, while in type (iii) and (iv) structures, both base pair as well as the hydrated metal and phosphate anion interactions occur. Therefore, the following interaction energies (E_{int}) were estimated.

For G‿C base pair interaction energy in the bare anion,

$$E1 = E(HPSG) + E(CSP^{-}) - E(HPSG‿CSP^{-}) + E1_{BSSE} \quad (1)$$

For G‿C base pair interaction energy in the bare dianion,

$$E2 = E((H_2O)_2‿^{-}PSG) + E(CSP^{-}) - E((H_2O)_2‿^{-}PSG‿CSP^{-}) + E2_{BSSE} \quad (2)$$

For G‿C base pair interaction energy in the metal bound anion systems,

$$E3 = E(\textit{HPSG}) + E(\textit{CSP}^{-}\_ M_{hyd}) - E(HPSG\_CSP^{-}\_ M_{hyd}) + E3_{BSSE} \quad (3)$$

For G_C base pair interaction energy in the metal bound dianion systems,

$$E4 = E((\textit{H}_2\textit{O})_2\_^{-}\textit{PSG}) + E(\textit{CSP}^{-}\_ M_{hyd}) - E((H_2O)_2\_^{-}PSG\_CSP^{-}\_ M_{hyd})) + E4_{BSSE} \quad (4)$$

For metal ion_phosphate interaction energy in the anion systems,

$$E5 = E(HPSG\_CSP^{-}) + E(M_{hyd}) - E(HPSG\_CSP^{-}\_ M_{hyd}) + E5_{BSSE} \quad (5)$$

For hydrated metal ion_phosphate interaction energy in the dianion systems,

$$E6 = E((H_2O)_2\_^{-}PSG\_CSP^{-}) + E(M_{hyd}) - E((H_2O)_2\_^{-}PSG\_CSP^{-}\_ M_{hyd}) + E6_{BSSE} \quad (6)$$

E is the total energy of the systems given in parenthesis. In order to get a reasonable estimate of the E_{int} values, the single point energies of the ONIOM optimized structures of all the anionic (HPSG**…**CSP^{-}**…**M_{hyd}) and dianionic ($(H_2O)_2$**...**$^{-}$PSG**…**CSP^{-}**…**M_{hyd}) are calculated with the B3LYP/6-31G(d) level. Further, E values at B3LYP/6-31G(d) level are calculated for the fragment structures HPSG, $(H_2O)_2$...$^{-}$PSG, and CSP^{-} taken from their respective full systems. Names in regular font are of fully optimized ONIOM level structures and those in italics are of the fragment structures taken from the fully optimized systems. The $E1_{BSSE}$ to $E6_{BSSE}$ are the BSSE (Basis Set Superposition Error) corrections to be obtained by employing the counterpoise correction method of Boys and Bernardi[41]. The BSSE-corrected interaction energies were used for comparing the stability of different structures.

2.B.4. Results and Discussion

2.B.4.1. *Bare Anion and Dianion Models of DNA.*

The ONIOM level optimized geometries of the bare anion and dianion models are given in Fig.2.B.4.a and b, respectively. As expected, in the optimized structures, the P-O bonds that are not connected to the sugar units are projected outward with respect to the G-C pair. The steric effect imposed by these sugar units is mainly responsible for this structural feature. The low level of MM theory proved useful, particularly to treat the steric effect of these sugar units. Since there are no electrons in the MM layer, the phosphate group will not interact electronically with this layer and therefore large twisting of phosphate groups leading to phosphate…GC interaction is prevented. Therefore, it is felt that the optimized geometries in Fig.2.B.3.a and b would serve as good models for the phosphate…hydrated-metal ion interactions.

It may be noted that compared to the anion model, the hydrogen bonds especially those of $CO_{(G)}$ ⎯ $HN_{(C)}$ and $NH_{(G)}$ ⎯ $N_{(C)}$ interactions in the dianion model are slightly weaker. Further, the values of the ordered triplet ($CO_{(G)}$ ⎯ $HN_{(C)}$, $NH_{(G)}$ ⎯ $N_{(C)}$, $NH_{(G)}$ ⎯ $OC_{(C)}$) may be compared with the corresponding values of (1.877, 1.870, 1. 717 Å) reported for the free G⎯C base pair by Sponer et al. at RI-MP2/TZVPP level[42]. In both anion and dianion models, $CO_{(G)}$ ⎯ $HN_{(C)}$ and $NH_{(G)}$ ⎯ $N_{(C)}$ hydrogen bonds are significantly shorter while that of $NH_{(G)}$ ⎯ $OC_{(C)}$ hydrogen bond is significantly larger than that found in the free G⎯C base pair by Sponer[42] which may be attributed to the excess charge in the present systems. According to eq.1 and 2, the base pair interaction

energies (E_{int}) are calculated for bare anion and dianion models, respectively. The BSSE corrected G_C base pair interaction energy was found to be 29.6 and 7.3 kcal/mol for the metal free anion and dianion models, respectively. According to Sponer et al. the E_{int} for a free GC pair obtained with RI-MP2/aug-cc-pVTZ level calculations was -27.0 kcal/mol[42]. Compared to this, the values obtained for both the anion and dianion models are significantly different. The value obtained for the bare anion model was 2.6 kcal/mol higher and it was 19.7 kcal/mol lower for the dianion model.

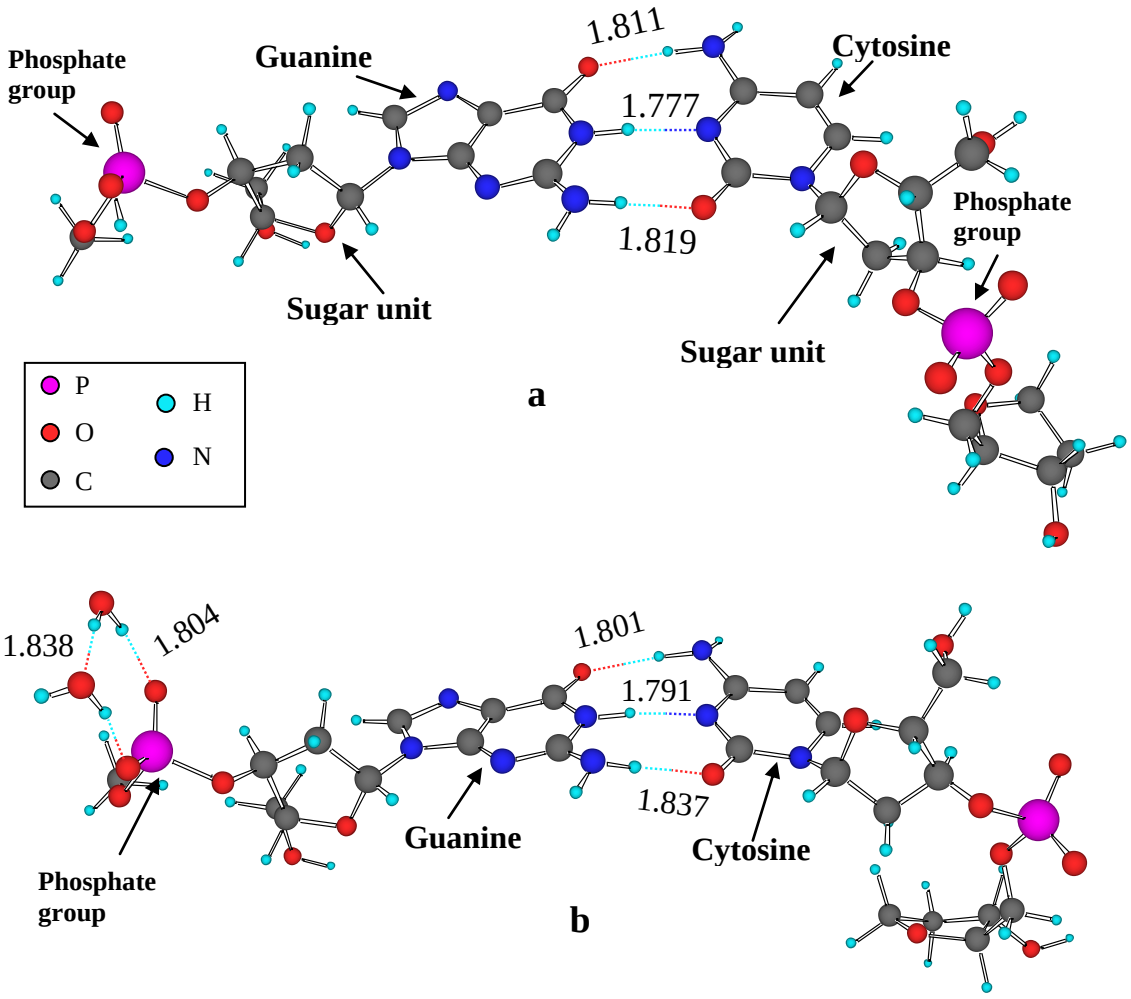

Fig.2.B.4. Optimized structures of bare (a) anion (HPSG…CSP^-) and (b) dianion ($(H_2O)_2$- PSG…CSP^-) model systems. All bond lengths are in Å.

However, this result is not surprising because the anion model can be visualized as the interaction between the neutral guanine fragment and the anionic cytosine fragment and this type of a (neutral…charged) interaction is expected to be higher than the (neutral…neutral) interaction found in a free GC pair. On the other hand, the electrostatic repulsion between the negatively charged guanine and the negatively charged cytosine fragments in the dianion model will induce some repulsive electrostatic interaction, and therefore a large reduction in the E_{int} value is found in its GC pair.

2.B.4. 2. *The HPS…CSP$^-$…M(H_2O)$_4$ Anion Models*

The hydration studies of alkali metal ions suggest that the primary solvation shell contains only four water molecules (See details in Appendix Fig.5, 6 and 7).

The binding of alkali metals such as Li^+, Na^+ and K^+ to the anionic phosphate group in the anion model with different binding mechanisms was optimized at the ONIOM level according to the scheme given in Fig.2.B.2 and 2.B.3. The ONIOM optimized full geometry for the outer sphere coordination of $Li(H_2O)_4$ with the HPSG**…**CSP^- model is depicted in Fig.2.B.5.a.

In order to have a closer look at the hydrated metal region interacting with the phosphate anion, the QM region of the ONIOM optimized geometry of the outer sphere coordination of $Li(H_2O)_4$ is also presented in Fig.2.B.5.b. Only the QM regions in the cases of inner sphere monodentate and bidentate structures of Li^+ are presented in Fig.2.B.5.c and d, respectively.

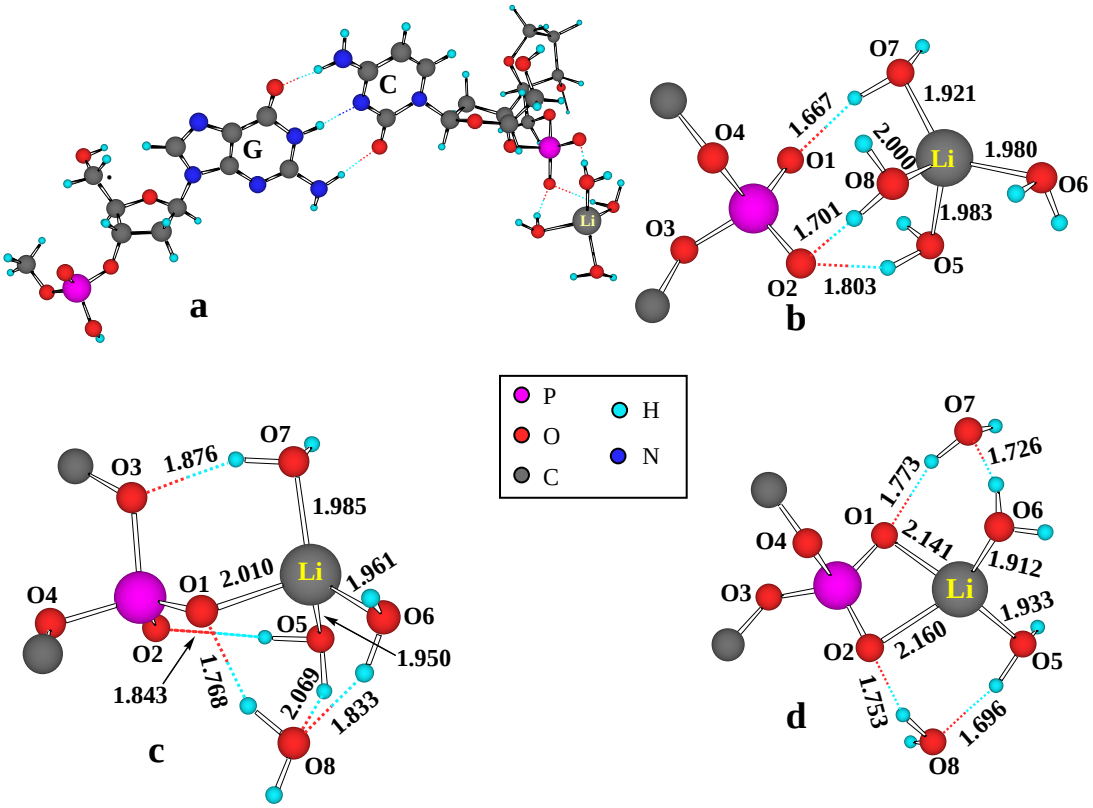

Fig.2.B.5. The HPS…CSP$^-$…Li$(H_2O)_4$ anion model (a) ONIOM level optimized full geometry for outer sphere binding. (b), (c) and (d) are the QM region of the ONIOM optimized geometries for outer sphere binding, inner sphere monodentate binding, and the inner sphere bidentate binding, respectively. All bond lengths are in Å.

The QM layer of the ONIOM optimized geometry of anion model for Na^+ and K^+ are presented in Fig.2.B.6. In the case of Na^+, the outer sphere-binding mode suggests that Na^+ has a distorted tetrahedral arrangement with respect to the surrounding oxygen atoms (Fig.2.B.6.a). For instance, in this geometry the O7-Na-O8 angle is found to be 134.6^o, which is quite large compared to a tetrahedral angle and this feature is mainly attributed to the O5…H-O8 hydrogen bond interaction between the two metal bound water molecules. The metal oxygen bond connections found in the inner sphere mono

and bidentate structures give largely a tetrahedral arrangement and are very similar to the corresponding Li^+ geometries (Fig.2.B.6.b and c).

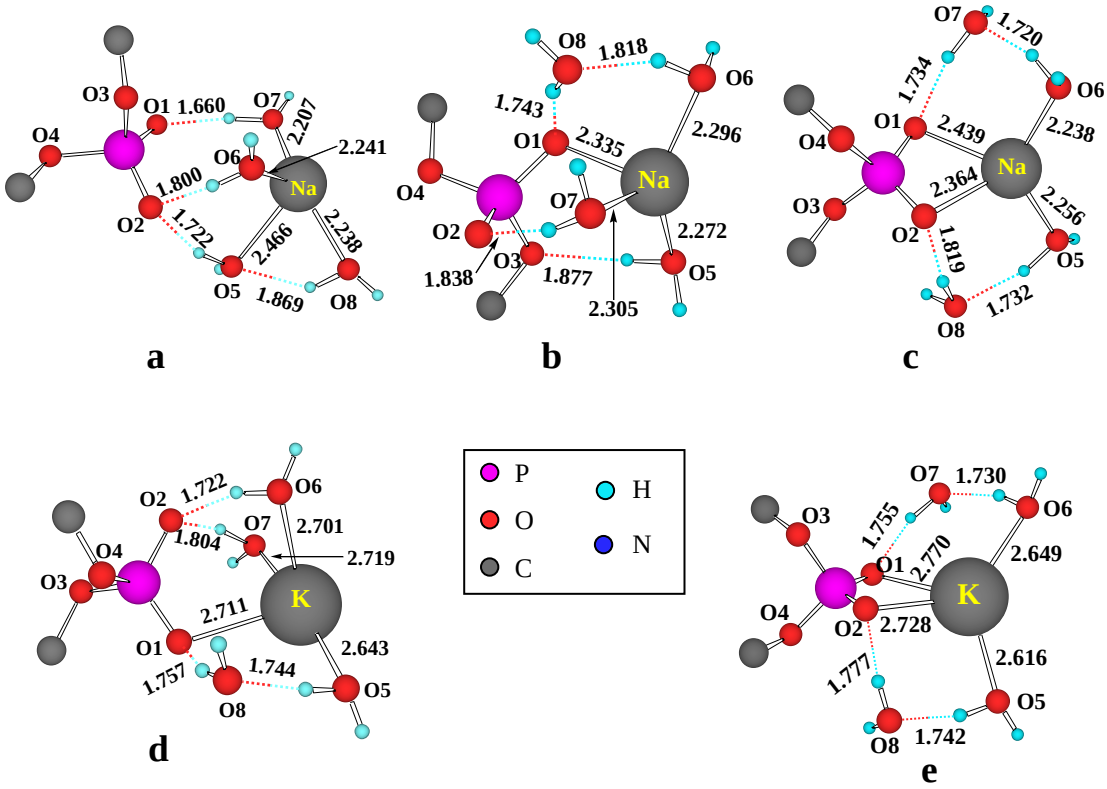

Fig.2.B.6. The HPSG…CSP$^-$…Na$(H_2O)_4$ and HPSG…CSP$^-$…K$(H_2O)_4$ Anion Model. The QM layer of the ONIOM optimized geometry for (a) outer sphere binding of Na^+ (b) and (d) for inner sphere monodentate binding (c) and (e) the inner sphere bidentate binding of Na^+ and K^+ respectively. All bond lengths are in Å.

In the case of K^+, the outer sphere structure was not found. All attempts to find the outer sphere coordination always gave the inner sphere mono-dentate structure as the optimized one (Fig.2.B.6.d). In this mono-dentate structure, the three water molecules bound to the metal nearly occupy the same plane. However, in the case of the bi-dentate structure, the oxygen atoms are arranged tetrahedrally to the metal ion (Fig.2.B.6.e). This can be attributed mainly to the large coordination sphere of the K^+ ion.

The average values of the metal-oxygen distances are 1.971 and 2.288 Å for outer sphere Li^+ and Na^+, respectively and that for the inner sphere mono-dentate structures are 1.977, 2.302, 2.694 Å for Li^+, Na^+, and K^+, respectively. A slightly higher value of 2.037, 2.324 and 2.691 Å are observed for the average metal-oxygen distances in the bi-dentate structures of Li^+, Na^+, and K^+, respectively. It can be understood that, the average metal-oxygen distances increase with increase in size of the metal ion. However, it does not change much with respect to the different binding modes preferred by the metal ions (See Appendix Table. 5, 6 and 7 for the bond lengths).

Table 2.B.1. Phosphate-hydrated metal ion interaction energy in anion (E5) and dianion (E6) models. Values in parenthesis are the BSSE corrections. All values are in kcal/mol.

Model Systems	Outer sphere		Inner sphere monodendate		Inner sphere bidendate	
	E5 (anion)	E6 (dianion)	E5 (anion)	E5 (anion)	E6 (dianion)	E5 (anion)
Li^+	-112.46	Not found	-98.73	-134.98	-88.28	-131.74
Na^+	-95.25	-129.46	-96.34	-126.46	-99.44	-128.24
Na^+	Not found	-126.80	-108.66	-124.42	-96.88	Not found

Table 2.B.1 lists the metal ion- phosphate interactions energy data (E_{int}^{M}) for tetrahydrated Li^+, Na^+, and K^+ ions, for anion and dianion models in the outer sphere, inner sphere monodentate and inner sphere bidentate binding modes. In the case of Lithium, the E_{int}^{M} values show the following order of stability: outer sphere > inner sphere monodentate > inner sphere bidentate. For Li^+ outer sphere coordination the binding energy value, -112.46 kcal/mol is superior to the value of -98.73 and -88.28 kcal/mol obtained for the inner

sphere mono and bidentate structures, respectively. On the other hand, in the case of Na^+, the order of stability is exactly the reverse to the above one and the inner sphere bidentate is the most stable structure. In the case of K^+, the inner sphere monodentate structure is the most stable one (E_{int}^{M} = -108.66 kcal/mol). As a whole, the E_{int}^{M} values suggest that Li^+ binds more strongly to DNA anion model than the Na^+ and K^+ ions. It should also be pointed out here that Li^+ has the highest affinity for DNA in aqueous solutions in terms of counter ion interactions[43].

Table 2.B.2. G_C base pair interaction energy in anion (E3) and dianion (E4) models. Values in parenthesis are the BSSE corrections. All values are in kcal/mol.

Model Systems	Outer sphere		Inner sphere monodendate		Inner sphere bidendate	
	E3 (anion)	E4 (dianion)	E3 (anion)	E4 (dianion)	E3 (anion)	E4 (dianion)
Li^+	25.2 (4.7)	Not found	25.4 (4.6)	21.0 (4.7)	25.9 (4.7)	20.8 (4.8)
Na^+	24.7 (4.7)	20.5 (4.8)	25.3 (4.6)	20.6 (4.8)	25.1 (4.7)	20.6 (5)
Na^+	Not found	20.6 (4.9)	24.9 (4.6)	20.7 (4.9)	25.2 (4.7)	Not found

Table 2.B.2 shows the GC base pair interaction energy data for tetrahydrated Li^+, Na^+, and K^+ ions with anion and dianion models calculated according to the equations 1-4. It may be seen that irrespective of the metal ions and their different binding modes, base pair interaction energy is nearly the same at 25.0 kcal/mol, which is 4.7 kcal/mol smaller than the E_{int} value of the GC pair of the bare anion model. In fact, the average value of the three

hydrogen bond lengths for the GC pair in all the systems is in the range of 1.802 to 1.805 Å (see Appendix Table 2 for hydrogen bond length information). This means that the hydrogen bond interactions in all the hydrated metal-anion model systems are nearly unchanged, which are in agreement with the nearly identical interaction energy values.

2.B.4.3. *The $[(H_2O)_2\ldots {}^{-}PSG\ldots CSP^{-}\ldots M(H_2O)_4]$ Dianion Models*

The dianion model was selected in order to understand the effect of excess negative charge on the DNA fragment. QM layer of the ONIOM level optimized geometries of dianion model for the Li^+, Na^+, and K^+ ions are depicted in Fig.2.B.7. In the dianion model, the outer sphere model for Li^+ and the inner sphre bi-dentate model for K^+ could not be located. In the optimized structures, the average metal-oxygen distances are 1.964, 2.024, 2.365, 2.291, 2.324, 2.751, and 2.652 Å for inner sphere mono-dentate Li^+, inner sphere bi-dentate Li^+, outer sphere Na^+, inner sphere mono-dentate Na^+, inner sphere bi-dentate Na^+, outer sphere K^+, and inner sphere mono-dentate K^+ respectively.

All these bond length values are shorter than the corresponding values found in the respective anion models (See Appendix for the distance Table 5, 6 and 7). This means that a stronger metal-phosphate binding is occurring in the dianion model than that in the anion model.

The metal phosphate interaction energy values of dianion models given in Table 2.B.1 also suggest a substantial increase in the metal phosphate binding energy in all types of binding modes, when compared with the corresponding values for the anion models.

For instance, compared to the anion models, in the case of inner sphere mono-dentate Li^+, the metal-phosphate binding energy is increased by 36.7 % and for the inner sphere bi-dentate Na^+, the increase in the binding energy is 29.0 %.

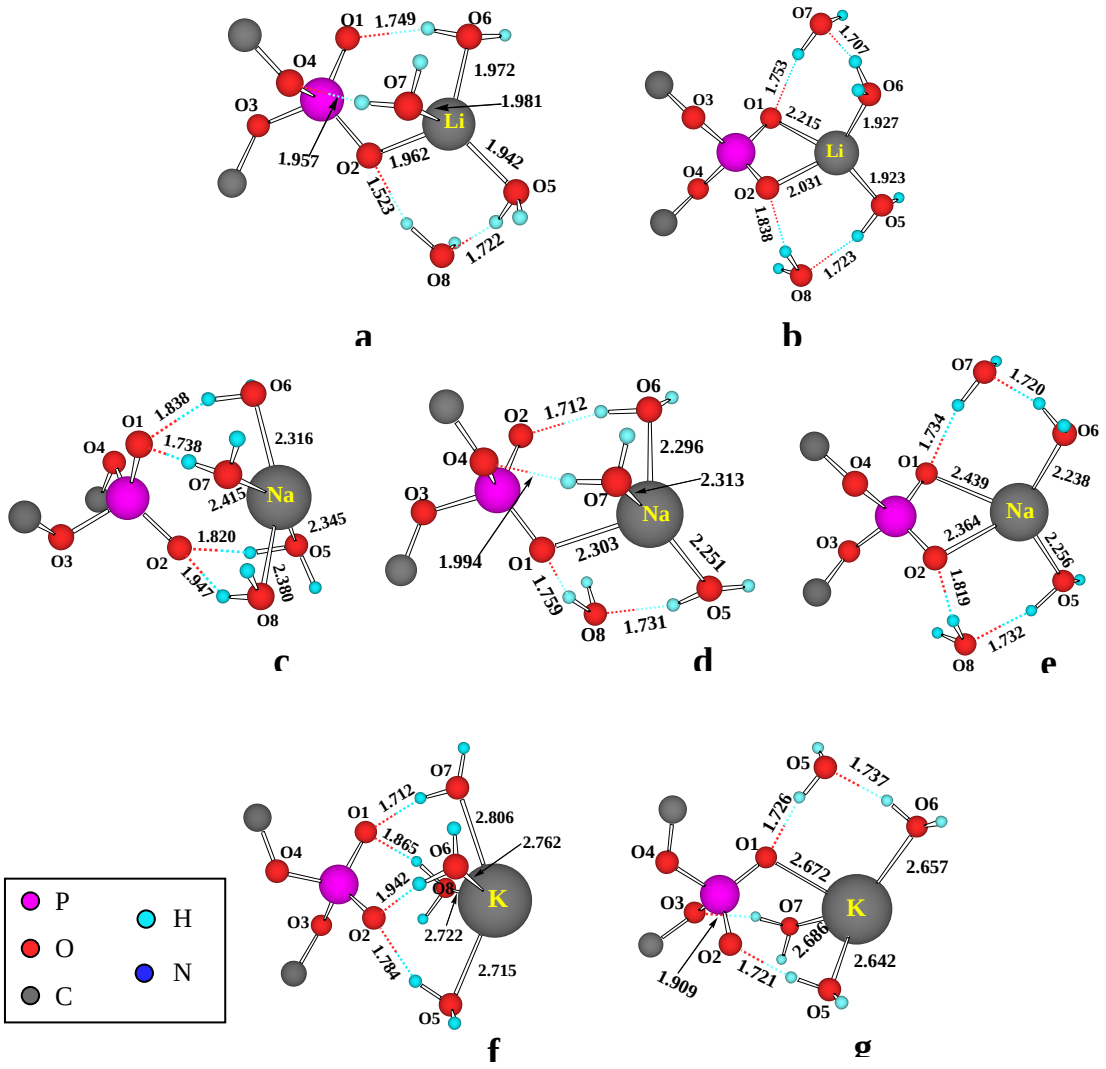

Fig.2.B.7. The $(H_2O)_2PSG\ldots CSP^-M(H_2O)_4$ dianion models for alkali metal ions. (a) and (b) are the inner sphere mono- and inner sphere bi-dentate structures for Li^+ ion, respectively. (c), (d), and (e) are the outer sphere, inner sphere mono- and bi-dentate structures of Na^+ ion, respectively, (f) and (g) are outer and inner sphere monodentate structures for K^+ ion respectively.

The G-C base pair interaction energy data of the three different binding modes (outer sphere, inner sphere monodentate and bidentate) of the hydrated alkali metal ions in the dianion model are given in Table 2.B.2.

In all the cases, the base pair interaction energies are nearly identical around 21 kcal/mol. However, this value is 5 kcal/mol smaller than the GC pair interaction in the anion model, which means that the excess negative charge on the DNA fragment is weakening of the GC hydrogen bond strength. The average value of the three hydrogen bond lengths (1.810 to 1.813 Å) in the GC pair is also increased as a result of the weakening of the GC pair interaction (See Appendix for the hydrogen bond lengths, Table 4).

In the case of Li^+ binding to dianion model, the E_{int}^{M} values obtained for inner sphere monodentate and inner sphere bidentate are -134.98 kcal/mol and -131.74 kcal/mol respectively, which suggest that Li^+ prefers inner sphere monodentate binding mode. In contrast, in the anion model the stable binding mode observed with Li^+ ion was the outer sphere one, which implies that charge of the model system is crucial in deciding the binding mechanism.

The difference in the binding mechanism could be due to the fact that, as the dianion model has higher negative potential, it can hold the lithium ion closer to the DNA than the anion model, accompanied by the dehydration of Li^+, resulting in an inner sphere monodentate binding mode. Moreover, in case of inner sphere binding, the metal–oxygen distances are shorter than that in anion model. Unlike lithium, it can be understood from the E_{int}^{M} values of Na^+ and K^+, that they prefer outer sphere binding mode in the dianion model.

Whereas in the anion model, the most stable binding mechanisms observed with Na^+ and K^+ were inner sphere bidentate and monodentate respectively. It can therefore be concluded that, the binding modes of alkali metal ions largely depend on the charge of the DNA fragment.

However, experimental reports show that Li^+ ions prefer outer sphere binding to DNA[44] and stabilizes the water structure around DNA[45], and Na^+ and K^+ binds to DNA in an inner sphere manner[46,47] which is in well agreement with the binding behavior of these ions with the anion model. This indicates that the anion model is more realistic, in the case of alkali metal ion binding to DNA, than the dianion model where the net charge of the system is negative. The outer sphere binding of Li^+ ion, to the anion model of DNA is a point of support to the unique LC behavior of DNA, in the presence of Li^+ ion. The inner sphere-binding mode of Na^+ and K^+, dehydrates DNA by establishing direct contact with it, which explains the lower C_D in the presence of Na^+ and K^+ compared to that with Li^+ ions.

2.B.5. Conclusions

The interaction of hydrated Li^+, Na^+ and K^+ ions to the phosphate group of DNA was studied by modeling a DNA fragment, both in an anion (one negative charge) and dianion (two negative charges) state, with the phosphate geometry maintained as in native DNA (projected towards the exterior), using a three layer ONIOM –based QM-MM method. Three combinations of metal ion–DNA binding were studied, which include the outer sphere, inner sphere mono-and inner sphere bi-dentate patterns. In the anion model, Li^+ preferred

the outer-sphere binding, whereas Na^+ and K^+ preferred inner-sphere bi- and mono-dentate binding respectively. However, in the case of the dianion model the Li^+ preferred the inner-sphere mono-dentate binding, whereas Na^+ and K^+ preferred outer-sphere binding respectively. Since the present data on the binding of Li^+, Na^+ and K^+ ions to anion model of DNA are in good agreement with the previous experimental results, the anion model reveals a more realistic picture of DNA-alkali metal ion interactions compared to the dianion model where the net charge on the system is not neutral. The present results which were supported by earlier experimental reports also showed a stronger binding of Li^+ ions to DNA anion model compared to Na^+ and K^+ ions. To the best of our knowledge, this is the first theoretical investigation on the interaction of Li^+, Na^+ and K^+ ions with a comparatively larger DNA model system. The outer sphere binding of Li^+ ion to the anion model of DNA is a point of support to the unique LC behavior of DNA in the presence of Li^+ ion.

2.B.6. References

1. Eichhorn, G. L., *Adv. Inorg. Biochem.* **1981,** 3, 1.
2. Martin, R. B., *Acc. Chem. Res.* **1985,** 18, 32.
3. Saenger, W., *Principles of Nucleic Acid Structure*. ed.; Springer-Verlag: New York, 1994.
4. Sigel, H., *Chem. Soc. Rev.* **1993,** 22, 255.
5. Glusker, J. P., *Adv. Protein Chem.* **1991,** 42, 1.
6. Misra, V. K.; Draper, D. E., *Biopolymers* **1998,** 48, 113.
7. Alexander, R. S.; Kanyo, Z. F.; Chirlian, L. E.; Christianson, D. W., *J. Am. Chem. Soc.* **1990,** 112, 933.
8. Laughton, C. A.; Luque, F. J.; Orozco, M., *J. Phys. Chem.* **1995,** 99, 11591.
9. Schneider, B. K.; Kabelac, M.; Hobza, P., *J. Am. Chem. Soc.* **1996,** 118, 12207.
10. Bamann, E.; Trapmann, H.; Fischler, F., *Biochem. Z.* **1954,** 328, 89.
11. Marzilli, L. G.; Kistenmacher, T. J.; Eichhorn, G. L., ed.; John Wiley and Sons: New York, 1980.
12. Missailides, S.; Anastassopoulou, J.; Fotopoulos, N.; Theophanides, T., *Asian J Phy* **1997,** 6, 481.
13. Chiu, T. K.; Dickerson, R. E., *301*, 915, *J. Mol. Biol.* **2000,** 301, 915.
14. Sponer, J.; Burda, J. V.; Leszczynski, J.; Hobza, P., *J. Biomol. Struc. & Dynam.* **1999,** 17, 61.
15. Sponer, J.; Hobza, P., *Colle. Czech. Chem. Comm.* **2003,** 68, 2231.
16. Sponer, J.; Leszczynski, J.; Hobza, P., *J. Mol. Stru. Theochem* **2001,** 573, 43.
17. Sponer, J.; Sabat, M.; Burda, J. V.; Leszczynski, J.; Hobza, P.; Lippert, B., *J. Biol. Inorg. Chem.* **1999,** 4, 537.
18. Sponer, J. E.; Sychrovsky, V.; Hobza, P.; Sponer, J., *Phys. Chem. Chem. Phys.* **2004,** 6, 2772.

19. Munoz, J.; Sponer, J.; Hobza, P.; Orozco, M.; Luque, F. J., *J. Phys. Chem. B* **2001,** 105, 6051.
20. Petrov, A. S.; Funseth-Smotzer, J.; Pack, G. R., *Int. J. Quant. Chem.* **2005,** 102, 645.
21. Petrov, A. S.; Lamm, G.; Pack, G. R., *J. Phys. Chem. B* **2002,** 106, 3294.
22. Petrov, A. S.; Lamm, G.; Pack, G. R., *J. Phys. Chem. B* **2004,** 108, 6072.
23. Bandyopadhyay, D.; Bhattacharya, D., *J. Biomol. Struc. & Dynam.* **2003,** 21, 447.
24. Bertran, J.; Rodriguez-Santiago, L.; Sodupe, M., *J. Phys. Chem. B* **1999,** 103, 2310.
25. Zeizinger, N.; Burda, J. V.; Sponer, J.; Kapsa, V.; Leszczynski, J., *J. Phys. Chem. A* **2001,** 105, 8086.
26. Murashov, V. V.; Leszczynski, J., *J. Phys. Chem. B* **1999,** 103, 8391.
27. Rodger, A.; Sanders, K. J.; Hannon, M. J.; Meistermann, I.; Parkinson, A.; Vidler, D. S.; Haworth, I. S., *Chirality* **2000,** 12, 221.
28. Marincola, F. C.; Denisov, V. P.; Halle, B., *J. Am. Chem. Soc.* **2004,** 126, 6739.
29. Kankia, B. I., *Biopolymers* **2004,** 74, 232.
30. Jerkovic, B.; Bolton, P. H., *Biochemistry* **2001,** 40, 9406.
31. Svensson, M.; Humbel, S.; Froese, R. D. J.; Matsubara, T.; Sieber, S.; Morokuma, K., *J. Phys. Chem.* **1996,** 100, 19357.
32. Humbel, S.; Sieber, S.; Morokuma, K., *J. Chem. Phys.* **1996,** 105, 1959.
33. Dapprich, S.; Komaromi, I.; Byun, K. S.; Morokuma, K.; Frisch, M. J., *J. Mol. Struct. THEOCHEM* **1999,** 461-462, 1.
34. Tschumper, G. S.; Morokuma, K., *J. Mol. Struct.: THEOCHEM* **2002,** 592,137.
35. Re, S.; Morokuma, K., *J. Phys. Chem. A* **2001,** 105, 7185.
36. Becke, A. D., *J. Chem. Phys.* **1993,** 98, 5648.
37. Becke, A. D., *Phys. Rev. A* **1988,** 38, 3098.

38. Hariharan, P. C.; Pople, J. A., *Mol. Phys.* **1974,** 27, 209.
39. Stewart, J. J. P., *J. Comp. Chem.* **1989,** 10, 209.
40. Rappé, A. K.; Casewit, C. J.; Colwell, K. S.; Goddard III, W. A.; Skiff, W. M., *J. Am. Chem. Soc.* **1992,** 114, 10024.
41. Boys, S. F.; Bernardi, F., *Mol. Phys.* **1970,** 19, 553.
42. Sponer, J.; Jurecka, P.; Hobza, P., *J. Am. Chem. Soc.* **2004,** 126, 10142.
43. Lyubartsev, A. P.; Laaksonen, A. J., *Biomol. Struct. Dyn.* **1998,** 16, 579.
44. Zheng, J.; Li, Z.; Wu, A.; Zhou, H., *Biophysical Chemistry* **2003,** 104, 37.
45. Mrevlishvili, G. M.; Carvalho, S. M. C.; Ribeiro da Silva, M. A. V.; Mdzinarashvili, T. D.; Razmadze, G. Z.; Tarielashvili, T. O., *J. Therm. Anal. Cal.* **2001,** 66, 133.
46. Stelwagen, N. C.; Magnusdottir, S.; Gelfi, C.; Righeti, P. G., *J. Mol. Biol.* **2001,** 305, 1025.
47. Tereshko, V.; Wilds, C. J.; Minasov, G.; Prakash, T. P.; Maier, M. A.; Howard, A.; Wawrzak, Z.; Manoharan, M.; Egli, M., *Nucleic Acids Res.* **2001,** 29, 1208.

CHAPTER 3

INDUCTION AND STABILIZATION OF LIQUID CRYSTALLINE PHASES OF DNA BY ALKALINE EARTH METAL IONS:

A. STUDIES ON LC BEHAVIOR USING POLARIZED LIGHT MICROSCOPY.

B. STUDIES ON BINDING BEHAVIOR OF ALKALI METAL IONS USING MOLECULAR MODELING.

CHAPTER 3 A

INDUCTION AND STABILIZATION OF LIQUID CRYSTALLINE PHASES OF DNA BY ALKALINE EARTH METAL IONS: STUDIES ON LC BEHAVIOR USING POLARIZED LIGHT MICROSCOPY

3.A.1. Abstract

A comparative study of the effects of alkaline earth metal ions, Mg^{2+}, Ca^{2+}, Sr^{2+} and Ba^{2+}, on the LC organization of high molecular weight DNA, was carried out using polarized light microscopy. All the alkaline earth metal ion-DNA systems show multiple LC textures, mainly a fluidic cholesteric phase, and a columnar hexagonal phase with restricted fluidity. Critical DNA concentration (C_D) required to exhibit anisotropic behavior in the presence of alkaline earth metal ions, was found to be higher than that of alkali metal ions, which suggests that both the size and charge of the counter ion had influenced the induction of LC behavior in DNA. C_D required to exhibit LC behavior in presence of Mg^{2+} was quite higher compared to Ca^{2+}, which in turn was higher than that of Ba^{2+} and Sr^{2+}. The difference in C_D can be attributed to their different hydration factor, and binding mechanisms. Mg^{2+} because of its outer sphere binding mode probably stabilizes the hydrogen bounded water network around DNA, and as a result prevents the dehydration of DNA strands, which is essential to exhibit LC

behavior. LC phases could be obtained only under defined ionic conditions in the presence of Mg^{2+} ions. The higher C_D required for Mg^{2+} like Li^+ can be correlated to their diagonal relationship (higher hydration factor). The rate of cholesteric to columnar phase transition was facilitated with increase in size of the counter ion, as observed in the case of alkali metal ions.

3.A.2. Introduction

Metal ion interactions play key roles in the control of DNA conformation and its supramolecular organization. Experimental results have proved that metal ions interact in vitro with nucleic acids and stabilize or destabilize the double helix[1,2]. The DNA-metal ion interactions are governed by several parameters such as the nature of the metal, its size and charge. All these parameters influence the conformation of DNA by direct or indirect interaction through the water molecules with the basic sites of the nucleotides[3]. Although monovalent cations have been found in a few cases to be localized at preferred binding sites of DNA with low occupancies, the stable and specific solvation geometries adopted by divalent cations endow them with the ability to strongly and selectively bind to DNA[4,5]. Moreover, divalent cations serve critical functions across a multitude of biochemical processes, and are necessary to reach the ultimate states of condensation[6,7].

Researchers have put forwarded a number of ideas, regarding the nature and type of metal binding, binding sites and the effect of metal binding on the conformation of DNA. It was demonstrated that divalent metal ions not only can

induce DNA condensation,[8] or aggregation,[9] but also can alter its secondary or tertiary structure[10]. A recent AFM study of equilibration of DNA molecules on mica indicated that, both the topological and secondary structures are dependent on the type of alkaline earth metal ions. The four alkaline earth metal ions (Mg^{2+}, Ca^{2+}, Ba^{2+} and Sr^{2+}) cause the B-A transition in different degrees, in which strontium induces the greater structural transition. The magnitude of inducing B-A conformation was in the following order Sr^{2}> Ba^{2+}> Ca^{2+}> Mg^{2+} [11].

It is well known that alkaline earth cations with greater binding specificity for the phosphates, neutralizes the negative charge of sugar–phosphate backbone and thus enhances the base stacking[12]. The alkaline earth cations, especially Mg^{2+} have long been known to stabilize the secondary and tertiary structure of DNA much more efficiently than the alkali metal ions, presumably through non-specific phosphate binding[13]. Mg^{2+} is the most prevalent intracellular divalent cation, occurring in millimolar quantity (≈40 mM) and has several essential biological roles[14]. Intracellular magnesium concentrations are highly regulated and magnesium acts as an intracellular regulator of cell cycle control to apoptosis[15]. Mg^{2+} ion stabilizes the DNA structures at physiological levels, whereas it destabilizes them at low or higher concentrations[8]. Besides stabilizing DNA structure, Mg^{2+} is also known to protect DNA from hydroxyl radical cleavage[16]. NMR works on the Mg^{2+} and Ca^{2+} interaction with calf thymus DNA showed that at small amounts of the cations, the interaction is specific and cannot be described by simple electrostatic association[17].

It is reported that magnesium competes for certain coordination sites with other common metal ions[18]. In addition to its interaction with the phosphate groups, Mg^{2+} ion with its six-coordinated water molecules can form hydrogen bonds as follows. One of the coordinated water molecules may be substituted by the N7 coordination site of the nucleotide or hydrogen bonded to it, another one can be involved in hydrogen bonding with O6, while others form more hydrogen bonds. The pentahydrated doubly charged magnesium $[Mg(H_2O)_5]^{2+}$ moiety could be bound directly to N7, whereas the hexahydrated doubly charged 'free' cation, $[Mg(H_2O)_6]^{2+}$ is bound with hydrogen bonds to the nucleotide at the N7 guanine site and O6. This may not allow approaching denaturants at this position,[19-21] and thus protecting the molecule, from attacks at this position. Magnesium ions also increase the activity of the O-H group of water, and hence increase the strength of the hydrogen bonds they form. The importance of magnesium ions is to stabilize the structure of t-RNA and DNA, by binding to specific sites, which depends on the hydration state of the metal. Recently, the crystal structure of B-DNA was resolved at 1 A° resolution, which shows sequence specific binding of DNA to Mg^{2+} and Ca^{2+} in the minor grooves[10]. This structure reveals sequence-specific binding of Mg^{2+} and Ca^{2+} to the major and minor grooves of DNA, together with a non-specific binding to backbone phosphate oxygen atoms.

According to another theory, when 'free' hexahydrated magnesium cation binds to DNA or RNA, it forms a supermolecular structure, by neutralizing the negative charge density locally and by hydrogen bonding to DNA, thus stabilizing

the DNA structure and conformation. This magnesium effect may be named as '**protection'** of DNA[22] or **'protective effect'**. However, when magnesium binds 'covalently' to DNA, it forms a bound coordination complex with an Mg-O coordinative bond in the inner sphere of coordination. In this case, the lesion is stronger and we have a deformation of DNA locally, and thus '**enhancement**' of the bending distortion of the double helix, which may lead to the destruction of the cell. At higher concentrations of magnesium, we most likely have both the effects of magnesium on DNA, with the 'enhancement' effect being stronger, since at higher concentrations more magnesium cations react covalently with DNA[8]. However, in a recent study on the interaction of divalent metal ions with DNA, Hackl et al. have shown that Mg^{2+} ions binds only to the phosphates and not to the bases[23].

It has been proved that DNA is condensed into LC states *in vivo* and the same can be obtained in vitro also under controlled conditions[24]. In a condensed state of DNA (fiber, gel, liquid crystal), the mean concentration of counter ion is known to be very high (1-2M)[25.] Effective diameter, axial ratio, excluded volume of DNA and persistence length of the DNA polyelectrolyte, are the parameters which changes with the ionic environment, and in turn will influence the LC phase behavior of the molecule[24]. After a certain critical local concentration (C_D), it has been shown that DNA gets transformed from isotropic to anisotropic LC states, which are again dependent on the ionic strength and counter ion type[26].

Thus, when the concentration of DNA is slowly increased, the macromolecule undergoes spontaneous phase transitions, to form at least three distinct LC phases, which are termed *lyotropic phase transitions* in the liquid crystal field[24]. Linear DNA fragments in aqueous solution form multiple LC phases whose nature depends on the polymer concentration. Linear DNA dispersed in water or salt solutions shows at least two first order transitions from the isotropic, through cholesteric, to the columnar hexagonal phase, when the DNA concentration is increased. There are reports of appearance of blue phases and/precholesteric phases before the cholesteric phase, whereas more concentrated phases are true crystals[24].

Investigations of LC domains of DNA, in the presence of magnesium and calcium ions have focused to date, on low molecular weight fragmented DNA alone, under defined ionic conditions[24]. But the effect of varying size of other alkaline earth metal ions such as barium and strontium, and their role in the induction and stabilization of LC behavior of high molecular weight DNA are not known. This chapter presents the influence of alkaline earth metal ions such as Mg^{2+}, Ca^{2+}, Sr^{2+} and Ba^{2+} on the induction and stabilization of LC behavior of high molecular weight calf thymus DNA.

3.A.3. Experimental Section

A) ***Preparation of Samples:*** Calf Thymus DNA was purchased from Worthington Biochemical Corporation, Freehold, NJ, USA, and has been used without further purification. The weight average molecular weight of DNA was 6×10^6.

Autoclaved millipore water was used as the medium in all the experiments. DNA was dissolved in 0.1M NaCl (pH 7). The dissolved DNA was then dialysed against NaCl (0.1M) 3-4 times. The observed A_{260}/A_{280} ratio of the DNA solution was 1.88, indicating that the DNA was free of protein contamination. The concentration of calf thymus DNA was determined by measuring the absorbance at 260 nm, and using the molar extinction coefficient (Є) of 6900 per M/cm. The final concentration of DNA was 7.143 mg/ml. Desired concentration of DNA solutions were prepared by dilution of stock solution with the buffer/salt solutions according to the requirement. $MgCl_2$, $CaCl_2$, $BaCl_2$ and $SrCl_2$ of analytical grade were used for our experiments.

The LC behavior of Calf Thymus DNA was studied under the following conditions: (1) Varying DNA concentration, keeping the concentrations of metal ions constant, to arrive at the critical DNA concentration, in the presence of each ions; and (2) varying the metal ion concentration, while keeping the DNA concentration fixed, to examine the effect of different metal ion concentrations on the LC organization of DNA.

B) ***Polarized Light Microscopy***: Microscopic glass slides and cover-slips were soaked in chromic acid, and further rinsed with deionised water, and dried using analar acetone prior to use. Desired concentrations of metal ion and DNA solutions, were mixed in an eppendorf tube and vortexed for 15 minutes and were then allowed to equilibrate at room temperature (26 °C) for two hours. 20 µL of each metal ion DNA solution was sandwiched between a clean microscopic glass

slide and a cover slip, and the cover slips were then sealed with DPX mountant (a neutral solution of polystyrene and plasticizers in xylene used in microscopy work, M/s Nice Chemicals Ltd., Mumbai) to prevent dehydration of the sample[27,28]. The preparations were then incubated at 37°C for extended time periods to observe the phase changes until crystallization or complete darkening (isotropization) occurred. The preparations were monitored periodically for phase changes under a Nikon Optiphot Polarized Light Microscope equipped with a Nikon camera and photographs were taken when the phases became prominent and distinct. The phases and granular boundaries were clear and sharp when the sample was incubated at 37°C. A triplicate of each sample was made to ensure the reproducibility of the phase changes. The results were reproducible in three sets of separate experiments. The following parameters were noted: (a) C_D – critical DNA concentration required to exhibit anisotropy, (b) C_M – critical metal ion concentration below which anisotropic behavior is exhibited, (c) T_{tr}- Time required for cholesteric to columnar phase transition, (d) T_{iso}- Time required for the LC phases to darken and disappear ie. isotropization.

C) ***FTIR Spectra:*** DNA-metal complexes were precipitated using ethanol and the precipitates were centrifuged and dried, and for recording the IR spectra[29,30]. IR spectra were recorded in a Shimadzu IR spectrophotometer using the KBr pellet technique.

D) ***Circular Dichroism Measurements:*** Circular Dichroism (CD) spectra of dilute DNA solutions were obtained with a Jasco-715 spectropolarimeter using a

quartz cuvette of 1 cm path length[31]. CD data (with concentrated DNA solutions) for the LC ordering could not be obtained because the instrumental parameters were apt only for very dilute DNA dilutions, but LC ordering can be obtained only at higher DNA concentrations.

Also, several attempts were made to obtain X-ray diffraction data, which faced problems in obtaining the required birefringence (even after keeping the sample filled in the capillary in an oven set at 37^0C for long periods) for the instrument to make measurements. Probably, it must be the difficulty with the high molecular weight DNA system in anchoring/ordering of the long DNA molecules when sandwiched between the glass slide and cover slip and within the capillary where the sample is filled.

3.A.4. Results and Discussion

Among the alkaline earth metal ions, Mg^{2+} and Ca^{2+}, are widely distributed in biological systems and play an important role in many enzymatic activities related to replication, transcription, and recombination[32-34]. These divalent cations are also known to induce the compaction of the chromatin fiber[35]. Eventhough, Salyanov et.al. in their study on the influence of Mg^{2+}/Ca^{2+} along with Na^{+} on low molecular weight DNA fragments have reported formation of LC phases, nature of the phases were not identified properly[36]. Catte et al. also reported the influence of Mg^{2+} on the LC phases of low molecular weight DNA[37]. Moreover, the influence of these ions on the LC organization of high molecular weight DNA is not known.

The effects of divalent alkaline earth metal ions, on the induction and stabilization of LC behavior of high molecular weight calf thymus DNA, were analyzed in the present work. According to Bloomfield et al.,[38,39] magnesium and calcium are inefficient in condensing pure DNA in aqueous solution. But the present results show that all the alkaline earth cations, including magnesium and calcium, induced LC states in DNA under defined ionic conditions.

A homogenous DNA solution of concentration, 7.14 mg/ml was used as the stock solution in the present experiments. Preparation of DNA solutions of further high concentration faced difficulty in dissolution and attaining homogeneity.

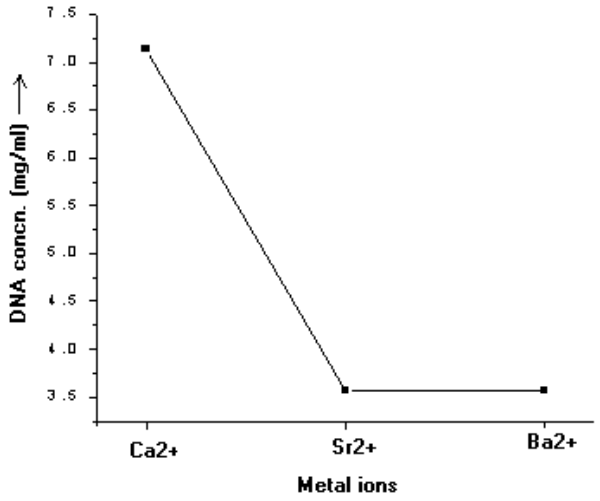

Fig.3.A.1. C_D required for LC behavior in the presence of alkaline earth metal ions

Table 3.A.1 show that on varying DNA concentrations and keeping metal ion concentration constant at 1M, DNA did not showed LC behavior in presence of Mg^{2+}, whereas the alkaline earth metal ion exhibited LC phases. Also, it can be seen from Fig. 3.A.1 that the critical DNA concentration (C_D) required for Ca^{2+} to exhibit LC behavior is far higher than those of Ba^{2+} and Sr^{2+}.

Table 3.A.1. LC phases obtained when DNA concentration was varied keeping metal ion concentration fixed.

DNA concn. mg/ml	$MgCl_2$ (1M)	$CaCl_2$ (1M)	$SrCl_2$ (1M)	$BaCl_2$ (1M)
7.14	Isotropic	Cholesteric	Iridescent fan shaped Texture	Weakly birefringent dendrimeric growth
3. 57	Isotropic	Isotropic	Weakly birefringent dendrimeric growth	Weakly birefringent fan shaped texture
1.79	Isotropic	Isotropic	Isotropic	Isotropic
0.89	Isotropic	Isotropic	Isotropic	Isotropic
0.45	Isotropic	Isotropic	Isotropic	Isotropic
0.22	Isotropic	Isotropic	Isotropic	Isotropic

So, it could be argued that the C_D for Mg^{2+} could be above that of Ca^{2+} under our experimental conditions, which could not be achieved due to the difficulty in dissolution of high molecular weight DNA.

Recent high-resolution X-ray studies indicate that, except in direct binding of Mg^{2+} ions with phosphate groups, Mg^{2+} immobilization of structural water by the grooves of the duplex take place[7]. Mg^{2+} binds to DNA molecule through a water bridge and stabilize the hydrogen bounded water network and, as a result prevents dehydration of the DNA strands, which is essential to exhibit LC behavior. In yet another study on volume and compressibility effects, it has been proved that Mg^{2+} binds to DNA in an outer sphere (water-mediated) manner, while larger cations, Ca^{2+}, Sr^{2+} and Ba^{2+}, bind to DNA in an inner-sphere (direct contact)

manner, which can be correlated with hydration energies of the cations[8] (see Table 3.A.2).

Our molecular modeling studies on the binding behavior of metal ions such as Mg^{2+} and Ca^{2+} to DNA fragment, using ONIOM approach, indicated that Mg^{2+} could bind both in an outer and inner sphere manner depending on the charge of the DNA fragment. However, Ca^{2+} preferred the inner sphere monodentate binding mechanism, irrespective of the charge on the DNA fragment (see Chapter 3B for details). The stable outer sphere-binding mode observed for Mg^{2+} ions and the innersphere-binding mode of Ca^{2+} ions, explains the reason for their difference in C_D. As inner sphere binding mode involves removal of water molecules from DNA strands to establish direct contact to the binding site, it can facilitate LC ordering compared to outer sphere binding mechanism, which does not involve the removal of water molecules. The different hydration energies and binding mechanism of the cations to DNA could be the reason for the observed difference in C_D required for anisotropic behavior. Table 3.A.3 show the results of variation of metal ion concentrations, keeping DNA concentrations constant at 7.143 mg/ml. It should be noted that at an Mg^{2+} concentration of 0.75 M, DNA showed a weakly birefringent fluidic texture pointing a cholesteric ordering which appears to be the critical magnesium concentration required for the induction of LC phase. Lower the amount of highly hydrated Mg^{2+} in the solution, the more will be the ordering of DNA molecules. As a whole, C_D required to exhibit anisotropy in the presence of alkaline earth metal ions was found to be higher than alkali metal ions

(C_D Mg^{2+} > C_D Ca^{2+} > C_D Sr^{2+} > C_D Ba^{2+} >C_D Li^+ > C_D Na^+ = C_D K^+ = C_D Rb^+ = C_D Cs^+), (described in Chapter 1) which suggests that both the size and charge of the counter ion had influenced the induction of LC behavior in DNA. Also the higher critical DNA concentration in the presence of Mg^{2+} and Li^+ (described in Chapter 1) can be correlated to their diagonal relationship (higher hydration factor, see Table 3.A.2.) in the periodic table.

Even though the phases obtained were not highly birefringent in presence of Mg^{2+}, they remained stable up to one week without undergoing complete transformation to columnar arrangement. Fig.3.A.3 shows the time dependent phase transitions of DNA in the presence of alkaline earth metal ions. It can be seen from Fig.3.A.3, that the transitions from lower ordered cholesteric to higher ordered columnar phase were more prominent at still lower Mg^{2+} concentrations (Fig.3.A.2. a and b), but the LC phases were less stable.

Table 3.A.2. Hydration energies of alkaline earth metal ions[40].

Metal ions	Enthalpy of hydration (kJ/mol)
Mg^{2+}	-1921
Ca^{2+}	-1577
Sr^{2+}	-1443
Ba^{2+}	-1305

It can be seen from, Fig.3.A.3.b that on variation of Ca^{2+} concentrations, at constant DNA concentrations, DNA showed LC behavior for all the Ca^{2+} concentrations studied. Nature of the textures obtained initially was weakly

birefringent, cholesteric planar like, which in the presence of lower Ca^{2+} concentrations adopted a more ordered columnar phase gradually. A biphasic region with restricted fluidity also coexisted at some regions. As the LC phases obtained were weakly birefringent in the presence of Ca^{2+}, no photographs were taken.

Table 3.A.3. LC phases obtained when metal ion concentration was varied keeping DNA concentration fixed (7.14 mg/ml).

Metal ion Concn.	**$MgCl_2$**	**$CaCl_2$**	**$SrCl_2$**	**$BaCl_2$**
1M	Isotropic	Weakly birefringent iridescent Cholesteric planar phase	Fan shaped texture and fine needle like crystallite	Columnar hexagonal and fan shaped texture turning to dendrimeric
0.75M	Weakly birefringent cholesteric phase	Cholesteric turning to columnar hexagonal phase.	Fan shaped+ dendrimeric	Fan shaped Texture of columnar phase
0.12 M	Cholesteric turning to columnar hexagonal	Cholesteric turning to columnar hexagonal phase	Fan shaped+ dendrimeric	Fan shaped texture Of columnar phase
0.06 M	Cholesteric turning to columnar hexagonal	Cholesteric turning to columnar hexagonal phase	Cholesteric+Fan Shaped	Cholesteric+ Columnar hexagonal
0.03 M	Cholesteric, turning to columnar hexagonal	Cholesteric turning to columnar hexagonal phase	Cholesteric+ fan shaped	Cholesteric+ Columnar hexagonal, dendrimeric growth

Table 3.A.3 presents the LC behavior of high molecular weight DNA in the presence of varying alkaline earth metal ion concentration. The transition from cholesteric to columnar hexagonal (T_{tr}) was found to be time dependent based on the size of the ion ($T_{tr}\,Mg^{2+} = T_{tr}\,Ca^{2+} < T_{tr}\,Ba^{2+} < T_{tr}\,Sr^{2+}$). On variation of metal

ion concentration, in case of Ba^{2+} and Sr^{2+}, higher metal ion concentrations favored formation of textures typical of columnar phase directly (Fig 3.A.3).

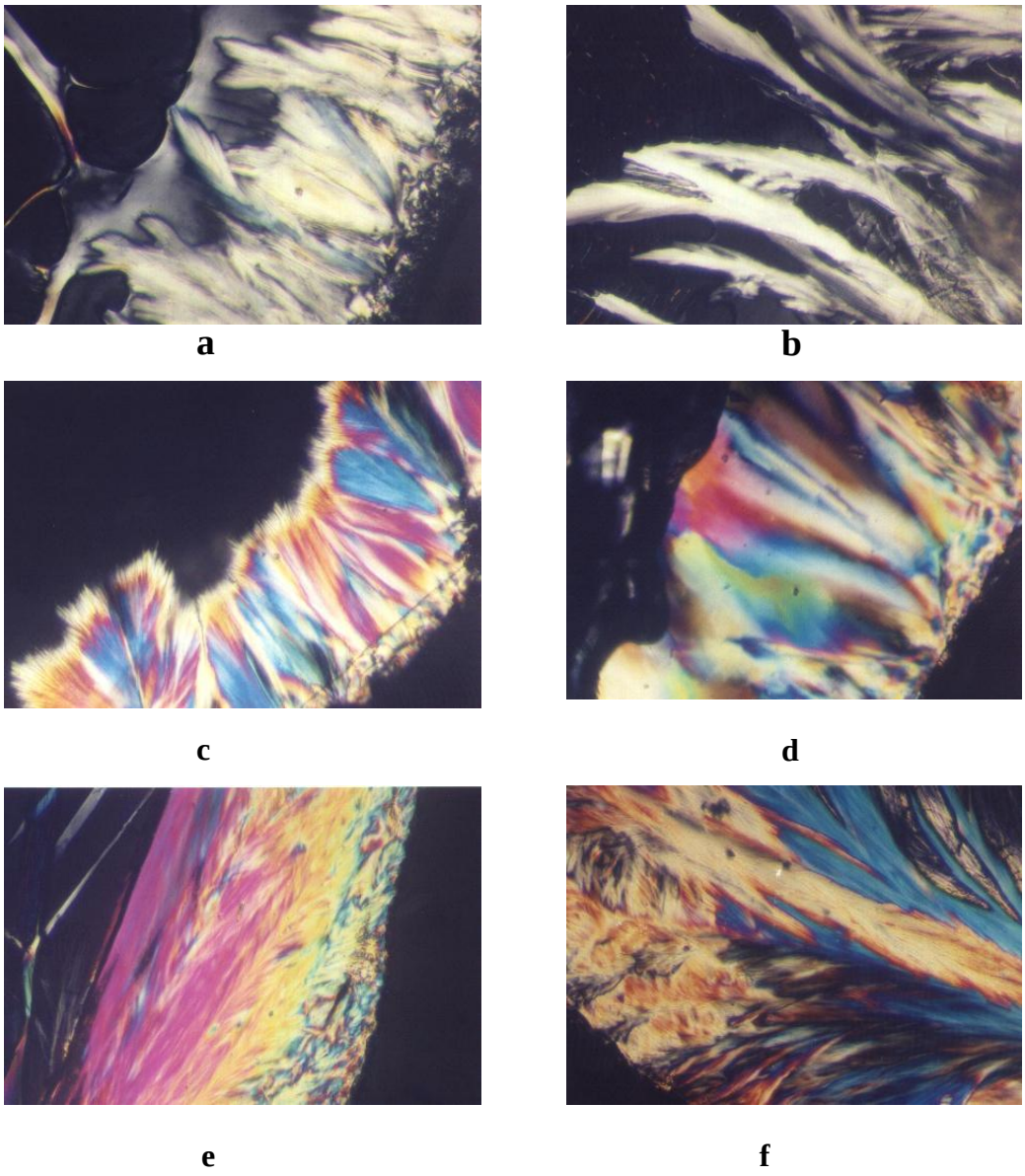

Fig.3.A.2. LC phases of high molecular weight DNA obtained in the presence of alkaline earth metal ions. a and b) shows the evolution of broken fan shaped textures typical of columnar phase from the fluidic cholesteric phase, obtained in the presence of 0.06 M Mg^{2+}, c and d) Textures typical of columnar hexagonal phase obtained with 0.06 M $BaCl_2$, e and f) Textures typical of columnar phase obtained with 0.06 M $SrCl_2$, Mag.10X obtained after 7 hrs of incubation at 37°C. Concentration of DNA ~5 mg/ml.

The columnar phase could easily be identified from its typical fan shaped textures with striated patterns (Fig 3.A.2.c, d, e and f). On the other hand, Mg^{2+} and Ca^{2+} exhibits the typical lower ordered cholesteric phase at similar concentrations (0.75 M in the case of Mg^{2+}) indicating that the size of the ion also possibly plays an important role in the stabilization of the LC phases of DNA.

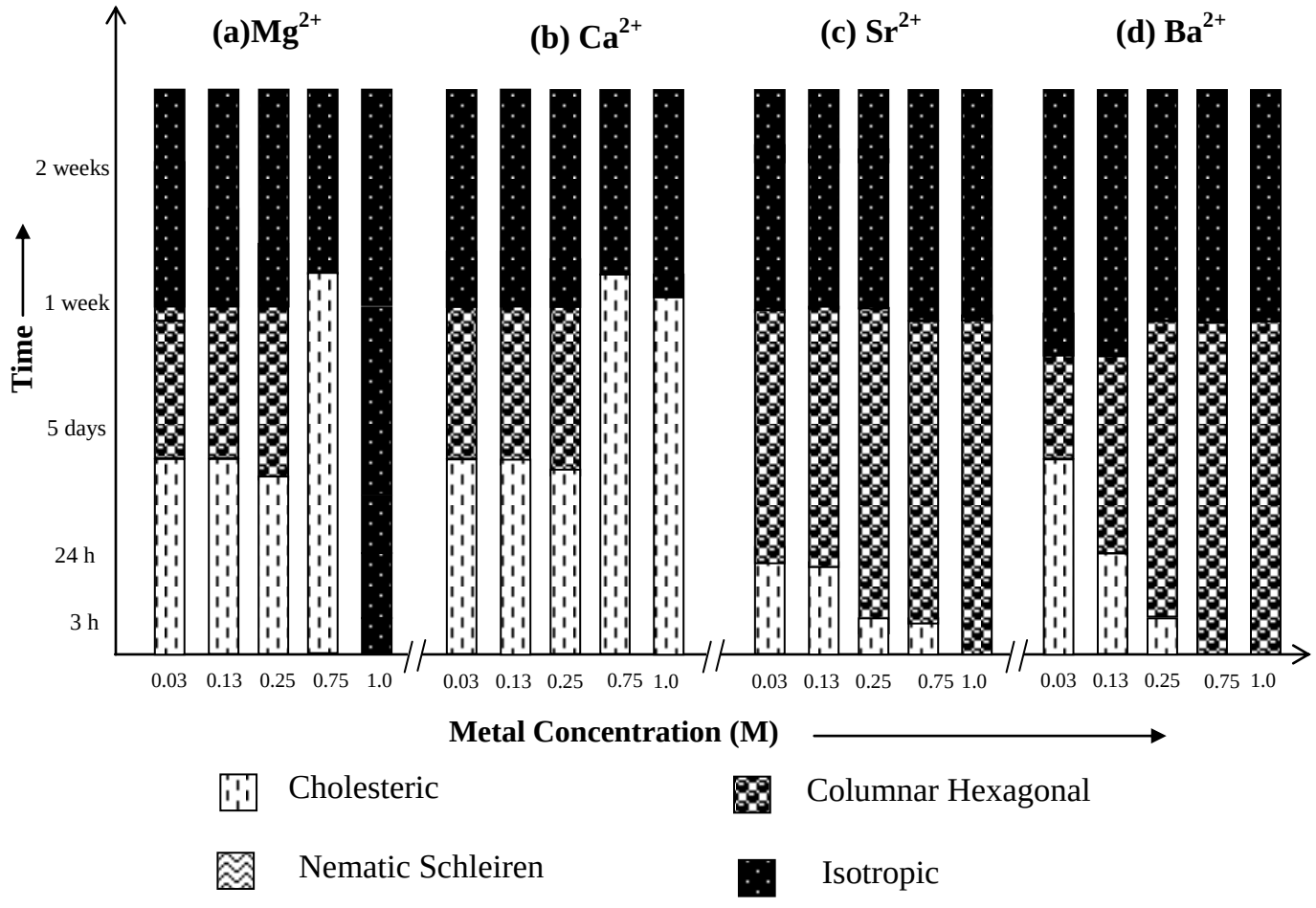

Fig.3.A.3. Time dependent phase transitions of LC DNA in the presence of alkaline earth metal ions (a) Mg^{2+}, (b) Ca^{2+}, (c) $Sr^{2+}$and (d) Ba^{2+}, (Y-axis Scales are not fixed arbitrary units.)

As the hydration energies of Ba^{2+} and Sr^{2+} are lower than Mg^{2+} and Ca^{2+}, lesser will be the water molecules around the ion, hence can dehydrate DNA faster, bringing rapid phase transitions. The fan shaped textures and striated and highly colored ribbon like textures obtained in the presence of Sr^{2+} and Ba^{2+} got darkened on prolonged incubation indicating lower stability of the phases obtained (Fig.3.A.3.c and d).

The T_{tr} values vary from hours to days and the nature of the phases obtained initially were birefringent cholesteric planar like textures, which adopted a more ordered columnar phase. All the phases obtained in the presence of alkaline earth metal ions started darkening after 8 days (T_{iso}) of sample preparation. The formation of columnar[41] textures in the presence of Mg^{2+} and Ca^{2+} also suggests their importance in inducing the most efficient packing of DNA molecules in vivo. It appears that the size dependency could be of use, in trapping a particular texture of DNA for applications, in designing DNA based devices such as biosensors, chips etc.

The binding sites of the alkaline earth metal ions on DNA were probed using IR spectra and CD measurements. The IR spectra obtained for alkaline earth metal-DNA complexes were almost similar to that of DNA without metal ions, except a slight shift of 1-2 cm^{-1} and an increase in intensity in the phosphate region 1223 cm^{-1},[42] which supports the phosphate binding nature of alkali metal ions (see Appendix Fig.1.B). Our CD experiments on the dilute solutions of DNA with these metal ions are also in agreement with this fact, and there was no significant

deviation from the B-conformation. Absence of shift in absorbance indicates that the binding of the metal ions were purely to phosphates and not to bases (see Appendix Fig.3). The present data on the mesophase structures, therefore, indicates that the alkaline earth metal ions stabilizes the helical rod like structures contributing to the supramolecular order in DNA through interaction with the negatively charged phosphate moieties.

3.A.5. Conclusions

The effects of alkaline earth metal ions such as Mg^{2+}, Ca^{2+}, Ba^{2+} and Sr^{2+} on the LC organization of high molecular weight DNA were studied using polarized light microscopy. DNA-alkaline earth metal systems show multiple LC textures depending on the type of the metal ion bound to DNA. C_D required to exhibit anisotropic behavior in the presence of alkaline earth metal ions was found to be higher than alkali metal ions, which suggests that both the size and charge of the counter ion had influenced the induction of LC behavior in DNA. C_D required to exhibit LC behavior in the presence of Mg^{2+}, was found to be quite higher, compared to Ca^{2+}, which in turn was higher than Ba^{2+} and Sr^{2+}. Mg^{2+} stabilizes the hydrogen bounded water network by its outer sphere binding to phosphate groups and, as a result prevents the dehydration of DNA strands, which is essential to exhibit LC behavior. The difference in C_D can be attributed to its different hydration factor and binding mechansims. The transition from cholesteric to columnar hexagonal (T_{tr}) was found to be time dependent, based on the size of the ion (T_{tr} Mg^{2+} = T_{tr} Ca^{2+} < T_{tr} Ba^{2+} < T_{tr} Sr^{2+}). The direct formation of higher

ordered columnar phase at higher concentrations of Ba^{2+} and Sr^{2+} might be due to their larger size and inner sphere-binding mode, which presumably facilitated the dehydration process, to achieve the textures typical of columnar phase. The formation of columnar textures in the presence of Mg^{2+} and Ca^{2+} also suggests their importance in inducing the most efficient packing of DNA molecules in vivo. It appears that the size dependency could be of use, in trapping a particular texture of DNA for applications in designing DNA based devices such as biosensors, chips etc.

3.A.6. References

1. Cini, R.; Burla, M. C.; Nunzi, A.; Polidori, G. P.; Zanizzi, P. F., *J Chem Soc Dalton Trans* **1984**, 2467.
2. Theophanides, T.; Anastassopoulou, J., *Metal binding and conformational changes.* Willey,1987.
3. Missailides, S.; Anastassopoulou, J.; Fotopoulos, N.; Theophanides, T., *Asian J Phy* **1997,** 6, 481.
4. Duguid, J. G.; Bloomfield, V. A.; Benevides, J. M.; Thomas, G. J., *Biophys. J.* **1995,** 69, 2623.
5. Christianson, D. W., *Prog. Biophys. Mol. Biol.* **1997,** 67, 217.
6. Glusker, J. P., *Adv. Protein Chem.* **1991,** 42, 1.
7. Holm, R. H.; Kennepohl, P.; Solomon, E. I., *Chem. Rev.* **1996,** 96, 2239.
8. Anastassopoulou, J.; Theophanides, T., *Critical Reviews in Oncology/Hematology* **2002,** 42, 79.
9. Misra, V. K.; Draper, D. E., *Biopolymers* **1998,** 48, 113.
10. Chiu, T. K.; Dickerson, R. E., *J. Mol. Biol.* **2000,** 301, 915.
11. Howerton, S. B.; Sines, C. C.; VanDerveer, D.; Williams, L. D., *Biochemistry* **2001,** 40, 10023.
12. Tereshko, V.; Wilds, C. J.; Minasov, G.; Prakash, T. P.; Maier, M. A.; Howard, A.; Wawrzak, Z.; Manoharan, M.; Egli, M., *Nucleic Acids Res.* **2001,** 29, 1208.
13. Ma, C.; Bloomfield, V. A., *Biophys. J.* **1994,** 67, 1678.
14. Duguid, J. G.; Bloomfield, V. A., *Biophys. J.* **1995,** 69, 2642.
15. Andrushchenko, V. V.; Kornilova, S. V.; Kapinos, L. E.; Hackl, E. V.; Galkin, V. L.; Grigoriev, D. N., *J. Mol. Struct.* **1997,** 408-409, (1), 225.
16. Krakauer, H., *Biopolymers* **1972,** 11, 811.

17. Sclavi, B.; Sullivan, M.; Chance, M. R.; Brenowitz, M.; Woodson, S. A., *Science* **1998,** 279, 1940.
18. Manfait, M.; Theophanides, T., *Magnesium* **1983,** 2, 323.
19. Suh, W. C.; Ross, W.; Record, M. T., *Science* **1993,** 259, 358.
20. Teeter, M. M.; Quigley, G. J.; Rich, A., *Nucleic acid- metal ion interactions*. ed.; Wiley: 1980.
21. Theophanides, T., *I. J. Quantum Chem* **1984,** 25, 933.
22. Craig, M. L.; Suh, W. C.; Record, M. T., *Biochemistry* **1995,** 34, 15624.
23. Hackl, E. V.; Kornilova, S. V.; Blagoi, Y. P., *Int. J. Biol. Macro.* **2005,** 35, 175.
24. Livolant, F.; Leforestier, A., *Prog.Polym.Sci.* **1996,** 21, 1115.
25. Korolev, N.; Nordenskiold, L., *Biomacromolecules* **2000,** 1, 648.
26. Davidson, M. W.; Strzelecka, T. E.; Rill, R. L., *Nature* **1988,** 331, 457.
27. Pelta, J.; Jr; Durand, D.; Doucet, J.; Livolant, F., *Biophys. J.* **1996,** 71, 48.
28. Strzelecka, T. E.; Rill, R. L., *Biopolymers* **1990,** 30, 57.
29. Tu, A. T.; Reinosa, J. A., *Biochemistry* **1966,** 5, 3375.
30. Sutherland, G. B. B. M.; Tsuboi, M., *Proc. Royal Soc. London* **1957,** 239, Ser. A., 446.
31. Besik, K. I., *Biophysical Chemistry* **2000,** 84, 227.
32. Widom, J., *Annu. Rev. Biophys. Biomol. Struct.* **1998,** *27*, 285.
33. Knowles, J. R., *Annu. ReV. Biochem.* **1980,** *49*, 877.
34. Bamann, E., Trapmann, H., Fischler, F., *Biochem. Z.* **1954,** *328*, 89.
35. Widom, J., *J. Mol. Biol.* **1986,** 190, 411.
36. Salyanov.V.I.; Lavrentev, P. I.; Chernuka, B. A.; Evdokimov, Y. M., Mol. Biol., **1995,** 28, 796.
37. Catte, A.; Cesare-Marincola, F.; Van der Maarel, J. R. C.; Saba, G.; Lai, A., *Biomacromolecules* **2004,** 5, 1552.

38. Bloomfield, V. A.; Ma, C.; Arscott., P. G.; Schitz, K. S.*Macro-Ion Characterization from Diluted Solutions to Complex Fluids.* ed.; American Chemical Society: Washington, D.C. 1994.

39. Bloomfield, V. A.; Crothers, D. M.; Tinoco, I., J. *Nucleic Acids: Structures, Properties and Functions.* ed.; University Science Books: Mill Valley, 2000.

40. Cotton, F. A.; Wilkinson, G., *Advanced Inorganic Chemistry*. 3 ed.; Wiley Eastern: 1992.

41. Strey, H., H; Wang, J.; Podgornik, R.; Rupprecht, A.; Parsegian, V. A.; Sirota, E., B., *Physical Review Letters* **2000,** 84, 3105.

42. Andrushchenko, V. V.; Kornilova, S. V.; Kapinos, L. E.; Hackl, E. V.; Galkin, V. L.; Grigoriev, D. N.; Blagoi, Y. P., *J Mol. Str.* **1997,** 408-409, (1), 225.

CHAPTER 3B

A BASE-SUGAR-PHOSPHATE THREE-LAYER ONIOM MODEL FOR CATION BINDING: BINDING AFFINITIES OF ALKALINE EARTH METAL IONS FOR PHOSPHATE GROUP IN DNA

3.B.1. Abstract

The interaction of hydrated Mg^{2+} and Ca^{2+} ions with a DNA fragment containing two phosphate groups, three sugar units and a G⎯C base pair was modelled in the anion (one negative charge) and dianion states (two negative charges) using a three layer ONIOM approach. Among the three metal binding combinations (outer sphere, inner sphere mono- and bi-dentate) studied, a mono-dentate binding mode was the most stable structure observed for both the ions in the anion model. However, the binding interactions of Mg^{2+} and Ca^{2+} to the DNA fragment in the dianion model gave rise to a large structural deformation at the base pair region, which led to the formation of "ring" structures. In both the anion and dianion models, Mg^{2+} bound structures were considerably stabler than the corresponding Ca^{2+} bound structures, which strongly supported the higher coordination power of the Mg^{2+} towards DNA systems, for its bending. The charge of the DNA fragment appeared to be crucial in deciding the binding strength as well as the binding mechanism of the metal ions. The outer sphere binding of Mg^{2+}

ion to the dianion model of DNA, is a point of support to the higher C_D required for LC behavior of DNA in the presence of Mg^{2+} ion.

3.B.2. Introduction

DNA-metal ion interactions play critical roles in the control of DNA conformation and its topology[1-7]. These interactions are governed by several parameters such as the nature of the metal, its size and charge[8-12]. All these parameters influence the conformation of DNA by direct or indirect interaction through the water molecules with the basic sites of the nucleotides[13]. Although monovalent cations have been found in a few cases to be localized at preferred binding sites of DNA with low occupancies, the stable and specific solvation geometries adopted by divalent cations endow them with the ability to strongly and selectively bind DNA[14-17]. For instance, coordination of phosphate moieties by alkaline-earth cations such as Mg^{2+} and Ca^{2+} is essential in folding and winding of the polynucleic acids, to assume compact arrangements (LC states) *in vivo*[18] for catalytic enzymatic reactions involving de-esterification of phosphate esters,[19, 20] for the stabilization of triple and quadruple helices, for the processes involving the transfer of genetic information and the synthesis of oligonucleotides[21] etc.

Theoretical studies performed by Sponer[22-27] et al. on small model systems such as base pairs nucleotides, solvated metal ions and by Petrov and co-workers[28-30] on dimethyl phosphate anion and works by other groups[31-38] has shed new insights into metal ion binding to nucleic acids. In native DNA, usually the electronegative oxygen atoms of the phosphate group are projected towards the

exterior of the double helix and the small models selected so far are largely ineffective in replicating such geometrical constraints. Moreover, a model containing dimethyl phosphate anion and a dication gives a net positive charge on the system, which is unrealistic because one would expect either neutralized or excess negative charge on DNA. This has prompted us to investigate the effect of excess electrons on the binding properties of divalent cations to a DNA fragment where the phosphate groups are projected towards the exterior. This chapter deals with the computational analysis of the interaction of a DNA fragment, with hydrated Mg^{2+} and Ca^{2+} ions using a three-layer ONIOM approach .

3.B.3. Computational Details and Models

3.B.3.1. *A three- layer ONIOM Model*

Scheme 1 gives the dianion model of DNA fragment interacting with the hexahydrated metal dication in the outer sphere-binding mode. This model is designated as $(H_2O)_2$—$^{-}$PSG—CSP^{-}— M_{hyd}, where P, S, G, and C stands for the phosphate, sugar, guanine, and cytosine moieties respectively and M_{hyd} for a hexahydrated dication. In order to avoid a bare phosphate group in the system, the water dimer is used as a micro solvation model. A three layer ONIOM method, developed by Morokuma and co-workers[39-41] as the QM-MM technique was utilized to study the metal ion interactions with the DNA segment. ONIOM is a general hybrid method, which can combine both molecular orbital as well as molecular mechanics methods and it is now becoming an effective and

indispensable tool to study the chemical structure and reactivity of large molecular systems[42,43].

According to the ONIOM terminology, the model $(H_2O)_2$_$^{-}$PSG_CSP^{-}_M_{hyd} is divided in to three layers, viz. (i) a high layer, (ii) medium layer and (iii) low layer which are illustrated in Scheme 1. The hexahydrated structure of the metal is chosen in the high layer because it is the most commonly observed primary solvation shell of Mg^{2+} and Ca^{2+} (See Appendix for the hydration studies). For the high layer, the hybrid density functional B3LYP method[44,45] in conjunction with the standard 6-31G(d) basis set was employed[46]. The medium layer was treated with the semiempirical PM3 method[47]. The low layer of the system is treated using the UFF (Universal Force Field) method of MM (Molecular Mechanics)[48]. This force field is particularly useful to treat the steric effect imposed by the sugar unit and by doing so the direct electronic interaction between the QM layer and the medium layer can be prevented which in turn will keep the phosphate moiety projecting towards the exterior of the DNA fragment. Because of the computational limitations, we could not extend our studies with other alkaline earth metal ions. In addition to the outer sphere-binding mode given in Scheme 1, the inner sphere mono- and bi-dentate binding modes (Scheme 2) were also studied. In these models, one or two water molecules move (s) out from the hexahydration shell (one for mono- and two for bi-dentate) to make room for the direct metal-phosphate oxygen bonds. Further, an anion model was also studied to compare the results obtained from the dianion model. In the anion model, the two

water molecules in the medium layer is replaced with a proton on the O^- and it is labeled as HPSG_CSP$^-$_ M_{hyd}. An anion HPSG_CSP$^-$ and dianion $^-$PSG_CSP$^-$ structures without the hexahydrated metal ions were also located.

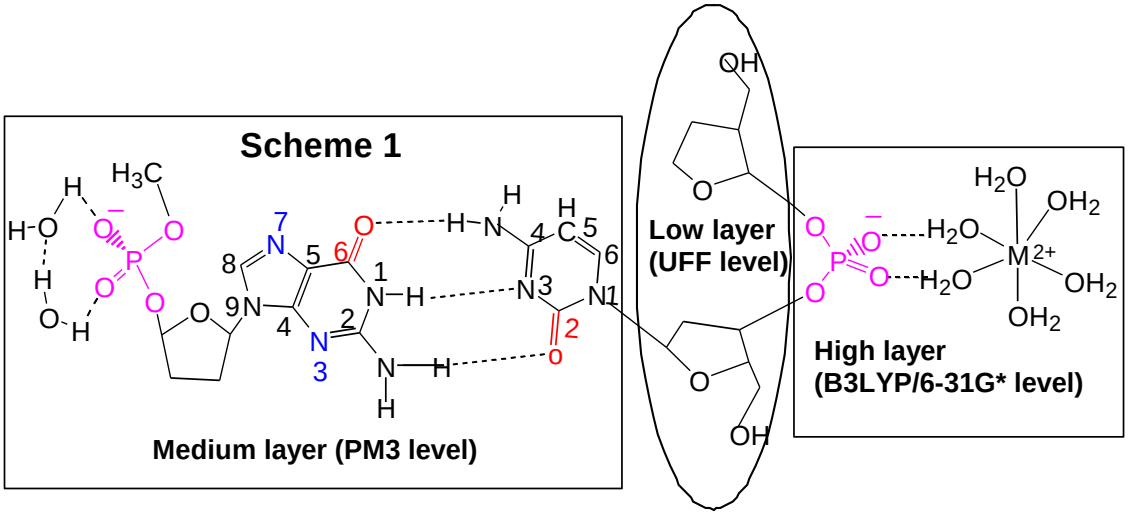

Fig.3.B.1. Scheme of the real and model system used in the ONIOM calculations for DNA-hydrated metal interaction.

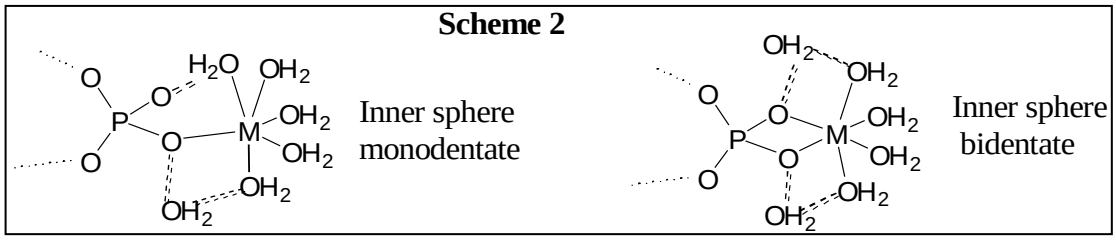

Fig.3.B.2. Scheme of the different binding modes selected to study hydrated alkaline earth metal ions and phosphate anion interactions.

For interaction energy calculations, structures of hydrated metal ions were also fully optimized at B3LYP/6-31G(d) level of theory (See Appendix for the details).

3.B.3.2. *Interaction Energy Calculations*

In the present calculations, the following four geometry types were optimized with a three-layer ONIOM method, viz.

(i) The bare anion HPSG…CSP^{-},

(ii) The bare dianion $(H_2O)_2$...$^{-}$PSG…CSP^{-}

(iii) Metal-anion system, HPSG…CSP^{-}…$M(H_2O)_n$, and

(iv) Metal-Dianion system $(H_2O)_2$...$^{-}$PSG…CSP^{-}…$M(H_2O)_n$.

In type (i) and type (ii) geometries, the main interaction is between the bases G and C, while in type (iii) and (iv) structures, base pair as well as the hydrated metal and phosphate anion interactions occur. Therefore the following interaction energies (E_{int}) were estimated.

For G_C base pair interaction energy in the bare anion,

$$E1 = E(HPSG) + E(CSP^{-}) - E(HPSG\_CSP^{-}) + E1_{BSSE} \quad (1)$$

For G_C base interaction energy in the bare dianion,

$$E2 = E((H_2O)_2\_^{-}PSG) + E(CSP^{-}) - E((H_2O)_2\_^{-}PSG\_CSP^{-}) + E2_{BSSE} \quad (2)$$

For G_C base pair interaction energy in the metal bound anion systems,

$$E3 = E(HPSG) + E(CSP^{-}\_ M_{hyd}) - E(HPSG\_CSP^{-}\_ M_{hyd}) + E3_{BSSE} \quad (3)$$

For G_C base pair interaction energy in the metal bound dianion systems,

$$E4= E((H_2O)_2\_^{-}PSG) + E(CSP^{-}\_ M_{hyd}) - E((H_2O)_2\_^{-}PSG\_CSP^{-}\_ M_{hyd})) + E4_{BSSE} \quad (4)$$

For metal ion_phosphate interaction energy in the anion systems,

$$E5 = E(HPSG\_CSP^{-}) + E(M_{hyd}) - E(HPSG\_CSP^{-}\_ M_{hyd}) + E5_{BSSE} \quad (5)$$

For hydrated metal ion–phosphate interaction energy in the dianion systems,

$$E6 = E((H_2O)_2\text{—}^{-}PSG\text{—}CSP^{-}) + E(M_{hyd}) - E((H_2O)_2\text{—}^{-}PSG\text{—}CSP^{-}\text{—}M_{hyd}) + E6_{BSSE} \quad (6)$$

E is the total energy of the systems given in parenthesis. In order to get a reasonable estimate of the E_{int} values, the single point energies of the ONIOM optimized structures of all the anionic ($HPSG\mathbf{\ldots}CSP^{-}\mathbf{\ldots}M_{hyd}$) and dianionic ($(H_2O)_2\mathbf{...}\,^{-}PSG\mathbf{\ldots}CSP^{-}\mathbf{\ldots}M_{hyd}$) are calculated with the B3LYP/6-31G(d) level. Further, E values at B3LYP/6-31G(d) level are calculated for the fragment structures HPSG, $(H_2O)_2...\,^{-}PSG$, and CSP^{-} taken from their respective full systems. Names in regular font are of fully optimized ONIOM level structures and those in italics are of the fragment structures taken from the fully optimized systems. The $E1_{BSSE}$ to $E6_{BSSE}$ are the BSSE corrections to be obtained by employing the counterpoise correction method of Boys and Bernardi[49].

3.B.4. Results and Discussion

3.B.4.1. *The Bare Anion and Dianion Models of DNA*.

The details of this section are same as given in the section 2.B.4.1 of Chapter 2 B.

3.B.4.2. *The HPS…CSP⁻…M(H₂O)₄ Anion Models*

The hydration studies of alkaline earth metal ions suggest that the primary solvation shell contains only six water molecules (See details in Appendix, Fig. 8).

The binding of alkaline earth metal ions such as Mg^{2+} and Ca^{2+} to the phosphate group in the anion model, with different binding mechanisms was optimized at the ONIOM level according to the schemes, given in Fig.3.B.1 and 3.B.2.

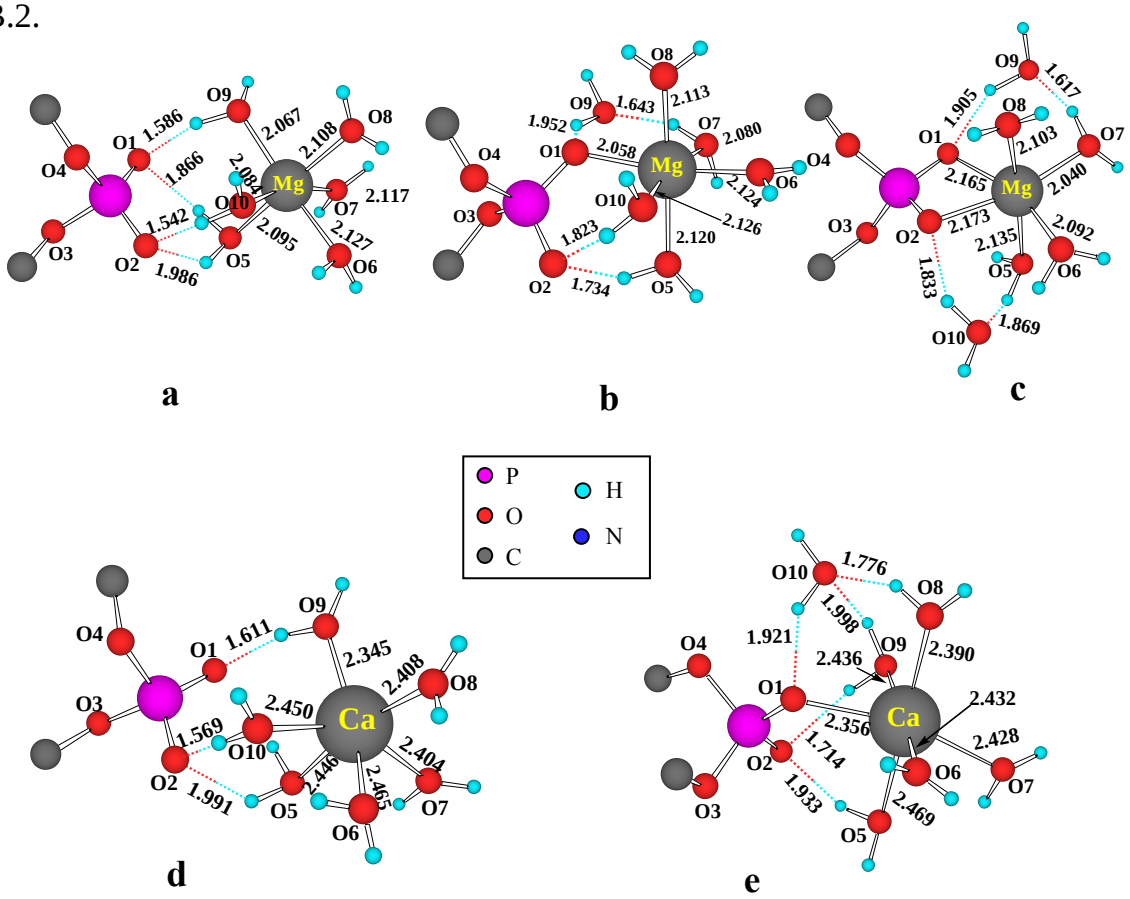

Fig.3.B.3. The HPSG…CSP$^-$ $M(H_2O)_6$ anion model. (a), (b) and (c) are the outer sphere, inner sphere mono- and inner sphere bi-dentate structures for Mg^{2+} ion respectively. (d) and (e) are the outer sphere and inner sphere mono-dentate structures of Ca^{2+} ion, respectively.

The ONIOM level optimization of the anion models gave outer sphere, inner sphere mono- and inner sphere bi-dentate structures for Mg^{2+} and outer sphere and inner sphere mono-dentate structures for Ca^{2+}. In order to have a closer look at the hydrated metal ion region interacting with the phosphate anion, the QM

layer of all the binding modes located with both Mg^{2+} and Ca^{2+} ions with the anion model is presented in Fig. 3.B.3.

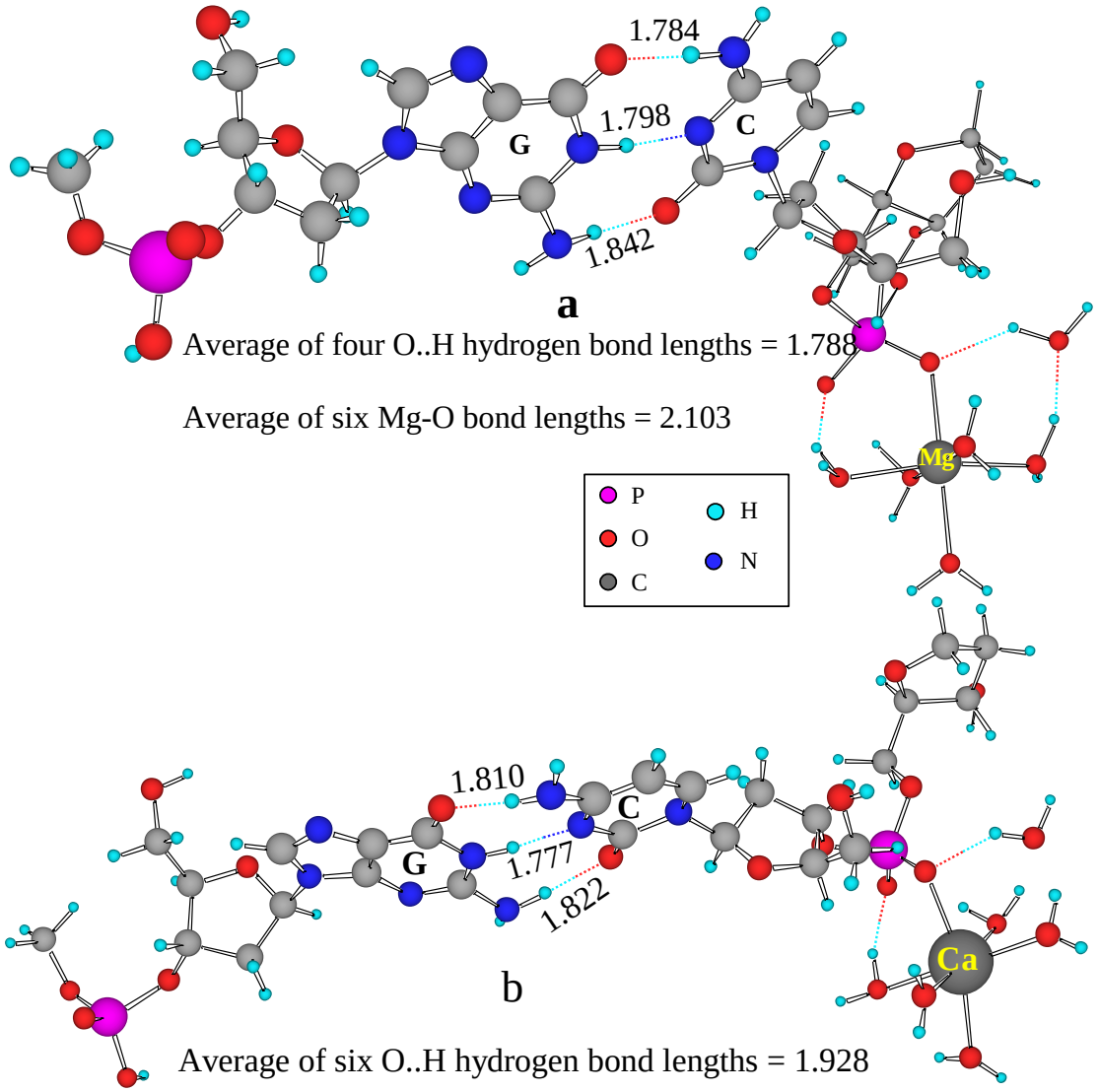

Fig.3.B.4. Inner sphere mono-dentate anion models of (a) Mg^{2+} and (b) Ca^{2+} binding. All bond lengths are in Å.

All attempts to find an inner sphere bi-dentate structure for Ca^{2+} ion failed. With both the metal ions, the most stable structure found was the inner sphere mono-dentate and the ONIOM optimized full geometries are depicted in Fig.

3.B.4.a and 3.B.4.b for Mg^{2+} and Ca^{2+} respectively. Both the structures were very similar to each other and the most significant difference between them was in their average O⎯H hydrogen bond lengths observed at the metal ion hydration region.

Compared to a shorter O⎯H value of 1.788 Å in Mg^{2+} system, a significantly large O⎯H value of 1.928 Å is found in the Ca^{2+} system. Similarly, compared to the average Mg-O distance of 2.103 Å, a larger value of 2.419 Å is observed for the average Ca-O distance, which may be attributed to the larger ionic radius of Ca^{2+} as compared to that of the Mg^{2+} ion (See Appendix for bond length information, Table 8, 9 and 10). These results indicate a stronger affinity of the hydrated Mg^{2+} compared to hydrated Ca^{2+} to bind with the phosphate anion of the DNA fragment. Table 3.B.1 lists the metal ion- phosphate interactions energy data (E_{int}^{M}), for tetrahydrated Mg^{2+} and Ca^{2+} ions in the outer-sphere, inner-sphere monodentate and bidentate binding modes for both anion and dianion models.

Table.3.B.1. Phosphate-hydrated metal ion interaction energy in anion (E5) and dianion (E6) models. Values in parenthesis are the BSSE corrections. All values are in kcal/mol.

Model Systems	Outer		Inner sphere monodentate		Inner sphere bidentate	
	E5 (anion)	E6 (dianion)	E5 (anion)	E6 (dianion)	E5 (anion)	E6 (dianion)
Mg^{2+}	175.2 (8.7)	315.7 (14.5)	185.4 (11.3)	304.2 (16.9)	180.8 (15.2)	295.8 (15.2)
Ca^{2+}	166.2 (10.2)	Not found	178.5 (12.3)	216.3 (14.6)[a] 286.1 (17.4)[b]	Not found	Not found

[a] "Linear" structure and [b] "ring" structure

The higher E_{int}^{M} values (E5) of anion models given in Table 3.B.1, also suggest the higher affinity of Mg^{2+} ions to DNA than Ca^{2+} ions, irrespective of the binding modes.

Table 3.B.2 shows the GC base pair interaction energy data of anion and dianion models calculated according to equations 1-4. It can be seen from the E3 values that in the case of anion model containing metal ion (HPSG_CSP^{-}_ M_{hyd}), both metal ions show nearly the same G_C base pair interaction energy, which is in the range of 21.7 to 22.3 kcal/mol.

Table. 3.B. 2. G_C base pair interaction energy in anion (E3) and dianion (E4) models. Values in parenthesis are the BSSE corrections. All values are in kcal/mol.

Model Systems	Outer sphere		Inner sphere mono-dentate		Inner sphere bi-dentate	
	E3 (anion)	E4 (dianion)	E3 (anion)	E4 (dianion)	E3 (anion)	E4 (dianion)
Mg^{2+}	22.9 (4.4)	Ring structure	22.6 (4.4)	Ring structure	22.3 (4.5)	Ring structure
Ca^{2+}	21.7 (4.4)	Not found	22.0 (4.4)	34.1 (4.6)	Not found	Not found

3.B.4.3. *The $[(H_2O)_2\ldots{}^{-}PSG\ldots CSP^{-}\ldots M(H_2O)_4$ Dianion Models*

For the dianion models, an outer sphere and inner sphere mono-dentate structures were located as the most stable binding modes for Mg^{2+} and Ca^{2+} respectively (Fig.3.B.5.a and b). The inner sphere mono- and inner sphere bi-dentate structures were also located for Mg^{2+} (Fig.3.B.6a and b). A structure search for the outer sphere and the inner sphere bi-dentate binding modes of Ca^{2+} always gave the inner sphere mono-dentate structure.

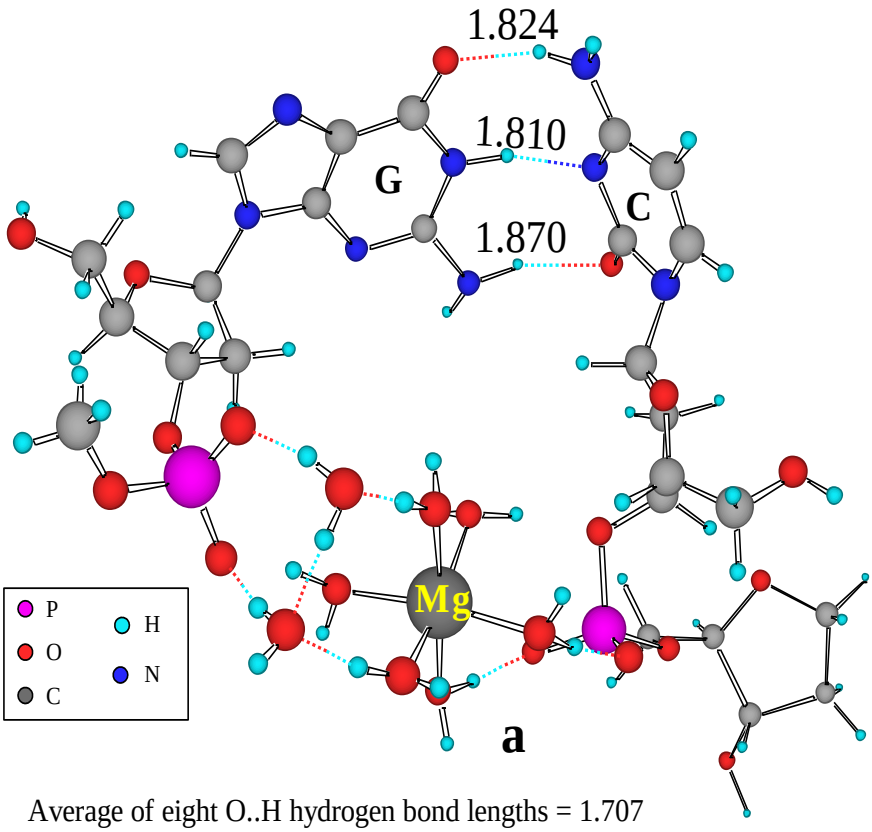

Average of eight O..H hydrogen bond lengths = 1.707

Average of six Mg-O bond lengths = 2.100

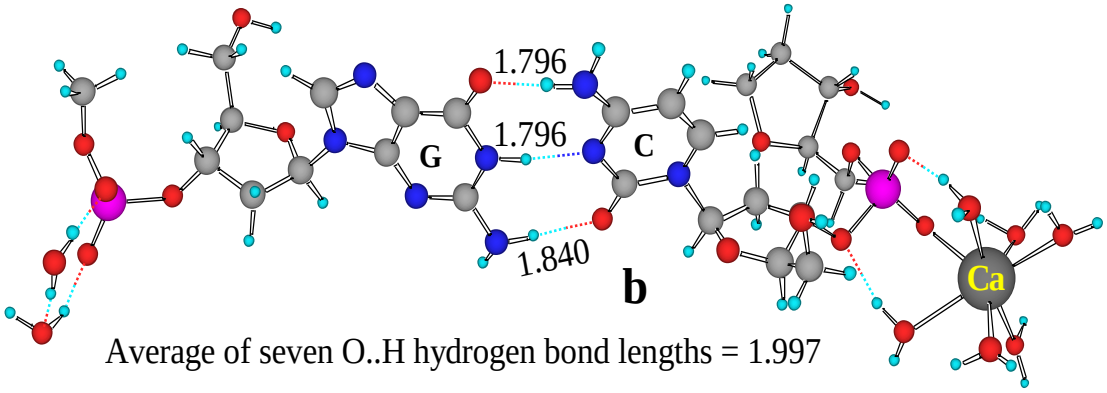

Average of seven O..H hydrogen bond lengths = 1.997

Average of six Ca-O bond lengths = 2.418

Fig.3.B.5. The $(H_2O)_2PSG\ldots CSP^-$ $M(H_2O)_6$ dianion models for alkaline earth metal ions. (a) Outer sphere binding of Mg^{2+} and (b) inner sphere mono-dentate binding of Ca^{2+}. All bond lengths are in Å.

The most interesting phenomenon occurred in the case of Mg^{2+}, where the otherwise linear fragment got bent into ring like structures in all the three binding modes studied. In this case, the Mg^{2+} binds to the cytosine end phosphate group in an outer sphere manner and to the guanine end phosphate group via water-mediated hydrogen bonds. It may be noted that in optimizing these "ring" structures, we always started with a structure where both the phosphate moieties were far apart, and these initial geometries were structurally very similar to the structures in Fig.3.B.4.a, 3.B.4.b and 3.B.5.b.

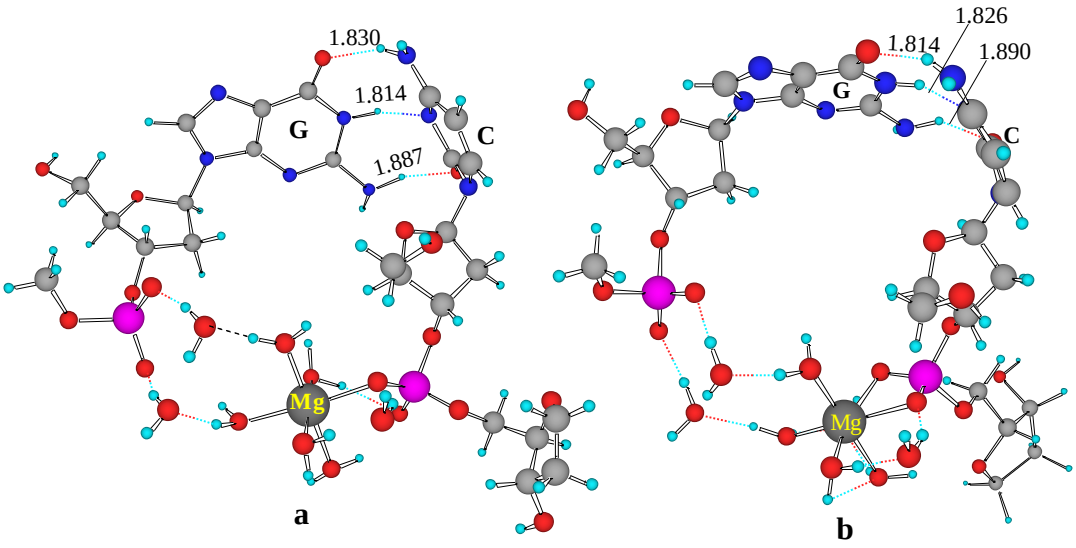

Fig.3.B.6. The $(H_2O)_2PSG\ldots CSP^{-}M(H_2O)_6$ dianion models (a) Inner sphere mono dentate binding of Mg^{2+} and (b) inner sphere bi-dentate binding of Mg^{2+}. All bond lengths are in Å.

The structures in Fig.3.B.4.a, 3.B.4.b and 3.B.5.b can be called as "linear" structures based on the linear arrangement of hydrogen-bonded atoms in their G_C base pair. In the case of Mg^{2+} dianion models, the optimization starting from a "linear" structure never converged back to such a structure, and it went all the way

to the “ring” structure. However, in the case of Ca^{2+}, starting from a “linear” structure, the optimization always gave the “linear” structure

In contrast to the “linear” mono-dentate binding mode of Mg^{2+} in the “linear” structures of the anion model, the “ring” structures of its dianion models preferred an outer sphere binding. On the other hand, Ca^{2+} ion preferred the inner sphere mono-dentate binding mode in both the anion and dianion “linear” models. The absence of “linear” structures, and the identification of “ring” structures in all the dianion models of Mg^{2+} (outer, inner mono- and inner bi- dentate) point towards to its higher coordinating, hence DNA bending ability as compared to Ca^{2+}. The drastic structural changes observed with the dianion DNA fragment on interaction with Mg^{2+} ion further suggest that the binding mode of the metal ion to DNA largely depends on the charge of the DNA fragment. These results also suggest that the typically used model of anion–dication combination giving a net positive charge is inadequate for understanding the proper binding behavior of the metal ion with DNA.

Since the automatic generation of “ring’ structures from “linear” starting structures was not succeeded in the optimization of dianion models with Ca^{2+} ion, we also attempted the geometry optimization by first constructing a “ring” structure as the initial guess geometry for the outer, inner mono- and inner bi-dentate coordination mode of hydrated Ca^{2+}. However, this procedure gave only an inner sphere mono-dentate ring structure for it. The optimization for the outer sphere converged to the inner sphere mono-dentate and for the bi-dentate structure

did not gave a meaningful structure. The optimized inner sphere mono-dentate "ring" structure of Ca^{2+} ion in the dianion model is presented in Fig.3.B.7. The interaction energies, E5 and E6 reported in Table 3.B.1 can be considered as a good measure of how strongly the hydrated metal ion bind with the phosphate groups in both the models. In anion and dianion models, Mg^{2+} binding to the phosphate groups are stronger than that of the Ca^{2+} binding. The binding energies observed for the most stable inner sphere mono-dentate anion models of both Mg^{2+} and Ca^{2+} are 85.7 and 178.5 kcal/mol respectively.

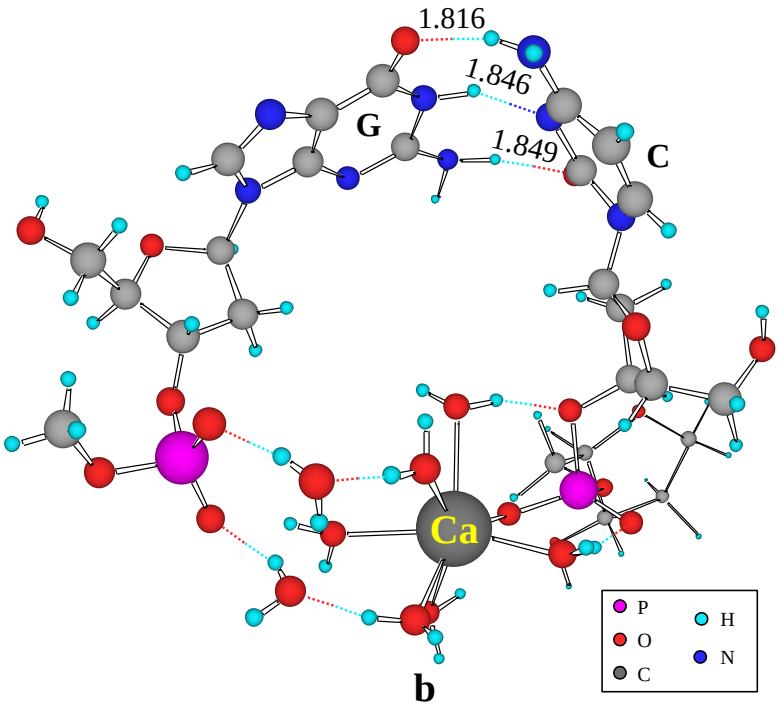

Average of eight O..H hydrogen bond lengths = 1.814

Average of seven Ca-O bond lengths = 2.483

Fig. 3.B.7. Dianion model showing the ring structure of the inner mono-dentate binding of Ca^{2+}. All bond lengths are in Å.

Very recently, Petrov and coworkers[28] studied the dimethyl phosphate anion systems with Mg^{2+} and Ca^{2+} and obtained values of 204.3 and 198.3 kcal/mol respectively for the mono-dentate structures. Although, the present model and the Petrov model are markedly different, the smaller value obtained in the present case can be attributed mainly to the weakening of the G⎯C base pair interaction. The drastic structural changes observed in the dianion models of Mg^{2+} are also reflected in their interaction energies. All the three bent structures of Mg^{2+} showed a substantial increase in their interaction energy as compared to the anion systems and the maximum increase of 80.3 % are observed in the most stable outer sphere dianion structure. On the other hand, the "linear" mono-dentate Ca^{2+} dianion structure showed an increase of 21.2 % in the interaction energy as compared to the anion structure. The high interaction energy of 315.7 kcal/mol observed for the Mg^{2+} outer sphere structure is attributed to the simultaneous interaction of the ion with both the phosphate groups. Further, this stabilization energy was 29.6 kcal/mol higher than the dianion "ring" structure of Ca^{2+} ion.

From the GC base pair interaction energy data given in Table 3.B.2, the E4 value (34.0 kcal/mol) of "linear" dianion model of Ca^{2+} (inner sphere mono-dentate) was quite high when compared to the corresponding value found in the metal free dianion system. This result is not surprising because in the "linear" dianion system, strong electrostatic interaction at the G⎯C region is expected because the dianion system can be considered as the interaction between the negatively charged $(H_2O)_2^-$PSG and the positively charged CSP^-⎯Ca^{2+} which in a

sense is an anion⎯cation interaction. It is expected that even in the dianion "ring" structures of Mg^{2+} and Ca^{2+}, a substantial amount of G⎯C base pair interaction energy is expected because in all these systems, the hydrogen bond lengths of $CO_{(G)}$ ⎯$HN_{(C)}$, $NH_{(G)}$ ⎯$N_{(C)}$, and $NH_{(G)}$ ⎯$OC_{(C)}$ were all well within the bonding region. For all the E1 to E4 energy calculations, the BSSE correction is found to be nearly a constant (4.4 to 4.6 kcal/mol).

In the "ring" structures, the interaction of the metal with phosphate groups is so dominant that the structural deformation leading to the weakening of the G⎯C base pair interaction is well compensated. In E5 and E6 calculation, the BSSE correction was found to be in the range of 8.7 to 17.4 kcal/mol.

As compared to the average O⎯H hydrogen bond length of 1.788 Å observed at the metal ion hydration region in the anion model of Mg^{2+}, the corresponding value in the dianion model ("ring" structure) was significantly shorter (1.707 Å). This suggests a stronger metal-phosphate interaction in the dianion model than the anion model and this could be attributed to the simultaneous interaction of hydrated metal ion with the two phosphate groups, leading to well -balanced charge neutralization, in the system. On the other hand, the charge is well separated in the "linear" Ca^{2+} dianion structure (negative charge at the guanine end and a net positive charge at the cytosine end), which in turn showed longer O⎯H hydrogen bond lengths (1.997 Å) than the anion model (1.928 Å). Similar to the dianion model of Mg^{2+} "ring" structures, the Ca^{2+} "ring"

structures also showed a significantly shorter average O⎯H hydrogen bond length (1.814 Å) as compared to the anion systems, which again pointed towards the importance of the simultaneous interaction of two phosphate groups to a dication (for hydrogen bond length information, see Appendix, Table 4).

Another observation is that the anion and dianion models showed nearly the same average metal-oxygen distance for Mg^{2+} as well as "linear" structures of Ca^{2+} ions. However, in the case of the "ring" structure of Ca^{2+} induced dianion systems, the average Ca-O distance of 2.483 Å is 0.064 Å larger than that found in the anion system. This difference may be attributed to the seven Ca-O bonds found in the "ring" structure (Fig.3.B.7) as compared to six metal-O distances in all other systems. Ca^{2+} has a larger coordination sphere than Mg^{2+} and therefore in the mono-dentate dianion coordination, it was able to retain the bonding interaction with all the six water molecules as well as the metal-phosphate oxygen bonding. This may be the reason for the absence of an outer sphere structure for the Ca^{2+} induced dianion systems.

The marked difference in the Mg^{2+} and Ca^{2+} binding modes have been reported in the experimental work of Tajmir-Riahi[50], where he noticed a direct binding of Ca^{2+} and indirect binding of Mg^{2+} to phosphates. Further support to the present results can be found in another study, where it has been proved that Mg^{2+} binds to DNA in an outer sphere (water-mediated) manner, while larger cations, Ca^{2+}, Sr^{2+} and Ba^{2+}, bind to DNA in an inner-sphere (direct contact) manner, which can be correlated with hydration energies of the cations. Outer sphere

complexes for Mg^{2+}-DNA were also suggested from ^{31}P-NMR and crystallographic studies.[51] One should also point out the recent study on CGCGAATTCGCG, GGCGAATTCGCG and GCGAATTCGCG crystals in the presence of Mg^{2+} and Ca^{2+} ions.[52] This work revealed that Mg^{2+} binds to the oligonucleotides in an outer sphere manner, while Ca^{2+} is engaged in more inner sphere complexes.

It is already seen that an anion-dication model of Mg^{2+} preferred the inner sphere mono-dentate binding mode while its dianion-dication model preferred the outer sphere coordination. The latter case is more realistic due to the net zero charge on the system and also it agreed with the experimental findings. In all the models used for Ca^{2+}, the inner sphere mono-dentate structure is the most stable one and this result also supported the experimental findings. The seven Ca-O bonds found in the more realistic dianion-dication "ring" structure model of Ca^{2+} suggest that the cation size is an important factor in deciding the binding mechanism. The outer sphere binding of Mg^{2+} ion to the dianion model of DNA is a point of support to the higher C_D required for LC behavior of DNA in the presence of Mg^{2+} ion. The outer sphere binding to DNA stabilizes the water structure around DNA, which does not favor LC formation, whereas inner sphere binding by Ca^{2+} ions can dehydrate DNA, which explains the reason for lower C_D in the presence of Ca^{2+} than Mg^{2+} ions.

3.B.5. Conclusions

The interactions of hydrated Mg^{2+} and Ca^{2+} ions to the phosphate group of DNA was studied by modeling a DNA fragment in an anion (one negative charge) and dianion (two negative charges) state with the phosphate geometry maintained as in native DNA (projected towards the exterior) using a three layer ONIOM – based QM-MM method. Three combinations of metal ion-DNA binding were studied, which includes the outer sphere, inner sphere mono- and inner sphere bi-dentate patterns. In the anion model, both the ions preferred the inner-sphere mono-dentate binding mechanism. However, in the case of the dianion model the metal ions induced major structural changes in the system, by bending the linear DNA fragment into stable ring like structures. Mg^{2+} induced ring structures were more stable compared to those with Ca^{2+} ion by 29.6 kcal/mol, wherein Mg^{2+} preferred outer sphere, and Ca^{2+} preferred inner sphere mono-dentate binding pattern. The present results indicate that unlike Ca^{2+} ion, the Mg^{2+} binding pattern to DNA largely depends on the charge of the DNA fragment and also give a clue to the biological roles of these metal ions in DNA bending. The binding of hydrated Mg^{2+} and Ca^{2+} ions to the dianion model of DNA revealed a more realistic picture of DNA- alkaline earth metal interactions in the cell compared to the anion model which is in good agreement with the experimental findings. To the best of our knowledge, this is the first theoretical investigation on the interaction of a comparatively larger DNA model system with the biologically important Mg^{2+} and Ca^{2+} ions. The outer sphere binding of Mg^{2+} ion to the dianion model of DNA,

is a point of support to the higher C_D required for LC behavior of DNA in the presence of Mg^{2+} ion compared to the other alkaline earth metal ions.

3.B.6. References

1. Rouzina, I.; Bloomfield, V. A. *Biophysical J.* **1998,** 74, (6), 3152.
2. Egli, M. *Curr. Opin. Chem. Biol.* **2004,** 8, (6), 580.
3. Egli, M. *Chem. & Bio.* **2002,** 9, (3), 277.
4. Subirana, J. A.; Soler-Lopez, M. *Ann. Rev. Biophys. Bimol. Struct.* **2003,** 32, 27.
5. Stellwagen, N. C.; Mohanty, U.In *Nucleic Acids: Curvature And Deformation* 2004
6. Maher, L. J., Mechanisms of DNA bending. *Curr. Opin. Chem. Biol.* **1998,** 2, (6), 688.
7. Hardwidge, P. R.; Pang, Y. P.; Zimmerman, J. M.; Vaghefi, M.; Hogrefe, R.; Maher, L. J., In *Nucleic Acids: Curvature And Deformation*, 2004.
8. Rueda, M.; Cubero, E.; Laughton, C. A.; Orozco, M. *Biophys. J.* **2004,** 87, (2), 800.
9. Anastassopoulou, J., Metal-DNA interactions. *J. Mol. Struct.* **2003,** 651, 19.
10. Sletten, E.; Froystein, N. A. In *Metal Ions In Biological Systems* 1996.
11. McFail-Isom, L.; Sines, C. C.; Williams, L. D., *Curr. Opin. Strcut. Biol.* **1999,** 9, (3), 298.
12. McConnell, K. J.; Beveridge, D. L., *J. Mol. Biol.* **2000,** 304, (5), 803.
13. Missailides, S.; Anastassopoulou, J.; Fotopoulos, N.; Theophanides, T., *Asian. J. Phy.* **1997,** 6, 481.
14. Duguid, J. G.; Bloomfield, V. A.; Benevides, J. M.; Thomas, G. J., *Biophys. J.* **1995,** 69, 2623.
15. Christianson, D. W., *Prog. Biophys. Mol. Biol.* **1997,** 67, 217.
16. Glusker, J. P., *Adv. Protein Chem.* **1991,** 42, 1.
17. Holm, R. H.; Kennepohl, P.; Solomon, E. I., *Chem. Rev.* **1996,** 96, 2239.
18. Widom, J., *Annu. Rev. Biophys. Biomol. Struct.* **1998,** 27, 285.
19. Knowles, J. R., *Annu. ReV. Biochem.* **1980,** 49, 877.
20. Bamann, E., Trapmann, H., Fischler, F., *Biochem. Z.* **1954,** *328*, 89.

21. Marzilli, L. G. K., T. J.; Eichhorn, G. L., *In Nucleic Acid-Metal Ion Interactions,* John Wiley and Sons 1980.
22. Sponer, J.; Burda, J. V.; Leszczynski, J.; Hobza, P. *J. Biomol. Struc. & Dynam.* **1999,** 17, (1), 61.
23. Sponer, J.; Hobza, P. *Chem. Comm.* **2003,** 68, (12), 2231.
24. Sponer, J.; Leszczynski, J.; Hobza, P *J. Mol. Stru. Theochem* **2001,** 573, 43.
25. Sponer, J.; Sabat, M.; Burda, J. V.; Leszczynski, J.; Hobza, P.; Lippert, B. *J. Biol. Inorg. Chem.* **1999,** 4, (5), 537.
26. Sponer, J. E.; Sychrovsky, V.; Hobza, P.; Sponer, J. *Phys. Chem. Chem. Phys.* **2004,** 6, (10), 2772.
27. Munoz, J.; Sponer, J.; Hobza, P.; Orozco, M.; Luque, F. J. *J. Phys. Chem. B* **2001,** 105, (25), 6051.
28. Petrov, A. S.; Funseth-Smotzer, J.; Pack, G. R. *Int. J. Quant. Chem.* **2005,** 102, (5), 645.
29. Petrov, A. S.; Lamm, G.; Pack, G. R. *J. Phys. Chem. B* **2002,** 106, (12), 3294.
30. Petrov, A. S.; Lamm, G.; Pack, G. R., *J. Phys. Chem. B* **2004,** 108, 6072.
31. Bandyopadhyay, D.; Bhattacharyya, D.*J. Biomol. Struc. & Dynam.* **2003,** 21, (3), 447.
32. Bertran, J.; Rodriguez-Santiago, L.; Sodupe, M. *J. Phys. Chem. B* **1999,** 103, (12), 2310.
33. Zeizinger, N.; Burda, J. V.; Sponer, J.; Kapsa, V.; Leszczynski, J. *J. Phys. Chem. A* **2001,** 105, (34), 8086.
34. Murashov, V. V.; Leszczynski, J. *J. Phys. Chem. B* **1999,** 103, (39), 8391.
35. Rodger, A.; Sanders, K. J.; Hannon, M. J.; Meistermann, I.; Parkinson, A.; Vidler, D. S.; Haworth, I. S. *Chirality* **2000,** 12, (4), 221.
36. Marincola, F. C.; Denisov, V. P.; Halle, B. *J. Am. Chem. Soc.* **2004,** 126, (21), 6739.
37. Kankia, B. I. *Biopolymers* **2004,** 74, (3), 232.

38. Jerkovic, B.; Bolton, P. H. *Biochemistry* **2001,** 40, (31), 9406.
39. Svensson, M.; Humbel, S.; Froese, R. D. J.; Matsubara, T.; Sieber, S.; Morokuma, K., *J. Phys. Chem.* **1996,** 100, 19357.
40. Humbel, S.; Sieber, S.; Morokuma, K., *J. Chem. Phys.* **1996,** 105, 1959.
41. Dapprich, S.; Komaromi, I.; Byun, K. S.; Morokuma, K.; Frisch, M. J., *J. Mol. Struct.THEOCHEM* **1999,** 461-462, 1.
42. Tschumper, G. S.; Morokuma, K., *J. Mol. Struct.: THEOCHEM* **2002,** 592, 137.
43. Re, S.; Morokuma, K. *J. Phys. Chem. A* **2001,** 105, (30), 7185.
44. Becke, A. D., *J. Chem. Phys.* **1993,** 98, 5648.
45. Becke, A. D. *Phys. Rev. A* **1988,** 38, (6), 3098.
46. Hariharan, P. C.; Pople, J. A., *Mol. Phys.* **1974,** 27, 209.
47. Stewart, J. J. P., *J. Comp. Chem.* **1989,** 10, 209.
48. Rappé, A. K.; Casewit, C. J.; Colwell, K. S.; Goddard III, W. A.; Skiff, W. M., *J. Am. Chem. Soc.* **1992,** 114, 10024.
49. Boys, S. F.; Bernardi, F., *Mol. Phys.* **1970,** 19, 553.
50. Tajmir-Riahi, H. A., *Biopolymers* **1991,** 31, 101.
51. McFail-Isom, L.; Shui, X.; Williams, L. D., *Biochemistry* **1998,** 37, 17105.
52. Minasov, G.; Tereshko, V.; Egli, M., *J. Mol. Biol.* **1999,** 291, 83.

CHAPTER 4

THE EFFECTS OF MULTIVALENT, TRANSITION AND HEAVY METAL IONS ON THE LIQUID CRYSTALLINE PHASES OF DNA

4.1. Abstract

The role of multivalent (Al^{3+}), transition metal ions (Cu^{2+}, Cd^{2+}, V^{4+}) and heavy metal ions (Hg^{2+}, Pd^{2+}, Au^{3+}, Pt^{4+}) on the LC phase behavior of high molecular weight DNA was studied. The multivalent, transition and heavy metal ions differed considerably from alkali and alkaline earth metal ions, in their induction and stabilization of LC phases, which could be attributed to their different binding modes. Unlike, alkali and alkaline earth metal ions, at very high metal ion concentrations (1M- ~0.625mM) transition metal ions and aluminium ions precipitated DNA into solid/translucent gel like aggregates, which were not liquid crystalline in nature, whereas heavy metal ions (1M-12mM) destroyed the viscosity required for LC ordering. However, below a certain critical metal ion concentration (C_M), LC phases could be observed with both transition and heavy metal ions, probably due to predominant phosphate interactions, which can maintain the rigidity of the DNA molecules, required for the LC behavior. In the presence of Al^{3+} and Cd^{2+}, the LC phases were highly unstable which can be correlated to their genotoxic effects. The heavy metal ions showed the highest instability in LC phase behavior of DNA, in

comparison to alkali, alkaline earth, multivalent and transition metal ions studied.

4.2. Introduction

Metal ion induced DNA condensation, has increasingly received attention for several decades, due to its applications in biological areas (anticancer drugs, probes of nucleic acid damage and cleavage agents)[1]**.** Compared to monovalent and divalent ions, transition and heavy metal ions are known to have strong base-affinity[2]. They can chelate or coordinate directly to the nucleophilic atoms of the bases; thus perturb the hydrogen bonding between base pairs, resulting in destabilization of DNA[3-5]. The interactions of metal ions with DNA may thus play key roles in the molecular mechanisms of metal toxicity affecting living organisms.

It has been shown that transition metal ions interact with N7 site of purines and N3 site of pyrimidines, by forming a chemical bond, M-N7 and/or M-N3[6]. They also interact with the phosphate groups of DNA, through the negatively charged oxygen atoms and water molecules of coordination[6]. The binding of transition metal particularly at G–C sites of DNA leads to its damage through radical generation, from oxidation by H_2O_2. The copper ion interaction with the N-7 and O-6 of the guanine, and N-3 of cytosine of the G-C pairs with no major perturbations of the A-T bases is well known[7-10]. At low metal ion concentrations, the copper ions bind mainly to the phosphate groups and consequently lead to increased base stacking and helical stability. At higher metal ion concentration, copper has a strong base affinity in concert with

phosphate groups, which results in the destabilization of the double helix[7-10]. Cu^{2+}, which is a biologically important metal is known to influence DNA interaction with drugs[11,12]. Moreover, Cu^{2+} ions ensuing conformational changes in DNA secondary structure is reported to enhance binding of tetracycline antibiotic and its derivatives to DNA[13]. On the other hand, it was reported that Cu^{2+} is involved in toxicity and oxidative damage in DNA and cause cancer[14,15].

Vanadium compounds are known to exert potent toxic effects on a wide variety of biological systems[16-20]. Epidemiological studies have shown a correlation between vanadium exposure and the incidence of lung cancer in human[17,21-23]. Vanadium (IV) compounds were reported to modify DNA synthesis and repair[24-27]. While biochemical mechanism of vanadium carcinogenicity and toxicity is still not fully understood, recent studies have indicated that vanadium mediated generation of hydroxyl radical ($^{\cdot}OH$) and related oxygen species may play an important role[28-31]. Vanadium (IV) is able to cause molecular oxygen-dependent dG hydroxylation and DNA strand breaks[32].

Cadmium is one of the most toxic heavy metal ions and is known to accumulate in marine food chains[33,34]. Binding of Cd^{2+} at guanine N7 has been verified by crystallographic studies on GMP (Guanosine Mono Phosphate)[35]. Even though the underlying mechanism for its genotoxicity has not been investigated in any marine species, several possible modes of action are already recognized for mammals. Cadmium is known to directly inflict damage on

DNA, through the induction of single strand breaks,[36] or indirectly by the production of free radicals[37], the inhibition of DNA repair enzymes,[38] or a reduction in the levels of glutathione, a free radical scavenger[39]. These effects combined with others such as the triggering of proto-oncogenes, the interference of Cd^{2+} with cellular signaling or the suppression of apoptotic response undoubtedly explain the widely recognized carcinogenic properties of this heavy metal[40,41]. The co-genotoxic influence of heavy metal ions must, therefore, be taken into account when evaluating the possible consequences of pollution impact on the cells.

Aluminum is a known neurotoxic agent and interferes with a large number of neurochemical reactions in vivo[42]. Al^{3+} appears to play a role, in the etiology of neurological disorders, such as Alzheimer's disease and amyotrophic lateral sclerosis- Parkinson dementia[43]. The neurotoxic effects of aluminum may be due to its binding to DNA. Literature dealing with the interaction of Al^{3+} with biological systems suggests that Al^{3+} has great affinity for phosphate ligating sites[44]. However, base-binding interactions of Al^{3+} was also reported[45].

Heavy metal ions are known to bind to the bases of DNA directly and disrupt the base stacking resulting in the destabilisation of the double helix and are specific to GC/AT content[46]. The distortion of the double helix will result in the loss of rod like shape of the DNA molecule, which is the determinant factor of its LC nature. Of all the metal ions, mercury has the highest affinity to bind to nitrogen ligand and it was therefore expected to have strong binding with the

purines and pyrimidines in nucleic acids. Yamane and Davidson reported that Hg^{2+} interacts predominantly with the bases, depending on the concentration of Hg^{2+}. Mercury, is known to form base-Hg complexes depending upon the metal concentration[47]. Luck and Simmer in a Tm and ORD study of Hg-DNA system, concluded that in the presence of sodium, Hg^{2+} might combine with phosphate sites[48].

Platinum (II) compounds are known to be anti-tumour active agents[49]. Certain platinum compounds are found to inactivate DNA, and the inactivation reaction was considered, due to the intra strand linking of the nucleic acids by Pt^{2+} ions. Cross linking of DNA strands are also known to occur with Pt^{2+}[50]. A kinetic study followed spectrophotometrically at 403 nm, reveals that Pt^{2+} binding apparently takes place within the helix[51]. $PtCl_4^{2-}$ was shown to react preferentially with adenine rather than guanine and cytosine. However, guanosine derivatives are found to react more rapidly with cis Pt(II). Both cis and trans Pt(II) interact monofunctionally to N-7 of guanosine[52]. Theophanides and his group[51] reported that the anti-tumour active Cis-Pt(II) $(NH_3)_2Cl_2$ binds to N7 and C_6O of guanine, whereas the other inactive trans compounds binds only to N7 of guanine.

Pd (II) complexes are also reported as anti-tumour active and they too bind to bases of DNA[53]. A ORD/CD study indicate, that Pd (II) interacts with both the phosphates and bases of DNA[54]. Pillai and Nandi reported that, as in the case of Cu(II), Gold(III) stabilizes the DNA initially followed by destabilization. Gold (III) binds initially to the phosphate probably as counter

ions, and binding to the base take place with time. Initially a mixed chelate between phosphate and base is formed. Disruption of the hydrogen bonds in the region where Au (III) binds, and cross linking between the two strands were also suggested[46,55,56].

The structural changes induced due to the base perturbation by the transition and heavy metal ions can destabilize DNA, resulting in loss of rigid like behavior and consequently affect the induction and stabilization of LC phases of DNA. The interaction of most of the multivalent ions with dilute solution of DNA have been studied extensively[1]. However, DNA exists *in vivo* in domains where the localized concentrations are very high, therefore, investigations on the behavior of concentrated DNA solutions in the presence of cationic species can be used as a probe in understanding the supramolecular ordering of DNA under various environments. Although, LC organization of DNA was investigated in the presence of various monovalent ions and divalent ions (phosphate binders), the induction and stabilization/destruction of LC phases of high molecular weight DNA in the presence of metal ions of varying charge (phosphate and base binders) such as V^{4+}, Al^{3+} etc. and heavy metal ions (base binders) are not known. In Chapters 2 and 3, we discussed the impact of metal ions of varying size, which are mainly phosphate binders (alkali and alkaline earth metal ions) on the LC behavior of DNA. Besides, examining the effect of phosphate binders, the aim of the present work was also to study the effect of metal ions of varying charge (+1, +2, +3, +4 etc.), which may be phosphate binders/phosphate cum base binders/base binders on the

induction, and stabilization of LC DNA. While, selecting the metal ions of higher charge after divalent alkaline earths, Al^{3+} fitted well in the series as it is also a phosphate binder like alkali and alkaline earths, but selecting the next ion with +4 was a problem. Vanadium (IV) and Platinum (IV) compounds are known, but V^{4+} binds both to the phosphate and base and Pt^{4+} is a well-known base binder. Metal ion binding to phosphate is known to stabilize the DNA structure where as binding to the bases destabilize the DNA helix. So, a comparison of the effect of increasing charge on the induction and stabilization of LC DNA becomes difficult, due to the different binding modes of metal ions to DNA. Although Cu^{2+}, Cd^{2+} are also divalent metal ions like alkaline earths, they are known to bind both to the phosphate groups as well as to the bases depending on the metal concentration. Likewise, a number of heavy metal ions such as Hg^{2+}, Pd^{2+}, Au^{3+} and Pt^{4+} are of different charge but they are predominantly base binders. In short, LC behavior of DNA cannot be compared only on the basis of increasing charge of the metal ion bound to it, but their different binding modes should be taken into account. In this respect, an organic cation such as spermine (tetravalent) is useful for comparison as spermine (the effect of spermine under various ionic environments is discussed in the forthcoming chapter), which is known to stabilize DNA. Based on the above parameters, Cu^{2+}, Cd^{2+}, Al^{3+}, V^{4+}, Hg^{2+}, Pd^{2+}, Au^{3+} and Pt^{4+} ions were selected for the present study. An investigation of the interaction between these metal ions and DNA could be beneficial to elucidate the cellular and molecular bases of metal toxicity in terms of their LC behavior. This chapter describes the

role of transition metal ions such as Cu^{2+}, $Cd^{2+}$and V^{4+}, multivalent ions such as Al^{3+}, and heavy metal ions such as Hg^{2+}, Pd^{2+}, Au^{3+} and Pt^{4+} on the induction and stabilization/destabilization of LC phases of high molecular weight DNA.

4.3. Experimental Section

A) ***Preparation of Samples***: Calf Thymus (CT) DNA was purchased from Worthington Biochemical Corporation, New Jersey, and has been used without further purification**.** The weight average molecular weight of DNA was 6 x 10^6. Autoclaved Millipore water was used as the medium in all the experiments. DNA was dissolved in 0.1M NaCl (pH 7). The dissolved DNA was then dialysed against NaCl (0.1M) 3-4 times. The observed A_{260}/A_{280} ratio of the DNA solution was 1.88, indicating that the DNA was free of protein contamination. The concentration of calf thymus DNA was determined by measuring the absorbance at 260 nm, using the molar extinction coefficient (Є) of 6900 per M/cm. The final concentration of DNA was 7.143 mg/ml. $CuCl_2$, $CdCl_2$, $Al(NO_3)_3$, $VOSO_4$, $HgCl_2$, $PdCl_2$, $HAuCl_4$ and H_2PtCl_6 of analytical grade were used.

In the presence of alkali and alkaline earth metal ions, DNA did not get precipitated from solution under our experimental conditions. But in the case of multivalent and transition metal ions, as their binding behavior to DNA differ from alkali metal ions, the same methodology could not be followed because Cu^{2+}, Cd^{2+}, V^{4+} and Al^{3+} when mixed with DNA, precipitated it into a solid gel/translucent gel like mass which did not show anisotropy, whereas heavy

metal ions drastically reduced the viscosity of DNA solution required for LC ordering.

So, in the case of transition metal ions, the C_M at which it does not induce DNA precipitation and in the case of heavy metal ions the C_M at which it does not reduce the viscosity required for LC behavior were optimized separately. To prepare metal-DNA complexes, DNA stock solutions were mixed with the corresponding metal ion solutions and were allowed to attain equilibrium for 3 hours at room temperature (26^0C).

The DNA concentration of 7.14 mg/ml was selected for the present series of experiments because LC phase transitions could be observed with this concentration of high molecular weight DNA.

B) ***Polarized Light Microscopy***: Microscopic glass slides and cover-slips were soaked in chromic acid and further rinsed with deionised water and dried using Analar acetone prior to use. 20 µL of each metal ion DNA solution was sandwiched between a clean microscopic glass slide and a cover slip, and the cover slips were then sealed with DPX mountant (a neutral solution of polystyrene and plasticizers in xylene used in microscopy work, M/s Nice Chemicals Ltd., Mumbai) to prevent the dehydration of the sample[57,58]. The samples were then incubated at 37^0C for 2-3 hours. Triplicates of each sealed and unsealed sample were prepared to ensure reproducibility. The slides were observed under a Nikon Optiphot Polarized Light Microscope equipped with a Nikon camera to study the effect of metal ions on the LC behavior of DNA. The preparations were examined periodically, for phase changes and

photographs were taken, when the phases became prominent and distinct. The phases and granular boundaries were clear and sharp when the sample was incubated at 37°C. The results were reproducible in three sets of separate experiments. The following parameters were noted: (a) C_D – critical DNA concentration required to exhibit anisotropy, (b) C_M – CM below which anisotropic behavior is exhibited, (c) T_{tr} – Time required for cholesteric to columnar phase transition (d) T_{iso} – Time required for the LC phases to darken and disappear ie. isotropization.

C) ***FTIR Spectra:*** DNA-metal complexes were precipitated using ethanol and the precipitate were centrifuged and dried for recording the IR spectra[59,60]. IR spectra were recorded in a Shimadzu IR spectrophotometer using the KBr pellet technique.

D) ***Circular Dichroism Measurements:*** Circular Dichroism (CD) spectra[61] of dilute DNA solutions were obtained with a Jasco-715 spectropolarimeter using a quartz cuvette of 1 cm path length. CD data (with concentrated DNA solutions) for the LC ordering could not be obtained because the instrumental parameters were apt only for very dilute DNA dilutions, but LC ordering can be obtained only at higher DNA concentrations.

E) ***Molecular Modeling Studies***: Due to computational limitations binding studies of multivalent, transition and heavy metal ions with DNA, could not be carried out.

Also several attempts were made to obtain X-ray diffraction data, which faced problems in obtaining the required birefringence (even after keeping the

sample filled in the capillary in an oven set at 37^0C for long periods) for the instrument to make measurements. Probably, it must be the difficulty with the high molecular weight DNA system, in anchoring/ordering of the long DNA molecules, when sandwiched between the glass slide and cover slip, and within the capillary where the sample is filled.

4.4. Results and Discussion

4.4.1. *Effect of multivalent and transition metal ions on the LC behavior of DNA*

It becomes clear from the previous chapters (2 and 3), that the size and charge of phosphate binding alkali and alkaline earths had influenced both the induction and stabilization of LC phase transitions of DNA. The C_D required for the induction of LC behavior was found to be same in case of alkali metal ions except with lithium, which may be due to its outer sphere binding nature and higher hydration factor. Moreover in the case of alkaline earth metal ions the C_D was found to be higher than that of alkali metal ions, which could be due to its smaller size, higher charge and higher hydration energy than the alkali metal ions. Unlike, alkali and alkaline earth metal ions, the transition and heavy metal ions are expected to bring about large perturbations to the double helix, by interacting with the bases of nucleic acids. Hence major structural and topological changes can be expected compared to alkali and alkaline earths, when these ions interact with the DNA macromolecule.

The strong base-affinity[62] of transition metal ions was indicated by the FTIR spectra. In the IR region, the bases of nucleic acids absorbs at 1400–1800 cm^{-1} region and the main absorption bands are: 1580 cm^{-1}, the vibrations of C -

N7 of guanine, 1650 cm^{-1} the vibration of C2-O of cytosine, 1680 $cm.^{-1}$ the vibrations of C6-O of guanine and C4-O of thymine[63]. IR spectra of Cu^{2+}, V^{4+} and Cd^{2+} ions showed significant changes in the base absorption region 1400–1800 cm^{-1} and slight changes in the phosphate absorption regions, which are indicative of both phosphate and base interactions (See Appendix Fig.1 D for the spectra); this may perturb the hydrogen bonding between base pairs, resulting in the destabilization of DNA or the distortion of rigid rod like behavior of DNA required for LC ordering.

In contrast to the behavior of alkali and alkaline earth metal ions, Cu^{2+}, Cd^{2+}, Al^{3+} and V^{4+} ions when mixed with stock DNA solution (7.14 mg/ml) precipitated DNA into solid gels at high metal ion concentration (~1M), and translucent gel like aggregates at lower concentrations (0.625mM-1M), which lacked the mobility required for LC behavior. The DNA aggregation could be due to rapid multi-step inter-strand/intra-strand cross -linking or chelation of metal ions to phosphates/and bases. As ionic strength is one of the parameters affecting critical DNA concentration, it appears that the C_D required to exhibit LC ordering might be quite high which could not be achieved with high molecular weight of DNA. So, the metal ion concentration was optimized to the point where DNA does not form gels. In other words, the critical metal ion concentrations (C_M) at which the sample had enough viscosity to exhibit LC behavior, were found out separately and the same are given in Table 4.1. Even though the electronic structure of Cu^{2+}, V^{4+} and Al^{3+} are different, C_Ms observed were almost same (0.625mM) except that of Cd^{2+} (5mM). One of the

reasons for the difference in C_M, may be due to their difference in their binding modes to DNA.

Table 4.1. Critical metal ion concentration (C_M) required to induce LC behavior.

Metal ions	Critical Metal Concentration
Cu^{2+}	0.625mM
Cd^{2+}	5mM
Al^{3+}	0.625mM
V^{4+}	0.625mM

As aluminium is believed to play a role on the etiology of neurological disorders, such as Alzheimer's disease and amyotrophic lateral sclerosis-Parkinson dementia[43], a study of the LC phases of DNA of those affected by Alzheimer's disease and amyotrophic lateral sclerosis- Parkinson dementia might throw much light on the understanding of such diseases. It may also lead to the identification of the causative factors involved and finally to appropriate medications. The present data on the highly disturbed LC phases of DNA in the presence of Al^{3+} further indicate a possible negative impact on the biological functions of DNA if aluminum concentration surpasses optimal levels within the cell.

Fu et al. have observed the aggregation and precipitation of chromatin in cultured neurons exposed to aluminum at neutral pH, which indicates that aluminum ions can induce the apoptosis of cortical neurons[64]. Hegde et al. have indicated that aluminum ions induce cell apoptosis in vivo and cause neuronal death partially by uncoiling the brain genomic DNA to a fully relaxed form[65].

Our observation of precipitation of DNA in the presence of Al^{3+} upto certain C_M (Table 4.1) is comparable to the above phenomenon. This could be due to the inter and/or intra strand cross linking of DNA molecules by Al^{3+} which in turn arrested the mobility of DNA molecules to carry out its biological functions such as transcription, replication etc. The impairing of DNA functions can eventually lead to the destruction of the cell.

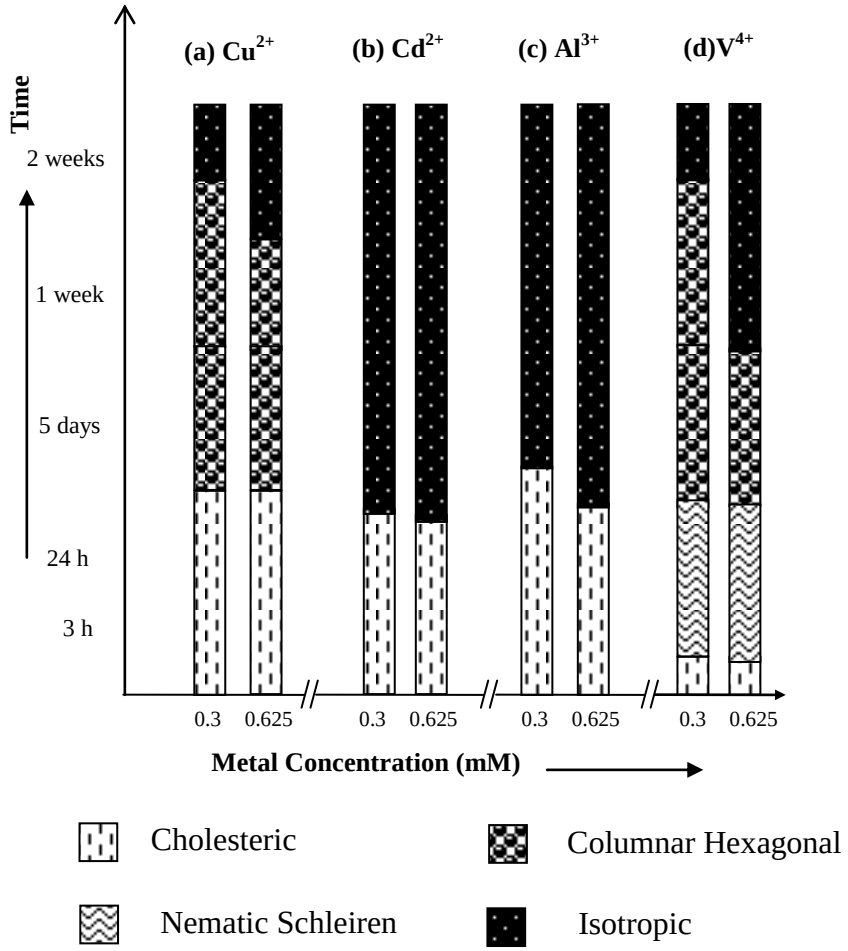

Fig.4.1. Time dependent LC phase transitions of DNA in the presence of multivalent (Al^{3+}) and transition metal ions. Y-axis Scales are not fixed arbitrary units.

Fig.4.1. presents the time dependent LC phase transitions of DNA in the presence of multivalent (Al^{3+}) and transition metal ions. It can be seen from

Fig.4.1 c that below the C_M, Al^{3+} gives a highly birefringent and fluidic cholesteric phase (Fig.4.2 c) initially below the C_M (0.625mM), but it soon becomes unstable as it darkens after 24 hrs (Fig.4.2 d) and isotropizes without getting transformed into the higher ordered columnar hexagonal phase. In comparison, the alkali and alkaline earth metal ions, which are phosphate binders, gave stable cholesteric phases, which transformed into columnar hexagonal phases with time. The highly unstable nature of the cholesteric phase is indicative of destabilization of DNA although Al^{3+} is a phosphate binder. As mentioned earlier, Al^{3+} is also reported to bind to the bases of DNA. The destabilization of DNA in the presence of Al^{3+} could be explained, if we assume a possible cross-linking (because of the multiple valence of aluminium ion) to another phosphate moiety of the same strand of DNA leading to possible destabilization. This might have ultimately disrupted the rigidity required for LC ordering for further transformation into columnar phase. The LC phases were more stable (Fig.4.1) at still lower Al^{3+} concentrations (~0.3mM) probably due to lesser metal ion induced distortion of double helical DNA molecules. Contrary to the earlier report[45], the IR spectra of Al-DNA system did not indicate any binding to the bases (see Appendix Fig.1 E for the spectra).

An over all survey of literature, on the interaction of vanadium with DNA did not provide any positive results. To understand the nature of interaction of vanadium with DNA system, the CD spectrum was measured. The CD spectrum at low metal concentration showed absence of shift in

absorbance indicating that it binds to the phosphate moiety of DNA. A red shift in the absorbance at high metal ion concentration indicated that it also binds to the bases like other transition metal ions (see Appendix Fig. 4 for the spectra). At very high concentrations (1M-0.625mM), V^{4+} precipitated DNA like Al^{3+}, but as it is a phosphate and base binder the aggregation may be due to the multi-step co-operative interaction with both phosphates and bases, thereby destabilizing DNA. Addition of V^{4+} provoked LC formation, in two-step manner, below a concentration of 0.625mM. A birefringent fluidic cholesteric phase was formed initially, on which threaded structures typical of nematic phase developed (Fig.4.2 e), probably due to the anchoring effects on the glass slide. On prolonged incubation it transformed into silkworm like texture probably of columnar phase (Fig.4.2.f), which remained stable up to 5 days (T_{iso}) at a concentration of 0.625mM and up to two weeks (T_{iso}) at lower metal ion concentrations (~0.3mM). The higher stability of DNA mesophases observed at the lower metal concentration might be due its phosphate interaction. Vanadium has been implicated in a number of publications as oncogenic[17,21-23]. The concentration dependent precipitation and destabilization of DNA observed in the presence of V^{4+} might play a role in vanadium-mediated disturbance of the supramolecular organization and the malfunctioning of DNA.

As copper ions are known to enhance the activity of chemotherapeutic drugs for curing human cancer[11,12] and as the toxicity of excess copper is well known in Wilson's disease (WD),[66] the study on the influence of Cu^{2+} on the

LC behavior of DNA would be interesting. Moreover, copper is also involved in carcinogenicity as catalytic copper[67].

At very high concentrations (1M-0.625mM) Cu^{2+} also precipitated DNA like Al^{3+} and V^{4+} that can result in the destabilization of DNA. Although Cu^{2+} is known to destabilize the double helical structure of DNA, it appears that below a certain concentration it mainly binds to the phosphate groups and reduces the charge density and intermolecular repulsion, thereby brings the ordered alignment required to exhibit anisotropic behavior. In the presence of Cu^{2+}, below C_M (<0.625mM), DNA initially exhibited cholesteric phase with two pointed brush defects (Fig.4.2.a) on which finger print pattern with antiparallel arrangement was developed (Fig.4.2.b) which later assumed a herring bone pattern of the columnar hexagonal phase (Fig.4.1.a). As in the cases of Al^{3+} and V^{4+}, still lower Cu^{2+} concentrations (0.3mM) favored formation of stable LC phases.

Cadmium is well known for its toxicity in biological systems. Langlais et al.[68] have interpreted Raman spectra of calf thymus DNA in the presence of Cd^{2+} to indicate binding to phosphates and AT regions, as well as to the N7 atom of guanine. Catte et al. reported the modification of LC phases with low molecular weight fragmented DNA, in the presence of Cd^{2+} ion[69]. The effect of Cd^{2+} on the LC behavior of high molecular weight DNA however was more drastic than that observed with Cu^{2+}, V^{4+} and Al^{3+}. At very high metal concentration (1M-5mM), DNA aggregation and precipitation, occurred as in the case of Cu^{2+}, V^{4+} and Al^{3+}. Cd^{2+}, however, showed a weakly birefringent

cholesteric phase, initially below C_M ie.5mM (because of very weak birefringence photographs could not be taken) which got darkened within ~24 hours (Fig.4.1.b) without transforming into higher ordered columnar hexagonal phase.

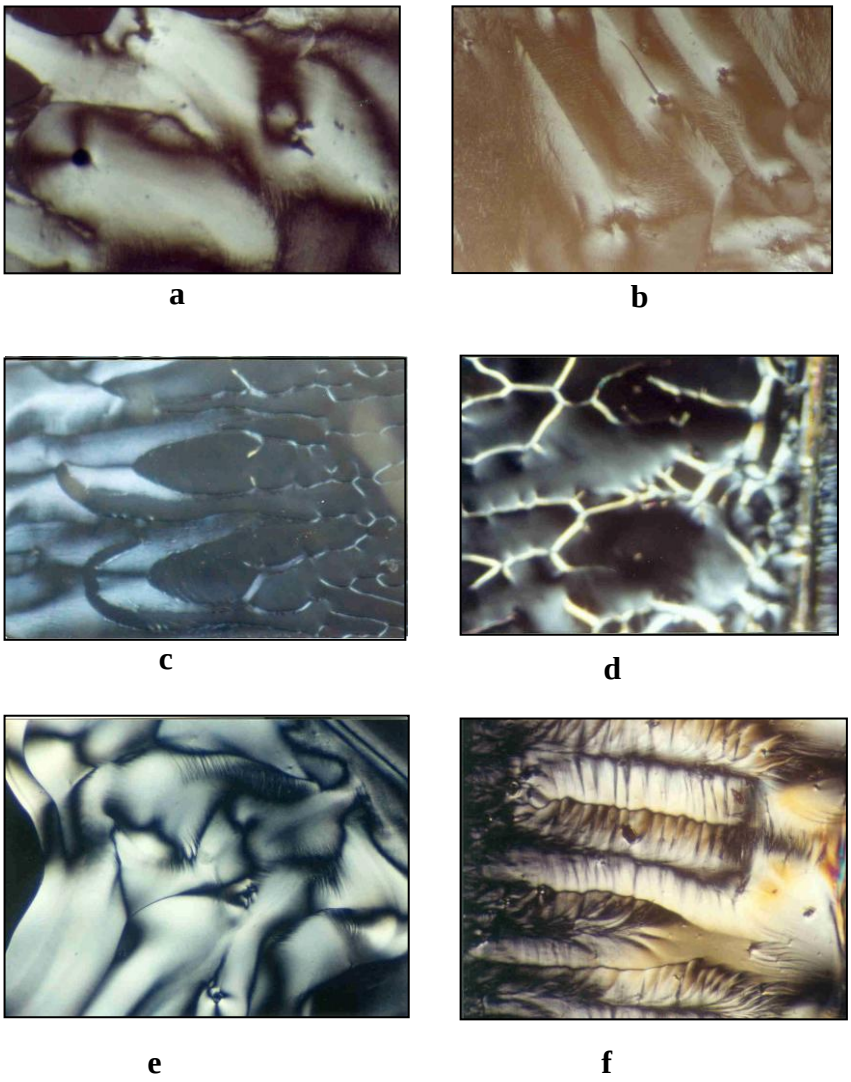

Fig.4.2. LC phase transitions of high molecular weight DNA obtained in the presence of transition and multivalent ions. a) Cholesteric fluidic phase formed after 3 hours and b) finger print pattern with antiparallel arrangement appeared on the cholesteric phase after 7 hours of incubation at 37^0C in the presence Cu^{2+}, (0.625mM) c) Cholesteric phase formed in the presence of Al^{3+} and d) Isotropization of the cholesteric phase in the presence of Al^{3+} (0.625mM), e) Cholesteric and Nematic threaded texture of DNA which flows spontaneously under the microscope obtained in the presence of V^{4+}ions (0.625mM). f) The same phase transformed into silkworm like texture probably of columnar phase in the presence of Al^{3+} (Mag.10X). Concentration of DNA is ~4 (mg/ml).

Cadmium is reported to inflict damage on DNA through the induction of single strand breaks,[70] which will distort the rigidity of the DNA molecule. This could be the reason for the weak birefringence and reduced stability of the LC phases. At still low metal concentration (~0.3mM), the LC phases were more stable which could be due to lesser interaction of metal with bases. Binding to phosphate probably favors the formation of cholesteric phase that is stable at low metal ion concentration (0.3mM), but at higher concentrations (0.625mM) LC phases were less stable, which could be due to double helix distorting interactions of metal ions. Figure 5 indicates that $T_{iso}\,Cu^{2+} > T_{iso}\,V^{4+} > T_{iso}\,Al^{3+} > T_{iso}\,Cd^{2+}$. This probably gives an indication that the stability of the DNA mesophase increases as the charge increases.

4. 4. 2. ***Effect of heavy metal ions on the LC behavior of DNA***

Heavy metal ions are known to bind to the bases of DNA directly, and disrupt the base stacking, resulting in the destabilization of the double helix and are specific to GC/AT content[71-74]. The IR spectra of all the heavy metal ions used here showed significant changes in the base absorption region (1580 cm^{-1}, the vibrations of C-N7 of guanine, 1650 cm^{-1}, the vibration of C2-O of cytosine, 1680 cm^{-1}, the vibrations of C6-O of guanine and C4-O of thymine)[63] and slight changes in the phosphate absorption regions, which are indicative of both phosphate (possibly at low concentration of the metal ions) and base interactions. (See appendix, Fig.1 D for the spectra).

Unlike transition metal ions, the behavior of heavy metal ions with DNA is interesting in the sense that instead of precipitation initially, one observes a

drastic reduction in viscosity. In the case of heavy metal ions, when 100mM metal solution was mixed with DNA solution (7.14 mg/ml in 0.1M NaCl) there was a sudden decrease in viscosity of DNA solution and it started flowing freely which appeared dark/isotropic under the microscope. The decrease in viscosity could be probably due to the uncoiling of DNA molecules, due to the rapid interaction of the heavy metal ions with DNA bases[71]. The heavy metal ions are known to form bridges between the stacked bases and between the strands[75], which will eventually perturb the double helix resulting in the destabilization of the molecule. The viscous nature and ordered alignment required for exhibiting liquid crystalline behavior presumably might have lost at higher metal ion concentration. Hence, it was extremely difficult to optimize the metal ion concentration to get an LC phase. So, the metal ion concentration was brought down where the DNA possesses the viscosity required for LC ordering.

In the case of all the heavy metal ions studied, the formation of the mesophases was observed at and below a critical metal ion concentration (12mM), as shown in Table 4.2.

Table 4.2. C_M required for the heavy metal ions to induce LC behavior.

Metal ions	C_M
Hg^{2+}	12mM
Pd^{2+}	12mM
Au^{3+}	12mM
Pt^{4+}	12mM

The C_M for the induction of LC phase appeared independent of the charge they carry. But as the metal ion concentration was reduced to 12mM, the reduction in viscosity was not very pronounced and the sample showed birefringent domains with homogenous illumination of cholesteric ordering under the polarized light microscope.

The time dependent liquid crystalline phase transitions of DNA, in the presence of heavy metal ions such as Hg^{2+}, Pd^{2+}, Au^{3+} and Pt^{4+} are presented in Fig.4.3.

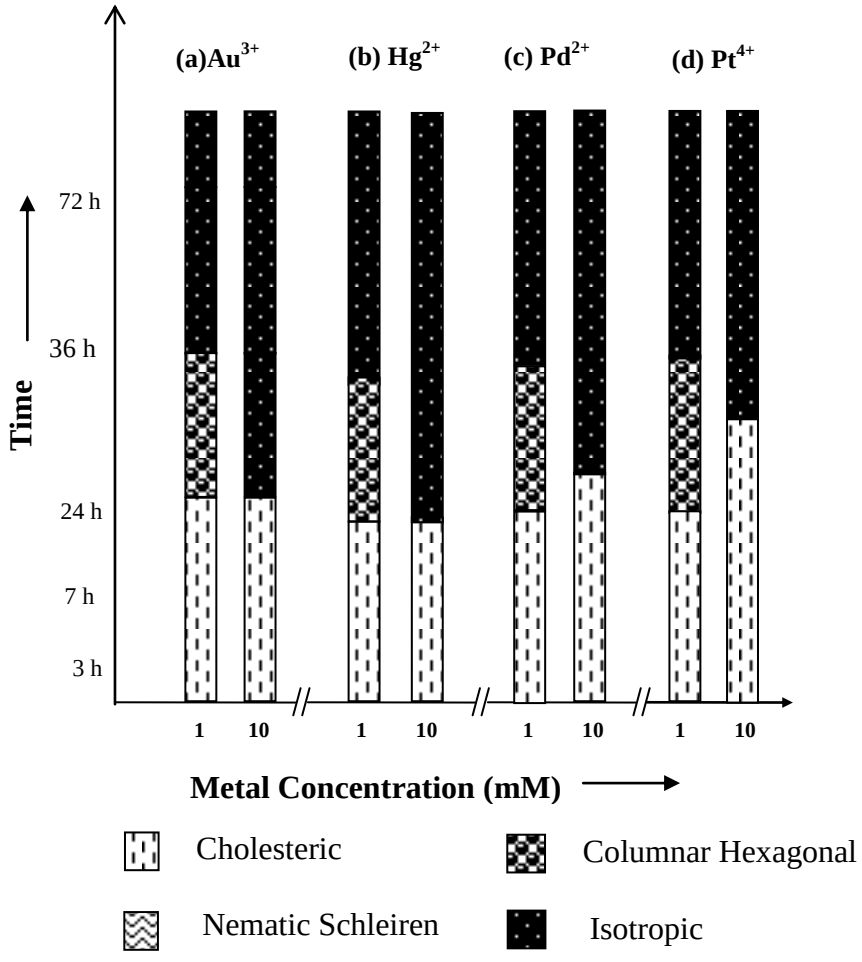

Fig.4.3. Time dependent LC phase transitions of DNA, in the presence of heavy metal ions (1mM) [(a) Hg^{2+}, (b) Pd^{2+}, (c) Au^{3+} and (d) Pt^{4+}] Y-axis Scales are not fixed arbitrary units.

With Hg^{2+}, Pd^{2+}, Au^{3+} and Pt^{4+}, the textures obtained were mainly cholesteric planar like in nature with homogenous illumination, irrespective of the metal ions studied and underwent isotropization after 24 hours (36 hrs in the case of Pt^{4+}) of sample preparation, indicating high level of instability, (T_{iso} $Hg^{2+} \leq T_{iso}$ $Pd^{2+} < T_{iso}$ $Au^{3+} < T_{iso}$ Pt^{4+}) of the phases and possible distortion of the double helix. There was no transition to the higher ordered columnar hexagonal phase; however, a columnar hexagonal phase (see Fig.4.3) was observed at still lower concentration (1 mM) possibly due some amount of phosphate interactions (Fig.4.4.a and b). The heavy metal ions, thus shows the highest instability in LC phase behavior in comparison to alkali, alkaline earth and other multivalent ions studied.

Mercuric chloride has been shown to be mutagenic in Chinese hamster ovary cells, while several studies have indicated that mercuric chloride or organic mercury can cause tumors in rodents[76].

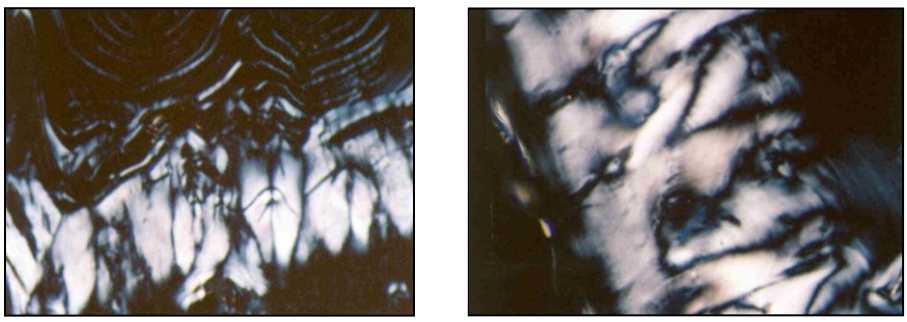

a **b**

Fig.4.4. LC phases of high molecular weight DNA, obtained in the presence of heavy metal ions. a) Cholesteric phase obtained after 3 hours of incubation in the presence of Pt^{4+}, 0.1mM. b) Cholesteric phase obtained after 3 hours of incubation in the presence of Hg^{2+}, 0.1mM.

The highly disturbed LC phases of DNA in the presence of Hg^{2+} might render support for the involvement of Hg^{2+} at the gene level for causing

tumor. Skuridin et al. have reported the modification of cholesteric phase of DNA on interaction with cis-Pt (II) complex,[77] which is anti-tumor active, but Pt^{4+} at a concentration of 1M to 12 mM reduced the viscosity of DNA and was completely isotropic indicating destabilization of DNA. So, it appears that the configuration of the metal complex might play a role in the stabilization of the liquid crystalline order as reported above[77].

4.5. Conclusions

The effects of multivalent, transition and heavy metal ions on the LC organization of high molecular weight DNA were studied. The overall phase behavior was found to be dependent on several parameters including the concentration, size, charge and binding modes of the metal ions and time. Two main phases, cholesteric and columnar hexagonal, are found either separately or in coexistence, with variations in the stability of the phases depending on local conditions and time. Multivalent, transition and heavy metal ions differed considerably from alkaline earths, in their induction and stabilization of LC phases, which could be due to their different binding modes. At very high metal concentrations (1 M), transition metal ions (Cu^{2+}, Cd^{2+}, V^{4+}) and Al^{3+} precipitated DNA into solid/translucent gel like aggregates whereas heavy metal ions (Hg^{2+}, Pd^{2+}, Au^{3+} and Pt^{4+}) reduced the viscosity of the DNA solution and appeared dark under the polarized microscope. The solid gel/translucent gel aggregates lacked the mobility required for LC behavior and DNA functions, indicating that these metal ions may influence the biological function of DNA if their concentration surpasses natural levels inside the cell.

Below a certain critical metal concentration, LC phases were formed, which could be due to their predominant phosphate interactions, which maintains the rigidity of DNA molecule, enough for exhibiting anisotropy. The precipitation of DNA in presence of certain metal ions up to certain concentrations can be correlated to their genotoxic effects**.** To the best of our knowledge, this is the first investigation of the effect of metal ions of varying size and charge with different binding modes on the LC organization of high molecular weight DNA. The present data on the LC phase behavior of DNA, in the presence of metal ions of varying size and binding modes, especially in the case of transition and heavy metal ions indicate that the mechanisms involved in the causation of certain diseases caused by an excess of these metal ions in the body may possibly be related to the supramolecular organization of diseased DNA in the cell. A comprehensive understanding of the LC behavior might lead to fundamental understanding on the etiology and finally appropriate solutions. There can also be tremendous possibilities of utilization of the structural specificity of the metal ions on the LC organization of DNA for the preparation of DNA biosensors which can be used in the determination of chemical compounds which form complexes with the nitrogenous bases of DNA testing of water, food, soil, and plant samples for the presence of analytes (carcinogens, drugs, mutagenic pollutants, etc.).

4.6. References

1. Bloomfiled, V. A., *Curr. Opin. Struct. Biol.* **1996,** 6, 334.
2. Anastassopoulou, J., *J. Mol. Str.* **2003,** 651, 19.
3. Duguid, J. G.; Bloomfield, V. A., *Biophys. J.* **1995,** 69, 2642.
4. Andrushchenko, V. V.; Kornilova, S. V.; Kapinos, L. E.; Hackl, E. V.; Galkin, V. L.; Grigoriev, D. N., *J. Mol. Struct.* **1997,** 408-409, (1), 225.
5. Hackl, E. V.; Kornilova, S. V.; Kapinos, L. E.; Andrushchenko, V. V.; Galkin, V. L.; Grigoriev, D. N., *J. Mol. Struct.* **1997,** 408-409, (2), 229.
6. Anastassopoulou, J.; Theophanides, T., *Critical Reviews in Oncology/Hematology* **2002,** 42, 79.
7. Eichorn, G. L.; Clark, P.; Becker, E. D., *Biochemistry* **1966,** 5, 245.
8. Eichorn, G. L.; Shin, Y. A., *J. Amer. Chem. Soc.* **1968,** 90, 7323.
9. Riahi, T. A. H.; Ahmad, R.; Naoul, M.; Diamantoglou, S., *Biopolymers* **1995,** 35, 493.
10. Mrevlishvili, G. M.; Sottomayor, M. J.; Manuel, A. V.; Silva, R. d., *Thermochim. Acta* **2002,** 394, 83.
11. Tachibana, M.; Iwaizumi, M.; Tero-Kubota, S., *J. Inorg. Biochem.* **1987,** 30,133.
12. Phillips, D. R.; Carlyle, G. A., *Biochem. Pharmacol.* **1981,** 30, 2021.
13. Khan, M. A.; Musarrat, J., *J. Int. Biol. Macromol.* **2003,** 33, 49.
14. Cheeseman K, H.; Slater, T., E., *Br Med Bull* **1993,** 49, 491.
15. Halliwell B; Aruoma O, I., *FEBS Lett* **1991,** 281, 9.
16. Chasteen, N. D., *Struct. Bonding* **1983,** 53, 107.
17. Zhong, B. Z.; Gu, Z. W.; Wallace, W. E.; Whong, W. Z.; Ong, T., *Mutat. Res.* **1984,** 321, 35.
18. Boyd, D. W.; Kustin, K., *Adv. Inorg. Biochem.* **1986,** 6, 311.
19. Erdmann, E.; Werdan, K.; Kraweitz, W.; Schmitz, W.; Scholz, H., *Biochem. Pharmacol.* **1984,** 33, 945.
20. Founes, M.; Kayser, E.; Strubelt, O., *Toxicology* **1991,** 70, 141.
21. Leonard, A.; Gerber, G. B., *Mutat. Res.* **1994,** 317, 81.

22. Hickey, R. J.; Schoff, E. P.; Clelland, R. C., *Arch. Environ. Health* **1967,** 15, 728.
23. Stock, P., *Br. J. Cancer*, **1960,** 14, 397.
24. Carpenter, G., *Biochem. Biophys. Res. Commun.* **1981,** 102,1115.
25. Smith, J. B., *Proc. Natl. Acad. Sci. USA* **1983,** 80, 6162.
26. Hori, C.; Oka, T., *Biochim. Biophys. Acta* **1987,** 610, 235.
27. Sabbioni, E.; Pozzi, G.; Pintar, A.; Casella, L.; Garattini, S., *Carcinogenesis* **1991,** 12, 47.
28. Keller, K. J.; Sharma, R. P.; Grover, T. A.; Piette, L. H., *Arch. Biochem. Biophys.* **1988,** 265, 524.
29. Ozawa, T.; Hanaki, A., *Chem. Pharm. Bull.* **1989,** 37, 1407.
30. Carmichael, A. J., *FEBS Lett* **1990,** 261, 165.
31. Carmichael, A., *Free Rad. Res. Commun.* **1990,** 10, 37.
32. Shi, X.; Jiang, H.; Mao, Y.; Jianping, Y.; Saffiotti, U., *Toxicology* **1996,** 106, 1996.
33. Romeo, M.; Gnassia-Barelli, M.; Lafaurie, M., *J. Eur. Hydrol.* **1995,** 26, (2), 227.
34. Devi, M.; Thomas, D. A.; Barber, J. T.; Fingerman, M., *Ecotoxicology and Environmental Safety* **1996,** 33, (1), 38.
35. Aoki, K., *Acta Crystallogr. B.* **1976,** 32, 1454.
36. Hassoun, E. A.; Stohs, S. J., *Toxicology* **1996,** 112, 219.
37. Zhong, Z.; Troll, W.; Koenig, K. L.; Frenkel, K., *Cancer Res.* **1990,** 50, 7570.
38. Hartwig, A., *Toxicol. Lett.* **1998,** 102-103, 235.
39. Shimizu, M.; Hochadel, J. F.; Waalkes, M. P., *J. Toxicol. Environ. Health* **1997,** 51, 609.
40. Beyersmann, D.; Hechtenberg, S., *Toxicol.Appl. Pharmacol.* **1997,** 144, 247.
41. Shimada, H.; Shiao, Y. H.; Shibata, M.; Waalkes, M. P., *J.Toxicol. Environ. Health* **1998,** 54, (2), 159.
42. Kiss, T., *Arch Gerontol Geriat* **1995,** 21, 99.

43. Perl, D. P.; Brody, A. R., *Science* **1980,** 208, 297.
44. Kiss, T.; Zatta, P.; Corain, B., *Coord. Chem. Rev.* **1996,** 149, 329.
45. Kasianenko, N. A.; Plotnikova, L. V.; Zanina, A. V.; Anderzhanov, A., Sh.; Defrenne, S., *Biofizika* **2002,** 47, 433.
46. Pillai, C. K. S. *Ph.D Thesis* 1974.
47. Yamane, T.; Davidson, N., *Biochem. Biophys. Acta J. Amer. Chem. Soc.* **1961,** 83, 2599.
48. Luck, G.; Zimmer, C., *Eur. J. Biochem.* **1971,** 18, 140.
49. Rosenberg, B., *Platinum Rev.* **1971,** 15, 42.
50. Shooter, K. V.; Howse, R.; Merrifield, R. K.; Robins, B., *Chem. Biol. Interactions* **1972,** 5, 289.
51. Zhakharenko, E. T.; Moshkovskii, Y. S., *Biofizika* **1972,** 17, 373.
52. Robins, A. B., *ibid* **1973,** 6, 35.
53. Mansy, S.; Rosenberg, B.; Thomson, A. J., *J. Amer. Chem. Soc.* **1973,** 92, 1633.
54. Pillai, C. K. S.; Nandi, U. S., *Biochim. Biophys. Acta* **1977,** 474, 11.
55. Pillai, C. K. S.; Nandi, U. S. *In Convention of Chemists*, 1972, 114.
56. Pillai, C. K. S.; Nandi, U. S., *Biopolymers* **1973,** 12, 1431.
57. Pelta, J., Jr; Durand, D.; Doucet, J.; Livolant, F., *Biophys. J.* **1996,** 71, 48.
58. Strzelecka, T. E.; Rill, R. L., *Biopolymers* **1990,** 30, 57.
59. Tu, A. T.; Reinosa, J. A., *Biochemistry* **1966,** 5, 3375.
60. Sutherland, G. B. B. M.; Tsuboi, M., *Proc. Royal Soc. London* **1957,** 239, Ser. A., 446.
61. Besik, K. I., *Biophysical Chemistry* **2000,** 84, 227.
62. Anastassopoulou, J., *Journal of Molecular Structure* **2003,** 651-653, 19.
63. Andrushchenko, V. V.; Kornilova, S. V.; Kapinos, L. E.; Hackl, E. V.; Galkin, V. L.; Grigoriev, D. N.; Blagoi, Y. P., *Journal of Molecular Structure* **1997,** 408-409, (1), 225.
64. Fu, H. J.; Hu, Q. S.; Lin, Z. N.; Ren, T. L.; Song, H.; Cai, C. K.; Dong, S. Z., *Brain Res* **2003,** 980, 11.

65. Hegde, M. L.; Anitha, S.; Latha, K. S.; Mustak, M. S.; Stein, R.; Ravid, R.; Rao, K. S. J., *J Mol Neurosci* **2003,** 22, 19.

66. Brewer, G., J., *Zinc acetate for the treatment of Wilsons disease*. ed.; 2001; 2, 1473.

67. Theophanides, T.; Anastassopoulou, J., *Critical Reviews in Oncology/Hematology* **2002,** 42, 57.

68. Langlais, M.; Tajmir Riahi, H. A.; Savoie, R., *Biopolymers* **1990,** 30, 743.

69. Catte, A.; Cesare-Marincola, F.; Van der Maarel, J. R. C.; Saba, G.; Lai, A., *Biomacromolecules* **2004,** 5, 1552.

70. Hassoun, E. A.; Stohs, S. J., *Toxicology* **1996,** 112, 219.

71. Yamane, T.; Davidson, N., *J. Amer. Chem. Soc.* **1961,** 83, 2599.

72. Pillai, C. K. S.; Nandi, U. S., *Biopolymers* **1977**, 17, 709.

73. Pillai, C. K. S.; Nandi, U. S., *Biopolymers* **1973,** 12, 1431.

74. Pillai, C. K. S.; Nandi, U. S., *Biochim. Biophys. Acta* **1977,** 474, 11.

75. Luck, G.; Zimmer., C., *Eur. J. Biochem* **1971,** 18, 140.

76. M.E. Ariza; J. Holliday; M.V. Williams, *Mutagenic effect of mercury(II) in eukaryotic cells, In Vivo*.1994.

77. Skuridin, S. G.; Schtykova, E. V.; Dembo, A. T.; Badaev, N. S.; Cheltsov, P. A.; Yevdokimov, Y. M., *Biofisika*, **1988,** 33, 55.

CHAPTER 5
SPERMINE INDUCED LIQUID CRYSTALLINE PHASES OF DNA IN THE PRESENCE OF ALKALI AND ALKALINE EARTH METAL IONS

5.1. Abstract

The effect of alkali and alkaline earth metal ions on the spermine induced LC behavior of high molecular weight DNA was studied. The spermine induced DNA precipitation was facilitated by the presence of alkali and alkaline earth metal ions, suggesting that the metal ions had acted in concert with spermine to precipitate out DNA from the solution. Spermine-DNA-metal ion condensates, exhibited mainly two different phases and at least one of them was fluid in nature, which is the cholesteric phase and a columnar hexagonal phase with a restricted fluidity where the DNA molecules are more closely packed. In the presence of alkali metal ions, spermine-DNA condensates were mainly in the cholesteric phase, but at higher spermine concentrations, in the presence of Rb^+ and Cs^+, they adopted a cholesteric to columnar arrangement, indicating the size effect of metal ions on the LC phase transitions. Among the alkaline earth metal ions, the existence of fluidic cholesteric textures in the presence of Mg^{2+}, suggest the possible synergistic role of polyamines and the Mg^{2+} in the cell nucleus, in preserving the fluidity required for the biological functions of DNA, within the condensates. The

evolution of columnar phase from cholesteric phase, in the presence of Ca^{2+} also indicates the probable role of spermine and Ca^{2+}, in packing DNA into hexagonal arrangement in vivo. Small angle X-ray diffraction peaks obtained at 2θ value in between 0 and 5 also indicates the formation of columnar hexagonal phase with Rb-DNA, Cs-DNA and Ca-DNA systems. Among all the metal ions studied, the behavior of Na^{+} was exceptional in inducing DNA resolubilization at 12 mM of spermine, whereas with the other metal ions, DNA resolubilization occurred at or above 400 mM concentration.

5.2. Introduction

The investigations on spermine and its chemical analogues, as perspective materials for condensing DNA into compact nanoparticles, for potential applications in DNA packaging and gene therapy, have given rise to encouraging results[1-9]. The cellular DNA is in a macromolecular crowded environment, surrounded by proteins and cationic molecules, including the polyamines. The condensation of DNA with polyamines such as spermine has been studied extensively, and they have been shown to induce DNA condensation, and to stabilize compact forms of DNA in vitro under controlled conditions[10-12]. Since polyamines associate with DNA by electrostatic interactions, a possible function of polyamines in the cell might involve the organization of DNA, including LC DNA[13]. In a series of experiments, Livolant and colleagues and Thomas and colleagues demonstrated that spermidine and spermine are capable of provoking multiple LC forms of fragmented DNA[14-20].

Polyamines are now believed to interact electrostatically with the charged DNA phosphates[21] and it has been shown recently that DNA exhibits possibly very weak, base sequence dependence[21,22]. It has been recently established that metal ions can be treated as factors modifying the character of interactions between polyamines and fragments of nucleic acids[23]. Similarly polyamines interfere in the reactions of metal ions and bioligands. The stability and character of complexes with polyamines and fragments of nucleic acids depend mainly on the type of metal ion. Generally "hard" ions of alkaline earth metals interact mainly with hard oxygen atoms from phosphate groups, whereas more soft nitrogen atoms from purine and pyridine bases interact with soft ions of transition metals[23-25].

In general, the affinity of a cation for a specific site on a polynucleotide is a function of its charge, hydration-free energy, coordination geometry, and coordinate bond forming capacity[26,27]. Those metal ions that bind primarily to the phosphates stabilize the helix by reducing the intermolecular repulsion, which provokes LC ordering by maintaining the rigid rod like shape of the DNA molecule, which is the determinant factor of its LC ordering.

Saminathan et al. in a recent study have reported the effect of spermine, spermidine and its synthetic analogues on the LC behavior of high molecular weight DNA. This study showed a structural specificity effect of polyamines, on LC phase transitions of DNA, and suggested a possible physiological function of natural polyamines. It is believed that some of the biologically important metal ions in combination with ubiquitous cellular molecules such as

polyamines serve critical functions across a multitude of biochemical processes, and are necessary to reach the ultimate states of condensation in the cell[26,28]. A comparative investigation of the expression of LC phases of high molecular weight DNA by its interaction with spermine in the presence of spermine alkali and alkaline earth metal ions might be beneficial to elucidate the role played by the condensed state of DNA *in vivo*. The spermine induced LC organization of low molecular weight fragmented DNA, was investigated in presence of Na^+, K^+, Mg^{2+} and Ca^{2+} under defined ionic conditions[9-12] but it remains unclear with high molecular weight DNA. As the stability and character of complexes with polyamines and fragments of nucleic acids depend mainly on the type of metal ion, the present work was undertaken to investigate the spermine induced LC organization of high molecular weight DNA, phase transitions and its stability in presence of alkali metal ions such as Li^+, Na^+, K^+, Rb^+ and Cs^+, and alkaline earth metal ions such as Mg^{2+}, Ca^{2+}, Ba^{2+} and Sr^{2+} using polarized light microscopy and small angle X-ray diffraction techniques.

5.3. Experimental Section

A) ***Preparation of Samples:*** Calf Thymus (CT) DNA was purchased from Worthington Biochemical Corporation, New Jersey, and has been used without further purification**.** The weight average molecular weight of the DNA was 6 x 10^6. The observed A_{260}/A_{280} ratio of the DNA solution is 1.88, indicating that the DNA is free of protein contamination. Preliminary experiments indicated that cacodylate buffer and phosphate buffer have interactions with various metal ions. Acetate/citrate buffer was noted to have minimal interactions. The

best results were obtained when DNA was dissolved in 0.1M NaCl (pH 7). A comparative study indicated that similar results are obtained with acetate/citrate buffer and with 0.1M NaCl at pH 7.

Spermine.4HCl was purchased from Sigma Chemical Co. (St Louis, MO). LiCl, NaCl, KCl, RbCl, CsCl, $MgCl_2$, $CaCl_2$, $BaCl_2$ and $SrCl_2$ of analytical grade were used. Autoclaved Millipore water was used as the medium in all the experiments. In the present experiments, the concentrations of alkali and alkaline earth metals for the preparation of metal-DNA complexes were selected as 300mM and 10mM respectively, considering their abundance at cellular level.

DNA-metal systems were prepared by dissolving 5mgs of DNA (15.01mM), 0.3 M LiCl, 0.3M NaCl, 0.3M KCl, 0.3M RbCl, 0.3M CsCl, 0.01M $MgCl_2$, 0.01M $CaCl_2$, 0.01M $BaCl_2$, 0.01M $SrCl_2$. The concentration of calf thymus DNA was determined by measuring the absorbance at 260 nm, and using the molar extinction coefficient (Є) of 6900 per M/cm. The DNA concentration of 15 mM was selected for the present series of experiments because LC phase transitions could be observed with spermine at this concentration. Spermine solutions of concentrations varying from 0.1mM to 600mM were prepared in autoclaved millipore water. DNA and spermine solutions were stored at 4°C. The solutions were homogeneous at the start of our experiments. The critical spermine concentration required for inducing DNA precipitation in the presence of each ion was determined by mixing spermine solutions of appropriate concentration with aliquots of DNA.

Following the addition of spermine to the solutions, the sample was incubated at room temperature (26^{o}C) for 15 minutes and centrifuged at 10,000× g for 5 minutes. The pellets were then sandwiched between a microscopic glass slide and cover slip and sealed using DPX[29,30] (DPX is a neutral solution of polystyrene and plasticizers in xylene) to prevent the dehydration of the sample.

B) ***Polarized Light Microscopy:*** Metal-DNA systems were precipitated, on addition of spermine solution either directly on the glass slide, or in an eppendorf tube. and centrifuged to sediment the precipitate for microscopic observation. The glass slides were soaked in chromic acid, cleaned with distilled water, rinsed with ethanol and dried prior to sample preparation. The DNA precipitate spread over the glass slides with a cover slip and sealed with DPX, as described above was observed under polarizing light or phase contrast light in a Nikon Optiphot microscope. After observing the initial phase appearance at room temperature, the preparations were incubated at 37°C for extended time periods to observe the phase changes until crystallization or complete darkening (isotropization) occurred[13]. The preparations were examined periodically for phase changes and photographs were taken when the phases became prominent and distinct. The phases and granular boundaries were clear and sharp when the sample was incubated at 37°C. A triplicate of each sample was made to ensure the reproducibility of the phase changes. The results were reproducible in three sets of separate experiments. The following parameters were noted: (a) C_{sp}– critical spermine concentration required to

exhibit anisotropy, (b) T_{iso}- Time required for the phases to darken and disappear ie isotropization to occur.

C) ***SAXS Measurements:*** Small angle X-ray diffractions of DNA samples were recorded by Philips Analytical diffractometer using CuK-α emission. The spectra were recorded in the range of 2θ = 0- 40 and analyzed using X' Pert software. The samples were deposited on the glass slides. Textures were allowed to stabilize for a few minutes to a few hours. The samples were then exposed for 5 minutes. Observation of LC textures on a polarizing Nikon Optiphot Microscope was also made in parallel with the X-ray measurements.

5.4. Results and Discussion

5.4.1. *General Observations*

As spermine is involved in a variety of cellular functions, and is largely responsible for the compact form of DNA in vivo, and metal ions are believed to be involved in this process,[2-4,31,32] it would beneficial to study in vitro the spermine induced LC phase behavior of DNA in the presence of metal ions. Previous studies of LC phase transitions of calf thymus DNA in the presence of polyamines, were carried out with low molecular weight fragments, prepared by either sonication or micrococcal nuclease digestion[16,17,29]. The first study using high molecular weight DNA and spermine and its synthetic analogues was reported by Saminathan et al[13]. Use of high molecular weight DNA in these studies would be beneficial as they may probably provide information on the supramolecular organization of DNA in the cell. In the present study, LC DNA could be obtained at concentrations (5mg/ml) that are far less than that

necessary for low molecular weight (150 mg/ml) DNA and the mesophases are comparable with those obtained with low molecular weight DNA.

The *in vitro* precipitation/condensation of DNA by spermine has been investigated by a number of researchers and it was found that the DNA precipitation efficacy of spermine is highly dependent on the other counter ions bound to DNA[10-16]. Spermine moiety because of its larger size is reported to prefer to bind along the major grooves of DNA[33] and alkali and alkaline earth metal ions because of their smaller size are reported to prefer A-T rich minor grooves of DNA as binding sites[34]. The spermine induced DNA pellets/aggregates appeared as transparent colloid like mass to white opaque gels, which exhibited multiple macroscopic polymorphic behaviors depending on the concentration of both spermine and the counter ions, whereas multivalent and transition metal ions precipitated DNA into translucent/solid gels, which were not liquid crystalline in nature. Spermine induced DNA condensates are either dense or partially fluid in nature flowing spontaneously under the microscope. The fluidity of the ordered phase suggests that spermine binds along the strands, which would allow the strands to slide on each other. When deposited between the glass slide and the cover slip these aggregates show multiple textures (Fig.5.4, 5.6), which depend on the nature of the phase and also on the thickness of the preparation. Two main phases, cholesteric and columnar hexagonal, are found in our study, either separately or in coexistence, with variations depending on local conditions. A cholesteric phase is frequently obtained in the samples, but its characteristic finger print pattern could not be

observed usually. Instead, birefringent domains are usually seen with homogenous illumination. But the presences of tear-shaped defects attest the formation of cholesteric phase. Numerous isotropic droplets of various sizes are also seen trapped in the birefringent cholesteric phase. Sometimes nematic textures were also observed with two or four branch brush defects. These textures probably correspond to the previously observed cholesteric phase, and are formed rarely where anchoring effects on the glass slides prevents the twist. They are slightly distorted into squares in very thin preparation.

It should be pointed here that blue phases commonly known as precholesteric phases[30] which are a transition from the isotropic to the cholesteric phase, are not observed in the present case. However, the higher ordered columnar hexagonal phases were observed when the concentration of spermine is above 200 mM, but only with metal ions of higher sizes. These domains are much more viscous than the cholesteric phase. In columnar hexagonal phase, the DNA molecules are unidirectionally aligned with a lateral hexagonal order[15]. Undulations typical of the hexagonally ordered columnar phase were also noticed. The fluidity and order required for a LC state are also observed here. It is important to note here that the time-dependent changes in LC textures of DNA occurred under conditions in which solvent evaporation was prevented by sealing the glass slides with a neutral solution of polystyrene and plasticizers in toluene. Therefore, the observed changes are a consequence of the reorganization of polyamines and metal ions on the DNA strands.

Fig.5.1 shows the C_{sp} values of spermine concentration required for the onset of DNA precipitation in the presence alkali and alkaline earth metal ions. Two distinct plateaus can be seen from Fig.5.1.

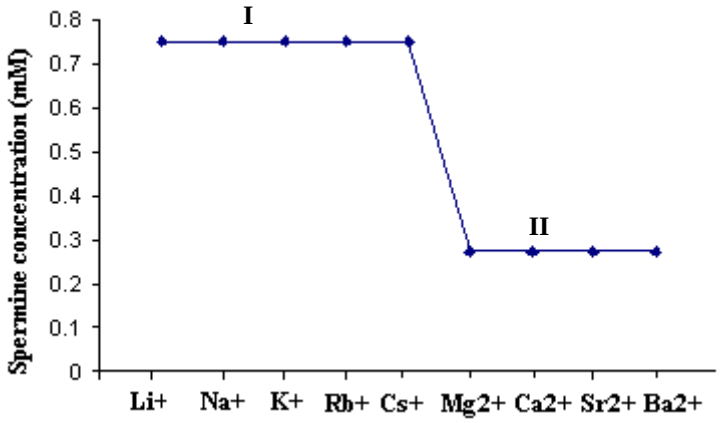

Fig.5.1. Critical spermine concentration (C_{sp}) required for the onset of DNA precipitation with alkali and alkaline earth metal ions

Plateau I for the alkali metal-DNA systems, occur around a concentration of 0.75 mM. It should be noted that spermine precipitates DNA, at a concentration of 0.85mM. Plateau II for the of alkaline earth metal ions, occured at a concentration of 0.275 mM. In short, C_{sp} (spermine alone) > C_{sp} alkali metal ions > C_{sp} alkaline earth metal ions. This suggests that alkali and alkaline earth metal might have acted in concert with spermine, which facilitated the precipitation range of spermine. Fig.5.1 also reveals that charge and size of the ion are playing important roles in the precipitation of DNA in the presence of metal ions.

Fig.5.2 gives the over all LC phase behavior of DNA in the presence of the alkali and alkaline earth metal ions studied, with respect to the change in spermine concentration.

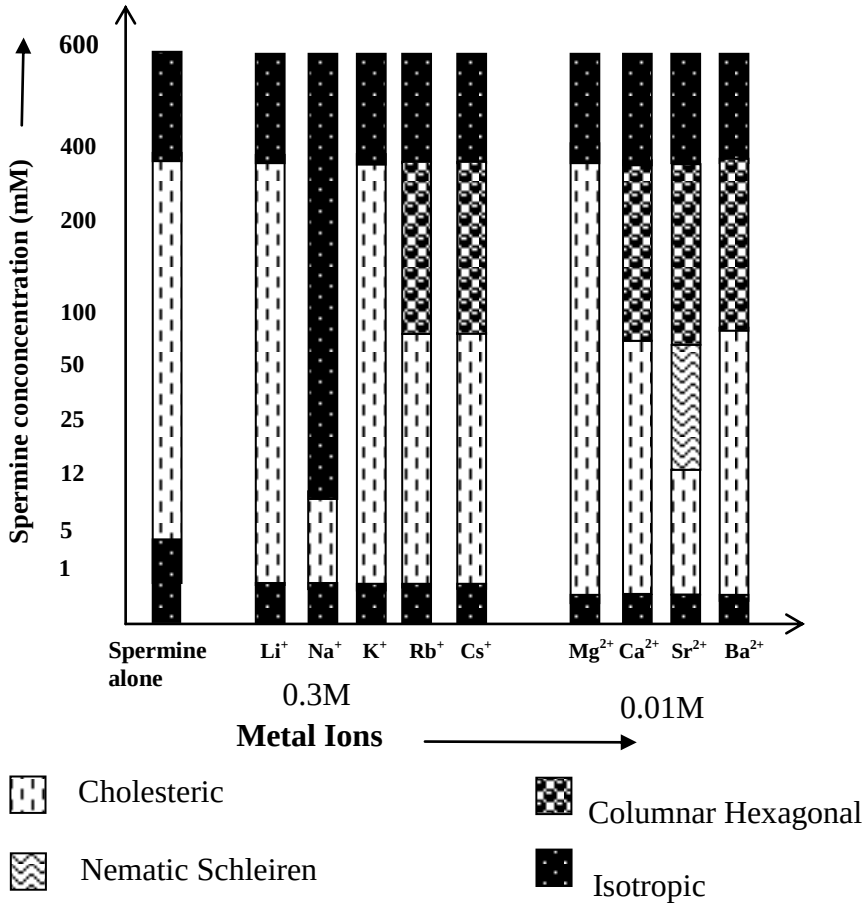

Fig.5.2. LC behavior of spermine induced DNA condensates in the presence of alkali and alkaline earth metal ions.

It can be seen from Fig.5.2 that after a threshold limit at or near 400 mM of spermine concentration, the precipitated DNA resolubilizes possibly due to the screening of short-range electrostatic interactions between the polyamine molecules and the DNA strands and goes to the isotropic state. Another important finding is that of sodium ion, which resolubilizes the DNA at extremely low spermine concentration. Any increase in spermine concentration after the precipitation of DNA, would naturally increase the osmotic stress of the medium. The increase in number of the spermine molecules around DNA would screen the intermolecular interaction between

DNA strands, thereby reduces the order parameter, and finally go to isotropic state.

5.4.2. *Effect of alkali metal ions on the spermine induced LC DNA*

Among the alkali metal ions, Na^+ and K^+ are widely distributed in most of the biological systems and are involved in a variety of cellular functions. In presence of Li^+, Na^+ and K^+, spermine-DNA aggregates were mainly in cholesteric phase (Fig.5.3.a, b and c) that flows spontaneously under the microscope (Fig.5.4 a, b and c) and no transition to columnar phase has been observed. Pelta et al. and Saminathan et al. have studied the precipitation of short DNA fragments by the polycations spermidine and spermine in the presence of Na^+, and have shown that resolubilization of DNA aggregate is essentially dependent on the Na^+ concentration present in the DNA solution[12,26]. This is comparable to the present observation with high molecular weight DNA molecules also. Na^+ appears to be exceptional among alkali metal ions in resolubilising precipitated DNA (see Fig.5.4.a), which suggests that spermine and Na^+ concentrations would be balanced in the cell nucleus to maintain DNA in the condensed states. Na^+ and K^+ are the major extra cellular and intracellular cations respectively in the body fluids of animals including human beings.

Even though, Na^+ and K^+ are abundant in biological systems, Na^+ concentration is always maintained low inside the cell (high K^+ inside the cell) by a Na^+-K^+ pump with the help of an enzyme Na-K ATPase present in the cell membrane through the active ion transport mechanism[35].

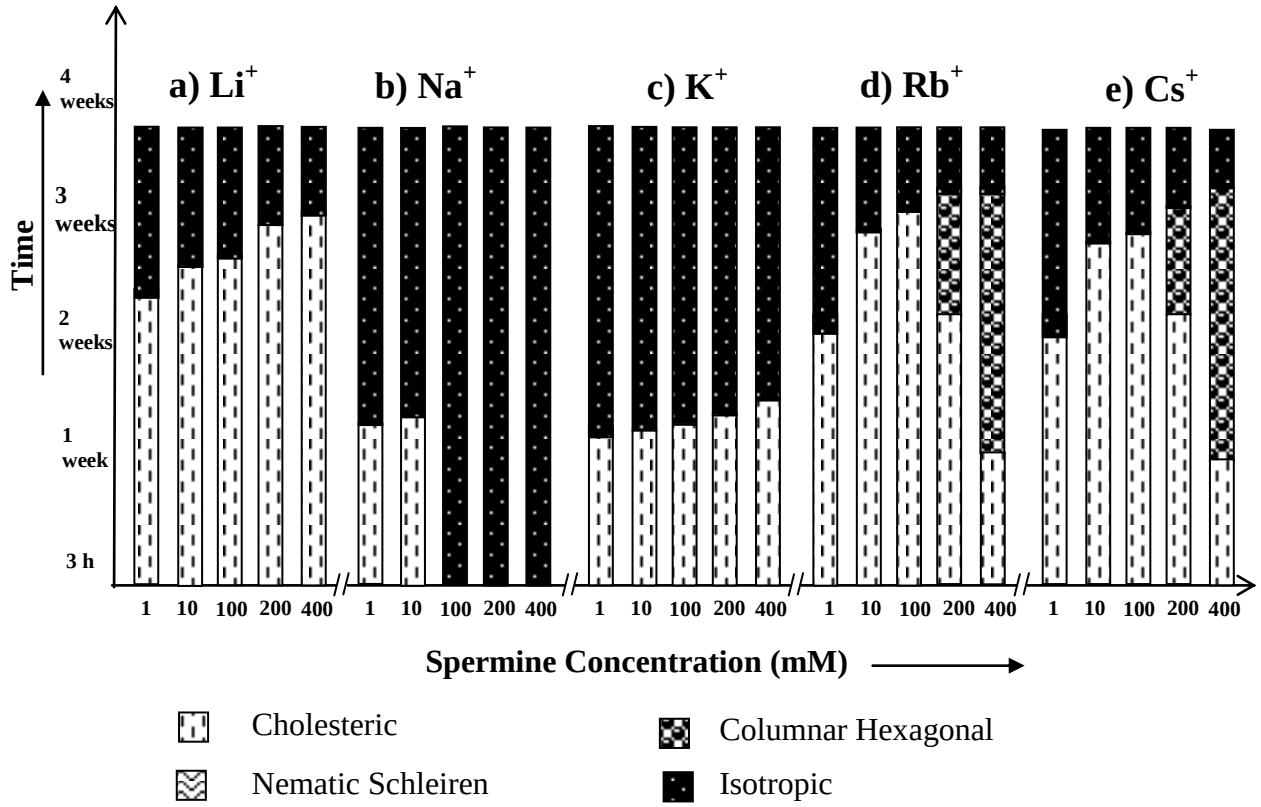

Fig.5.3. Time dependent phase transitions of spermine induced DNA condensates in the presence of alkali metal ions.

Each operation of the pump pulls out larger number of sodium ions from the cell, than the number of K^+ ions it pumps into the cell. The maintenance of low Na^+ concentration inside the cell could also be due to the fact that higher Na^+ concentration does not favor the existence of condensed states of DNA essential for its biological functions such as replication etc. Below 12mM spermine, DNA exhibited iridescent fluidic cholesteric phase in the presence of sodium, which remained stable for two weeks. The influence of Na^+ in the presence of a polyamine in controlling the supramolecular order of DNA will have many biological implications.

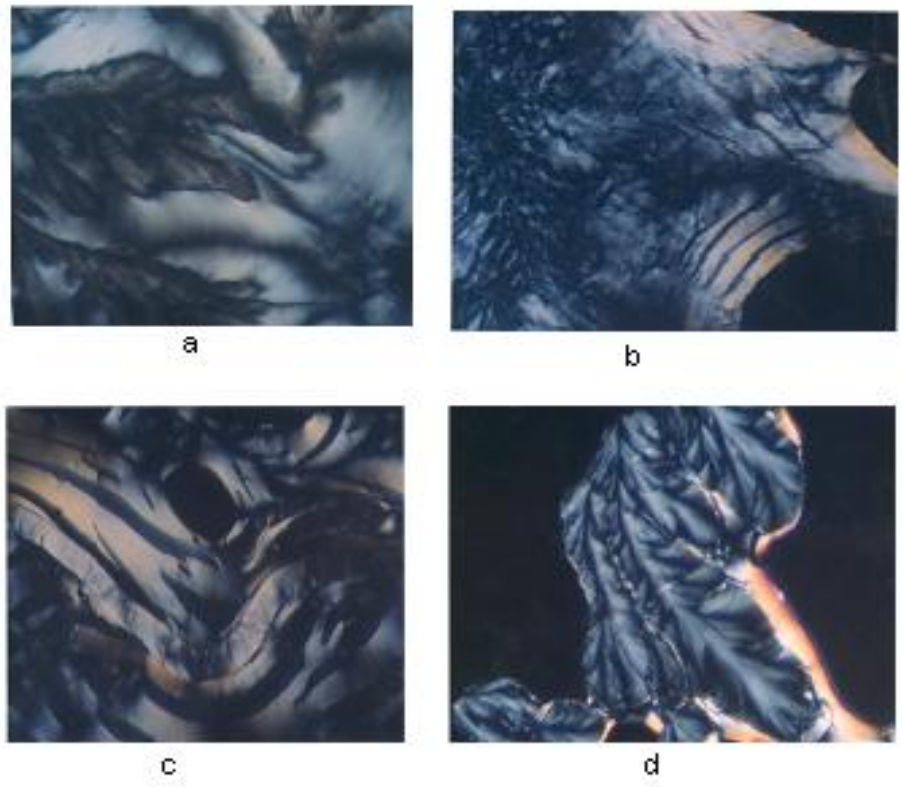

Fig.5.4. Spermine induced LC phases of high molecular weight DNA obtained in the presence of alkali metals. a) Li-DNA was treated with 200mM spermine and incubated in a glass slide at 37^{o}C- Fluid cholesteric phase was obtained after 3 hrs. b) Cholesteric phase obtained after 3 h with Na-DNA when treated with 200mM spermine and incubated in a glass slide at 37^{o}C. c) Cholesteric phase with tear shaped defects obtained after 3 h with K-DNA when treated with 200mM spermine and incubated in a glass slide at 37^{o}C. d) Dendrimeric growth obtained after 1 week with Rb -DNA when treated with 200mM spermine and incubated in a glass slide at 37^{o}C.

Fig.5.3 show that at higher spermine concentrations (200 and 400mM), in presence of Rb^{+} and Cs^{+}, spermine-DNA condensates adopted a cholesteric to columnar arrangement, showing broken-fan shaped textures (Fig.5.4.d) but at lower spermine concentrations transition from cholesteric to columnar phase was not observed, and the cholesteric phase directly underwent isotropization. It appears that the size of the ion exerts additional influence, on the induction, phase transitions and stabilization of the LC phases of DNA.

The X-ray diffraction patterns of few spermine-metal ion-DNA condensates are presented in Fig.5.7. In general, a sharp and strong peak at low angle ($1^0<2\theta<4^0$) in the small angle X-ray scattering (SAXS) curve and a broad peak associated with lateral packing in the wide angle X-ray diffraction region (WAXD) can be observed for the columnar structure. For cholesteric structure no patterns appears in SAXS, however a broad peak occurs at 2θ=16~18. The diffraction angles of cholesteric structure at wide angle are obviously less than that of columnar and nematic structure and this is a very important character to judge the cholesteric structure[36,37]. Small angle X-ray diffraction patterns obtained at 2θ value in between 0 and 5 also indicate the formation of columnar hexagonal phase in the presence of Rb^+ and Cs^+ ions. The broad peak obtained at the wide-angle region could be of the cholesteric phase. It appears that at higher spermine concentration and the increased size of Rb^+ and Cs^+ presumably facilitated the cholesteric to columnar transition. In the presence of Li^+, an unusual stability of DNA mesophase was reported in our recent work[38]. However, in the presence of spermine, lithium ions did not imparted the unusual stability. The hydrated structure of Li^+ ions,[39] which is responsible for the stability factor might have got disturbed in the presence of spermine. The stability of the phases was in the order: $T_{iso}Cs^+ = T_{iso}Rb^+ > T_{iso}Li^+ > T_{iso}K^+ > T_{iso}Na^+$. In the presence of all the alkali metal ions, except sodium, higher spermine concentrations rendered more stability to the LC phases.

5.4.3. *Effect of alkaline earth metal ions on the spermine induced LC DNA*

Magnesium and calcium ions are the most abundant alkaline earths metal ions in the biological systems. They serve a number of critical functions across a multitude of biochemical processes and are also necessary to reach the ultimate states of condensation[26,28]. They are reported to be essential in folding and winding of the polynucleic acids and to assume compact arrangements in vivo[40]. A previous study on the influence of Mg^{2+}/Ca^{2+} on low molecular weight DNA fragments has reported the formation of LC phases, but the phases were not identified[41]. Fig.5.5 shows that except Mg^{2+}, all the alkaline earth metal ions exhibit both cholesteric and columnar hexagonal phases as a time dependent phenomenon above a spemine concentration of 200 mM. It also shows that the cholesteric to columnar transitions depend on the size of the ion. In the presence of Mg^{2+}, below 400mM spermine concentrations cholesteric with nematic thread like fluidy structures (Fig.5.5.a and c) were formed initially which got darkened eventually without transforming into the higher ordered columnar phase (Fig.5.6.a). But in the absence of spermine cholesteric to columnar transition was observed. The existence of fluidic textures gives a clue to the possible physiological role of polyamines and the Mg^{2+} in the cell nucleus, where chromatin is condensed, still maintaining the mobility of the double strands required for the biological functions of DNA within the condensates.

A cholesteric organization of DNA was reported in dinoflagellate chromosomes[42-44] and in certain bacterial nucleoids[45]. It was also shown that

the condensed DNA in the presence of polyamines can stimulate the functional properties of DNA such as the efficiency of replication and transcription of DNA[17]. A cholesteric with nematic thread like fluidic structure (Fig.5.5.c) was observed with Sr^{2+} also, the phase instead of darkening transformed itself into the higher ordered columnar phase.

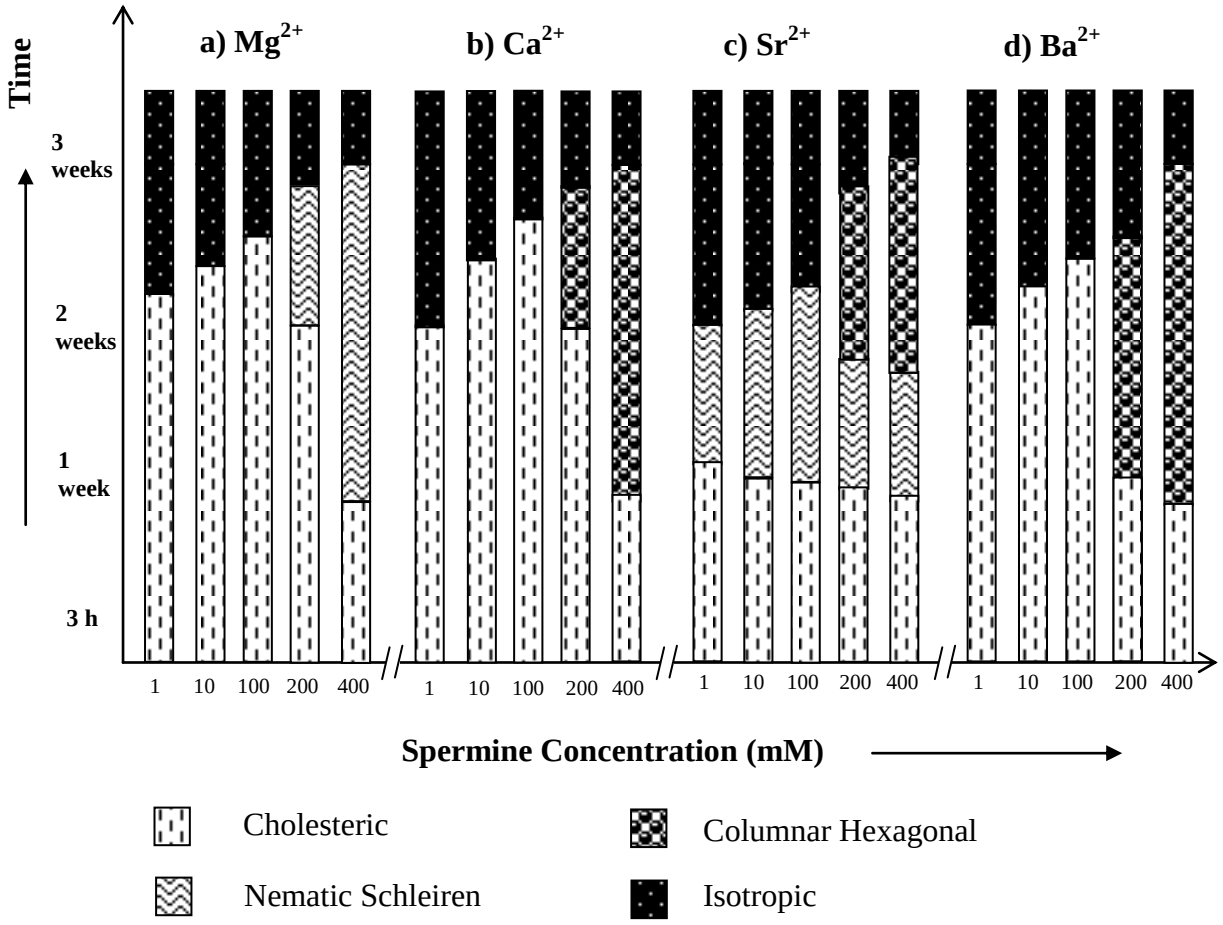

Fig.5.5. Time dependent phase transitions of spermine induced DNA condensates in the presence of alkali metal ions.

In the presence of calcium and barium below 400mM spermine concentrations, cholesteric phase was formed initially which developed striped appearance followed by broken fan shaped textures typical of columnar phase (Fig.5.6 b and d) and got darkened subsequently (Fig.5.5.b and d). Small angle

X-ray diffraction patterns obtained at 2θ value in between 0 and 5 also indicates the formation of columnar hexagonal phase (Fig.5.7).

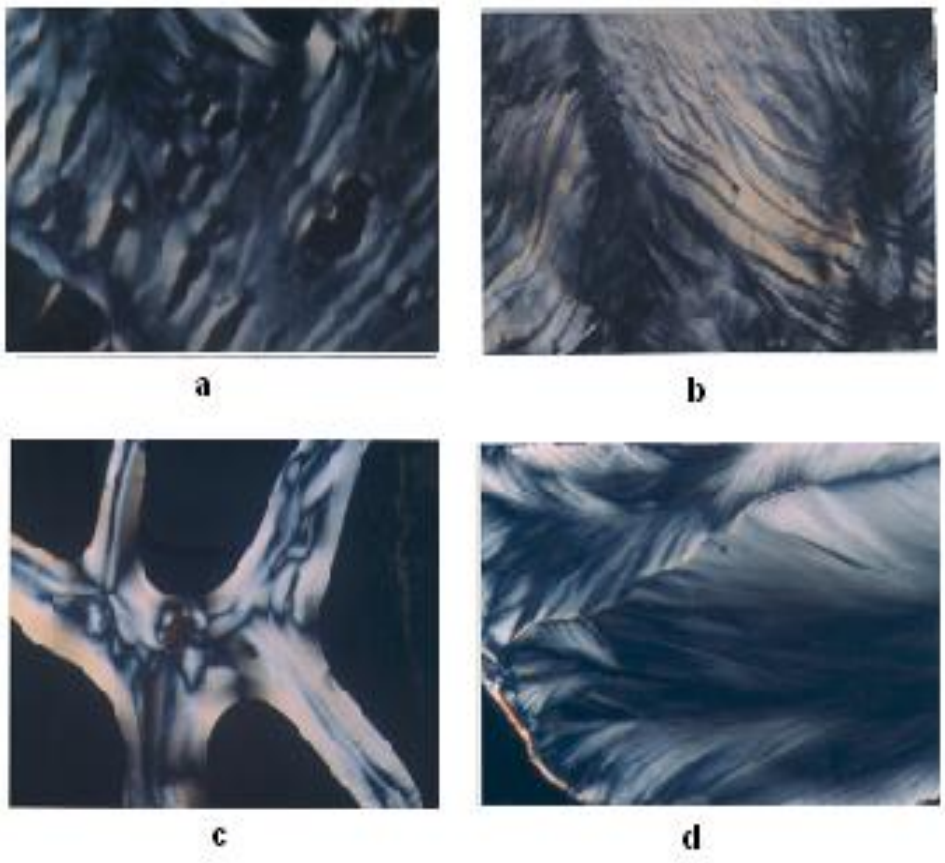

Fig.5.6. Spermine induced LC phases of high molecular weight DNA obtained in the presence of alkaline earth metals. a) Fluid cholesteric phase obtained after 3 hrs when Mg-DNA was treated with 100mM spermine and incubated in a glass slide at 37^{o}C. b) Cholesteric phase with striped pattern obtained after 12 hrs. with Ca-DNA when treated with 200mM spermine and incubated in a glass slide at 37^{o}C. c) Cholesteric phase with nematic threaded structures obtained after 3 hrs. with Sr-DNA when treated with 200mM spermine and incubated in a glass slide at 37^{o}C. d) Fan shaped textures of columnar phase obtained after 1 week with Ca-DNA when treated with 200mM spermine and incubated in a glass slide at 37^{o}C.

The comparatively faster formation of a well defined broken fan shaped textures typical of columnar phase, compared to those without spermine, suggests the importance of the synergistic effect calcium ions and spermine in inducing the most efficient columnar packing of DNA molecules in vivo. A

hexagonal packing of DNA was observed in bacteriophages and certain sperm heads[46]. As alternate condensation and decondensation of DNA is believed to occur when DNA functions in cell nucleus, both cholesteric and columnar phases may exist according to the local requirement.

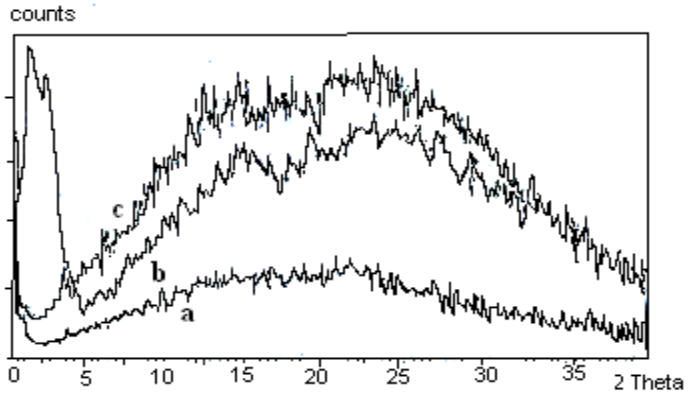

Fig.5.7. XRD patterns obtained with the biphasic sample obtained on precipitation with 200mM spermine. The low angle peak corresponds to the columnar packing of DNA molecules and wide- angle broad peak is related to the cholesteric phase of the sample. a) Rb-DNA and b) Cs-DNA c) Ca-DNA system.

Previous studies described in Chapter 2A and 3A, on the induction and stabilization of the LC phases, with metal ions of varying sizes indicated that the transition from cholesteric to columnar hexagonal phase was facilitated by the size of the concerned ion. Fig.5.4 and 5.6 also indicates a similar effect. It can also be noted for Fig. 5.5 that as the spermine concentration increases the stability of the phases also increases. Thus at 400 mM, $T_{iso}Mg^{2+} = T_{iso}Ca^{2+} = T_{iso}Sr^{2+} = T_{iso}Ba^{2+}$ and < 400 mM, $T_{iso}Mg^{2+} > T_{iso}Ca^{2+} = T_{iso}Sr^{2+} > T_{iso}Ba^{2+}$.

5.5. Conclusions

The effect of spermine on the induction and stabilization liquid crystalline phases of high molecular weight DNA in the presence of alkali and

alkaline earth metal ions was investigated. The spermine induced DNA pellets/aggregates exhibited multiple macroscopic polymorphic behaviors depending on the concentration of both spermine, charge and size of the metal ions, and time. The LC phases were observed at concentrations (5mg/ml), that are far less than that necessary for low molecular weight (150 mg/ml) DNA and the mesophases, both cholesteric and columnar hexagonal were comparable with those obtained with low molecular weight DNA with, of course, local variations in stability and texture. The concentration of spermine to precipitate DNA in the presence of the metal ions followed an order (C_{sp} spermine alone> C_{sp} alkali metal ions > C_{sp} alkaline earth metal ions) based both on the charge and size of the ion. However, the higher ordered columnar hexagonal phases were observed with metal ions of higher sizes at a spermine concentration of above 200 mM. The stability of the spermine induced LC DNA phases in the presence of alkali metal ions was in the order: $T_{iso}Cs^+ = T_{iso}Rb^+ > T_{iso}Li^+ > T_{iso}K^+ > T_{iso}Na^+$.

The alkaline earth metal ions with the exception of Mg^{2+}, exhibited a more mobile cholesteric phase that got transformed into broken fan shaped columnar hexagonal phases as a time dependent phenomenon above a spermine concentration of 200 mM. The transformation of the cholesteric phase with striped appearance into a stable higher ordered columnar hexagonal phase in the case of Ca^{2+} might suggest a probable role of Ca^{2+} in packing DNA in vivo into hexagonal arrangement. The existence of a stable fluid cholesteric phase induced by spermine in presence of Mg^{2+} can be thought of possibly as a clue

to the role of Mg^{2+} in condensing DNA synergistically with spermine in the cell nucleus and preserving the mobility required for the biological functions in the condensed state due to its (Mg^{2+}) higher hydration energy.

Among all the metal ions studied, the behavior of Na^{+} was exceptional in inducing resolubilization at a very low concentration of 12 mM spermine whereas, with the other metal ions DNA got resolubilized at or above 400 mM concentration of spermine.

Small angle X-ray diffraction peaks obtained at 2θ value in between 0 and 5 also indicates the formation of columnar hexagonal phase with Rb-DNA, Cs-DNA and Ca-DNA system. It appears that the alkali and alkaline earth metal ions might have involved in a condensation process in concert with spermine, which facilitated the precipitation of DNA. The data generated could be useful in selecting a particular metal for generating a particular LC phase for the preparation of spermine based DNA nanoparticles.

5.6. References

1. Zimmerman, S. B.; Murphy, L. D., *FEBS Lett.* **1996, 390**, 245.
2. Tabor, C. W.; Tabor, H., *1Annu. Rev. Biochem* **1976,** 45, 285.
3. Canellakis, E. S.; Viceps-Madore, D.; Kyriakidis, D. A.; Heller, J. S., *Curr. Top. Cell. Regul.* **1979,** 15, 155.
4. Thomas, T.; Thomas, T. J., *Cell. Mol. Life Sci.* **2001, 58**, 244.
5. Dam, L. V.; Korolev, N.; Nordenskiöld., L., *Nucleic Acids Research* **2002,** 30, (2), 419.
6. Santhakumaran, L. M.; Chen, A.; Pillai, C. K. S.; Thomas, T.; He, H. X.; Thomas, T. J., *Nanotechnology in Non-Viral Gene Delivery,book chapter in "Nanofabrication for Biomedical Applications."* ed.; Wiley-VCH: 2004.
7. Vijayanathan, V.; Thomas, T.; Thomas, T. J., *Biochemistry* **2002,** 41, 14085.
8. Vijayanathan, V.; Thomas, T.; Sigal, L., H.; Thomas, T. J., *Antisense Nucleic Acid Drug Dev* **2002,** 12, 225.
9. Vijayanathan, V.; Thomas, T.; Shirahata, A.; Thomas, T. J., *Biochemistry* **2001,** 40, 9387.
10. Bloomfield, V. A., *Biopolymers* **1991**, 31, 1471.
11. Gosule, L. C.; Schellman, J. A., *Nature* **1976,** 259, 333.
12. Raspaud, E.; Chaperon, I.; Leforestier, A.; Livolant, F., *Biophys. J.* **1999**, 1547.
13. Saminathan, M.; T., T.; Shirahata, A.; Pillai, C. K. S.; Thomas, T. J., *Nucl. Acids. Res* **2002,** 30, 3722.
14. Pelta, J.; Livolant, F.; Sikorav, J. L., *J. Biol. Chem.* **1996,** 271, 5656.
15. Livolant, F.; Leforestier, A., *Prog. Polymer Sci.* **1996,** 21, 1115.
16. Leforestier, A.; Livolant, F., *Biophys. J.* **1993,** 65, 56.
17. Sikorav, J. L.; Pelta, J.; Livolant, F., *Biophys. J.* **1994,** 67, 1387.
18. Leforestier, A.; Fudaley, S.; Livolant, F., *J. Mol. Biol.* **1999,** 290, 481.

19. Raspaud, E.; Olvera de la Cruz, M.; Sikorav, J. L.; Livolant, F., *Biophys. J.* **1998,** 74, 381.
20. Andreasson, B.; Nordenskiöld, L.; Braunlin, W. H., *Biopolymers,* **1996,** 38, 505.
21. Robinson, H.; Wang, A. H. J., *Nucleic Acids Res.* **1996,** 24, 676.
22. Deng, H.; Bloomfield, V. A.; Benevides, J. M.; Thomas, G. J., Jr, *Nucleic Acids Res.* **2000,** 28, 3379.
23. Lomozik, L.; Jastrzab, R.; Gasowska, A., *Polyhedron* **2000,** 19,1145.
24. Gąsowska, A.; Łomozik, L., *J. Coord. Chem* **2001,** 52, 375.
25. Gąsowska, A.; Jastrząb, R.; Bregier-Jarzębowska, R.; Łomozik, L., *Polyhedron* **2001,** 20, 2305.
26. Glusker, J. P., *Adv. Protein Chem.* **1991, 42**, 1.
27. Misra, V. K.; Draper, D. E., *Biopolymers,* **1998,** 48, 113.
28. Holm, R. H.; Kennepohl, P.; Solomon, E. I., *Chem. Rev.* **1996, 96**, 2239.
29. Pelta, J., Jr; Durand, D.; Doucet, J.; Livolant, F., *Biophys. J.* **1996,** 71, 48.
30. Strzelecka, T. E.; Rill, R. L., *Biopolymers* **1990,** 30, 57.
31. Pillai, C. K. S.; U. S. Nandi, *Indian J. Phys* **1976,** Commomorative Volume, 277.
32. Pillai, C. K. S.; Nandi, U. S.; Levinson, W., *Bio-inorganic Chem.* **1977,** 7, 151.
33. Bryson, K.; Greenall, R. J., *J. Biomol. Struct. Dyn.*, **2000,** 18, 393.
34. Theophanides, T., *Int. J. Quantum Chem.* **1984,** 26, 933.
35. Jorgensen, P. L.; Hakansson KO; D, K. S. J., *Annu Rev Physiol* **2003,** 65, 817.
36. Wang, L. G.; Huang, Y., *Chinese J Cell Sci Tech* **2000,** 8, 7.
37. Dong, Y. M.; Yuan, Q.; Xiao, Z. L., *Chem J Chinese Univ* **1999,** 20, 140.
38. Sundaresan, N.; Thomas, T.; Thomas, T. J.; Pillai, C. K. S., *Macromol. Biosci.* **2006,** 6, 27.

39. Puri, B. R.; Sharma, L. R.; Kalia, K. C., *Principles of Inorganic Chemistry*. ed.; Shobhan Lal Nagin Chand & Co.: 1998.
40. Widom, J., *Annu Rev Biophys Biomol Struct* **1998,** 27, 285.
41. Salyanov.V.I.; Lavrentev, P. I.; Chernuka, B. A.; Evdokimov, Y. M., Mol. Biol., **1995,** 28, 796.
42. Livolant, F., *Eur. J. Cell Biol.* **1984,** 33, 300.
43. Bouligand, Y.; Soyer, M. O.; Puiseux-Dao, *Chromosoma* **1968,** 24, 251.
44. Rill, R. L.; Livolant, F.; Aldrich, H. C.; Davidson, M. W., *Chromosoma* **1989,** 98, 280.
45. Gourett, J. P., *Biol. Cell* **1978,** 32, 299.
46. Lepault, J.; Dubochet, W.; Baschong, W.; Kellenberger, E., *EMBO J.* **1987,** 6, 1507.

CHAPTER 6

SUMMARY AND CONCLUSIONS

The condensation of DNA into Liquid crystalline (LC) domains has become a lively area of research due to its potential applications in diverse fields ranging from nanoelectronics to gene delivery. The condensation of DNA is known to involve neutralization of the highly anionic phosphate moieties of DNA by positively charged counter ions. The highly ordered and condensed LC phases of nucleic acids in *vivo* are largely due to their interaction with basic proteins, polyamines and metal ions. The LC phase behavior of DNA is known to be, influenced largely by the nature and concentration of counter ion, because the effective particle radius and excluded volume of DNA are determined by the counter ion shielding. Studies on the DNA LC domains can therefore be used as a probe to obtain vital information on its supramolecular organization *in vivo* and also the functioning of DNA in the condensed states. However, the present level of understanding on the LC phase behavior of DNA is inadequate and a thorough investigation is required to understand the nature, texture, stability, and the influence of various environmental conditions on the structure of these phases. The earlier studies were mostly carried out with low molecular weight DNA that established a polymorphic phase behavior in the presence of a few biologically important metal ions. It becomes, therefore, clear that the effect of metal ions of varying

size, charge, hydration, binding modes on the LC behavior of high molecular weight DNA might provide vital information on the phase behavior of DNA.

Some of the metal ions such as sodium, potassium, magnesium, calcium etc. are involved in a variety of cellular functions (enzymatic activities related to replication, transcription, recombination etc.) including DNA condensation, whereas certain metal ions such as cadmium, aluminium, vanadium etc. are known for their genotoxic effects. Those metal ions that bind primarily to the phosphates stabilize the helix by reducing the intermolecular repulsion, which provokes LC ordering, whereas a distortion of the double helix by base binding metal ions might result in the loss of rigid rod like shape of the DNA molecule, which is the determinant factor of its LC ordering. The present work, therefore, is an attempt towards understanding the LC behavior of DNA with selected cations of varying size, charge, mode of binding, hydration and other environmental conditions. Therefore, the objectives of the present work were:

1) Investigations on the induction and stabilization of LC phases of high molecular weight DNA by alkali metal ions.

2) Investigations on the induction and stabilization of LC phases of high molecular weight DNA by alkaline earth metal ions.

3) Effects of multivalent, transition and heavy metal ions on the LC phase behavior of high molecular weight DNA.

4) Investigations on spermine induced LC behavior of high molecular weight DNA in the presence of alkali and alkaline earth metal ions.

In an attempt to understand the binding affinities of few biologically important metal ions to DNA, the thesis also included molecular modeling studies on the binding modes of metal ions such as Li^+, Na^+, K^+, Mg^{2+} and Ca^{2+} to DNA.

Chapter 1 of the thesis out of six chapters gave a brief review of LC behavior DNA, DNA condensation by multivalent ions and its potential applications.

Chapter 2A described the comparative study of the effects of alkali metal ions Li^+, Na^+, K^+, Rb^+ and Cs^+ on the LC organization of high molecular weight calf thymus DNA using polarized light microscopy which indicated major differences in behavior for Li^+ ions (See Fig.6.1). Multiple LC phases of DNA were generated at concentrations (7.14 mg/ml) that are far less than that required for low molecular weight (200 mg/ml) DNA. Two main phases, cholesteric and columnar hexagonal and sometimes nematic Schlieren like texture, were found either separately or in coexistence, with variations in the stability of the phases depending on local conditions and time. Critical DNA concentration (C_D) required to exhibit anisotropic behavior was same for all the monovalent ions (See Fig.6.1), except Li^+ ion, which could be due to its higher hydration factor and also to its outer sphere (water mediated contact to DNA) binding mode to DNA. The inner sphere binding mode (direct contact to DNA) of Na^+, K^+, Rb^+ and Cs^+ ions to DNA might have facilitated the dehydration of DNA which favors the formation of liquid crystalline phase (see below for data obtained from molecular modeling studies).

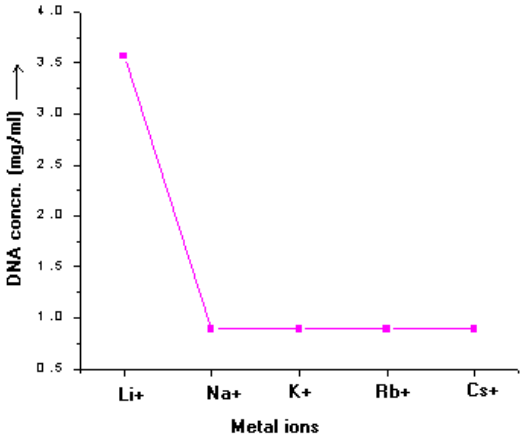

Fig.6.1. Critical DNA concentration required for anisotropy in the presence of alkali metal ions.

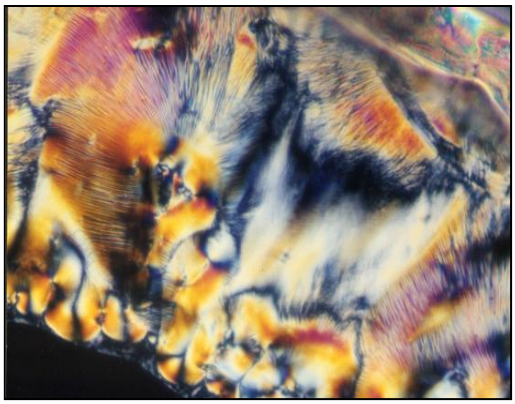

Fig.6.2. The biphasic cholesteric-columnar arrangement obtained in the presence of Li^+ ions.

DNA initially showed cholesteric textures, which later on turned to a more ordered columnar phase, but the cholesteric-columnar transition was facilitated by increased size of the ion. In the case of Li^+ ion, a nematic Schlieren like texture was formed initially, which after a few days changed to a higher ordered and highly stable (for more than two months) biphasic cholesteric-columnar arrangement (Fig.6.2). The observed differences between Li^+ and other alkali metal ions could be understood on the basis of the higher hydration factor and its outer sphere-binding mode. Chapter 2B presented the Molecular Modeling studies of the interactions of Li^+, Na^+ and K^+ ions to a DNA fragment both in an anion and dianion state using a three-layer ONIOM approach. Three hydrated metal-DNA binding combinations were studied which include, outer sphere (water mediated contact to DNA) and inner sphere mono- and bi dentate (direct contact to DNA) patterns. These studies revealed

that the metal ions could bind to DNA both in an outer and inner sphere (mono- and bi-dentate) manner, which in turn depends on the charge of the DNA fragment. The outer sphere binding of Li^+ ion to the anion model (see Fig.6.3) of DNA and its strong binding compared to Na^+ and K^+ is a point of support to the unique LC behavior of DNA in the presence of Li^+ ion.

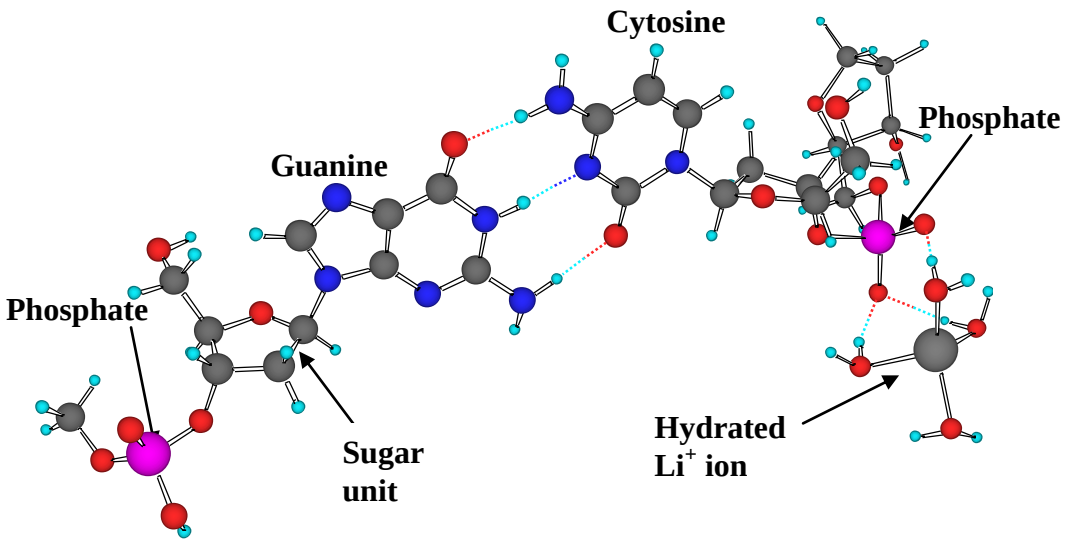

Fig.6.2. ONIOM optimized full geometry of Li^+ ion outer sphere binding to anion model of DNA.

Chapter 3A described the comparative study of the effects of alkali metal ions Mg^{2+}, Ca^{2+}, Sr^{2+} and Ba^{2+}on the LC organization of high molecular weight calf thymus DNA, using polarized light microscopy. As a whole, the C_D required to exhibit anisotropy was found to be higher for alkaline earth metal ions than alkali metal ions, which suggests that both the size and charge of the metal ions had influenced the induction of LC behavior in DNA. C_D required to exhibit LC behavior in presence of Mg^{2+} was higher than that of Ca^{2+}, which in turn is higher than Ba^{2+} and Sr^{2+} (see Fig.6.4). This might be due to their difference in hydration energy, and also to the outer sphere binding mode of

Mg^{2+} (see Chapter 3B) and the inner sphere binding modes of Ca^{2+}, Sr^{2+} and Ba^{2+} ions to DNA. LC phases could be obtained only under defined ionic conditions in the presence of Mg^{2+} ions. It should be noted that both Mg^{2+} and Li^{+} required a higher C_D for inducing the LC states and this behavior, which can be correlated to their diagonal relationship. The formation of higher ordered columnar phase at higher concentrations of Ba^{2+} and Sr^{2+} might be due to their larger size, which presumably facilitated the dehydration process to achieve the textures typical of the higher ordered columnar phase. All the alkaline earth metal ions studied exhibited prominent cholesteric to columnar phase transition (Fig.6.5) at lower metal ion concentrations(<0.5 M).

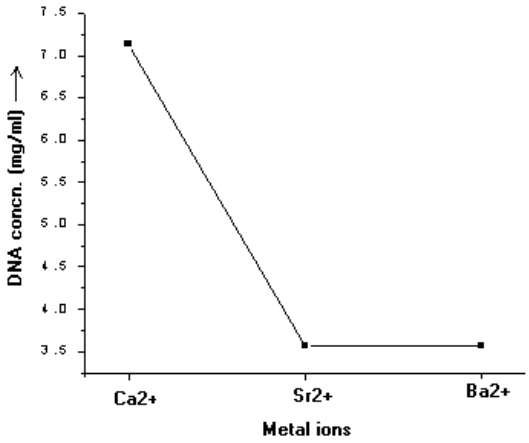

Fig.6.4. Critical DNA concentration in the presence of alkaline earth metal ions

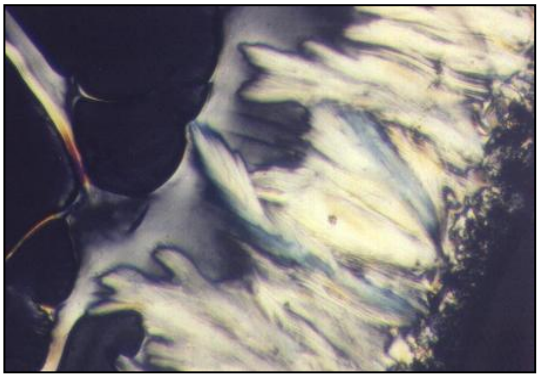

Fig.6.5. Evolution of columnar phase from cholesteric phase in the presence of Mg^{2+}ion.

Chapter 3B dealt with the Molecular Modeling studies on the interactions of Mg^{2+} and Ca^{2+} ions to a DNA fragment both in an anion and dianion state using a three layer ONIOM approach. Three hydrated metal-DNA binding combinations were studied as in the case of alkali metal ions, which include outer sphere and inner sphere mono- and bi dentate patterns. One of the

main findings from this study was that, DNA has more affinity for alkaline earth metal ions than alkali metal ions. A mono-dentate binding mode was the most stable structure observed for both ions in the anion model. However, the binding interactions of Mg^{2+} and Ca^{2+} to the dianion model of the DNA fragment gave rise to a dramatic structural deformation at the base pair region, which led to the formation of "ring" structures. The formation of "ring" structures with Mg^{2+} and Ca^{2+} strongly supports the role of Mg^{2+} and Ca^{2+} in DNA bending. However, in both the anion and dianion models, Mg^{2+} bound structures were considerably more stable than the Ca^{2+} bound structures. Unlike Ca^{2+} ion, the charge of the DNA fragment appeared to be crucial in deciding the binding strength as well as the binding mechanism of Mg^{2+} ion. The outer sphere binding of Mg^{2+} ion to the dianion model (See Fig.6.6) of DNA is a point of support to the higher C_D required for LC behavior of DNA in the presence of Mg^{2+} ion.

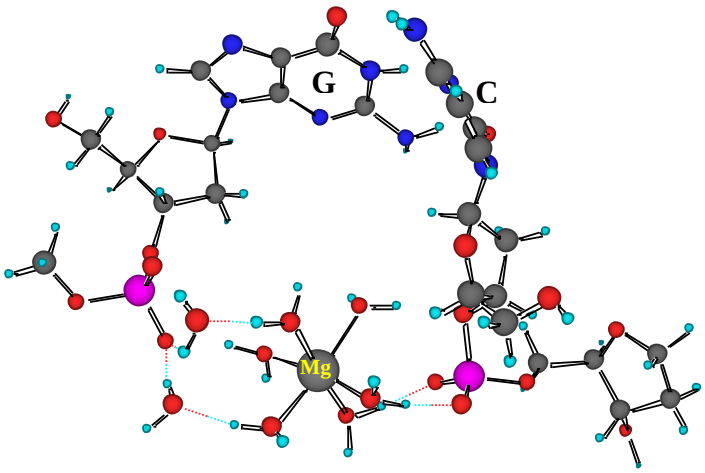

Fig.6.6. ONIOM optimized full geometry of bent structure of the DNA fragment (dianion model) in the presence of Mg^{2+} ion.

Chapter 4 presented the effect of transition and multivalent metal ions such as Cu^{2+}, Cd^{2+}, V^{4+}, Al^{3+} and heavy metal ions such as Hg^{2+}, Pd^{2+}, Au^{3+} and

Pt^{4+} on the LC phases of high molecular weight DNA. The overall phase behavior of DNA was complex, with multiple textures exhibiting below a certain critical metal ion concentration, which in turn depends on the binding mode of the metal ion to DNA. In contrast to the behavior of alkali and alkaline earth metal ions, Cu^{2+}, Cd^{2+}, Al^{3+} and V^{4+} ions when mixed with stock DNA solution (7.14 mg/ml) precipitated DNA into solid gel at high metal ion concentration (~1M) and translucent gel like aggregates at lower concentrations (0.625mM-1M), which lacked the mobility required for LC behavior.

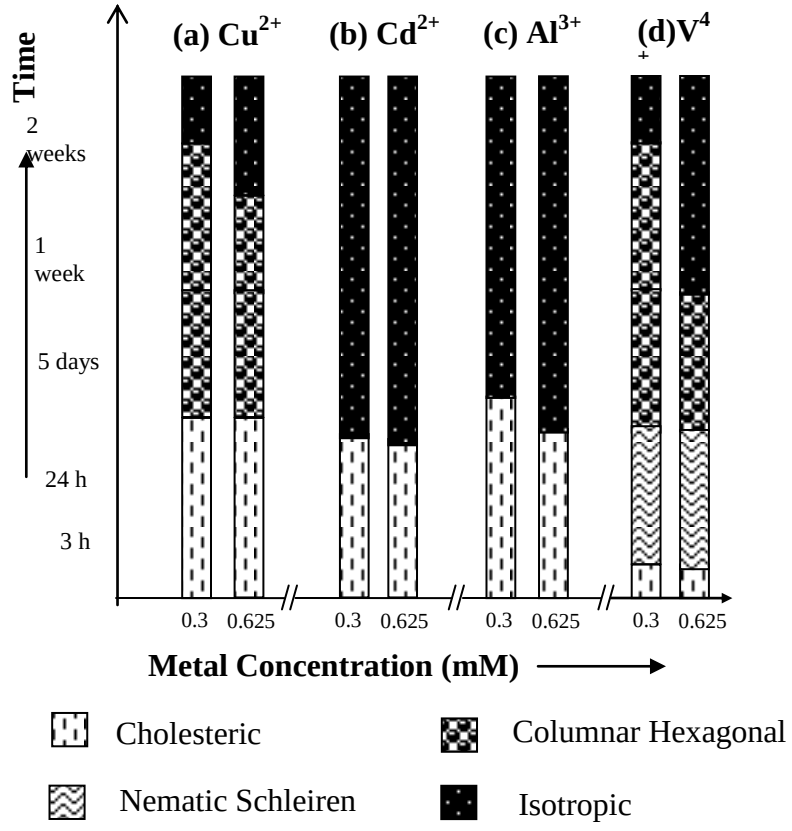

Fig.6.7. Time dependent phase transitions of DNA in the presence of transition and multivalent ions.

Heavy metal ions such as Hg^{2+}, Pd^{2+}, Au^{3+} and Pt^{4+} ions up to certain critical metal ion concentration reduced the viscosity of DNA solution required

for anisotropic behavior by disrupting the rigid rod like behavior, which was the determinant factor for LC behavior.

Transition and heavy metal ions differed considerably in their induction and stabilization of LC phases due to their different electronic structure. Among the transition and multivalent metal ions the LC phase in the presence of Cd^{2+} was highly unstable (Fig.6.7) because of its toxic nature. The heavy metal ions, showed the highest instability in LC phase behavior in comparison to alkali, alkaline earth and other multivalent ions studied.

Besides metal ions, polyamines are also known to stabilize the compact form of DNA in the cell nucleus and spermine based drugs have become chemotherapeutically important.

Chapter 5 described the nature and stability of the LC phases of the spermine-induced DNA aggregates in the presence of alkali and alkaline earth metal ions. The precipitation of DNA by spermine was found to increase with the alkali, and alkaline earth metal ions (see Fig.6.8), suggesting alkali, and alkaline earth metal ions instead of getting into competition with spermine in DNA binding, had acted in concert to precipitate DNA from solution. Spermine moiety because of its larger size is reported to prefer to bind along the major grooves of DNA and alkali and alkaline earth metal ions because of their smaller size are reported to prefer A-T rich minor grooves of DNA as binding sites. DNA remained in the resolubilised/isotropic state above 400mM spermine in presence of all the ions except in case of Na^{+} ions, which was above 12mM, indicating that spermine and Na^{+} concentrations may be well

balanced in the cell nucleus to maintain DNA in the condensed states for its biological functions. Spermine-DNA-metal ion complexes exhibited mainly two different phases and at least one of them was fluid in nature, which was the cholesteric phase and a columnar hexagonal phase with a restricted fluidity in which DNA molecules were more closely packed.

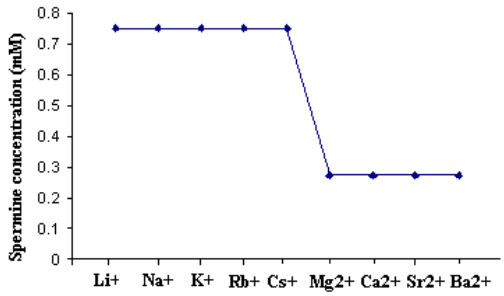

Fig.6.8. Critical spermine concentration (C_{sp}) required for the onset of DNA precipitation with alkali and alkaline earth metal ions

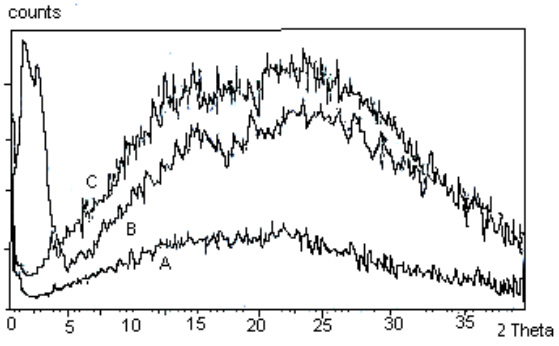

Fig.6.9. XRD patterns obtained with the biphasic sample obtained on precipitation with 200mM spermine. The low angle peak corresponds to the columnar packing molecules and wide-angle broad peak is related to the cholesteric phase of DNA. A) Rb-DNA and B) Cs-DNA

In the presence of alkali metal ions spermine-DNA aggregates were mainly in cholesteric phase but at higher spermine concentrations, in the presence of Rb^+ and Cs^+, they adopted a cholesteric to columnar arrangement, suggesting the size effect on the LC phase transitions. Among the alkaline earth metal ions, the existence of fluidic textures in the presence of Mg^{2+} gave a clue to the possible synergistic role of polyamines and the Mg^{2+} in the cell nucleus, in preserving the fluidity required for the biological functions within the condensates. The evolution of columnar phase from cholesteric phase in the presence of Ca^{2+} also indicated the probable role of Ca^{2+} in packing DNA into

hexagonal arrangement in vivo. Small angle X-ray diffraction peaks obtained at 2θ value in between 0 and 5, also indicates the formation of columnar hexagonal phase with Rb-DNA, Cs-DNA and Ca-DNA systems (see Fig.6.9).

In summary, the present work showed that multiple LC phases of high molecular weight DNA could be generated at concentrations that are far less than that required for low molecular weight DNA. The overall phase behavior was found to be dependent on several parameters including the concentration, size, charge, hydration and binding modes of the metal ions and time. Alkali and alkaline earth metal ions differed considerably from transition and heavy metal ions in their induction and stabilization and/or destruction of LC phases depending on their mode of binding to DNA. The alkali and alkaline earth metal ions stabilized DNA and gave the typical cholesteric/columnar structures even at high metal ion concentration, whereas the transition metal/multivalent ions precipitated DNA into solid/translucent gel like aggregates and heavy metal ions reduced the viscosity of the DNA solution, disrupting the rigid rod like structure, which was the determinant factor for its liquid crystalline behavior.

These results might find applications in gene therapy, in developing DNA based devices, in nanoelectronics, in designing biosensing units, in DNA chips, in biomarkers etc. The present data on the behavior of the LC phases of DNA in the presence of metal ions of varying size and binding modes especially in the case of divalent transition metal ions and heavy metal ions thus indicated that the mechanisms involved in the causation of certain diseases

caused by an excess of these metal ions in the body might possibly be related to the supramolecular organization of DNA in the cell.

Future directions: Since, the metal induced damage to LC organization of DNA *in vitro* can be correlated with the LC organization of the various diseased cells due to metal toxicity, a serious study on the LC phase behavior of DNA of the metal induced diseased cell would be worthwhile, which might shed new light on the mechanisms of causation of the disease and finally appropriate solutions.

APPENDIX

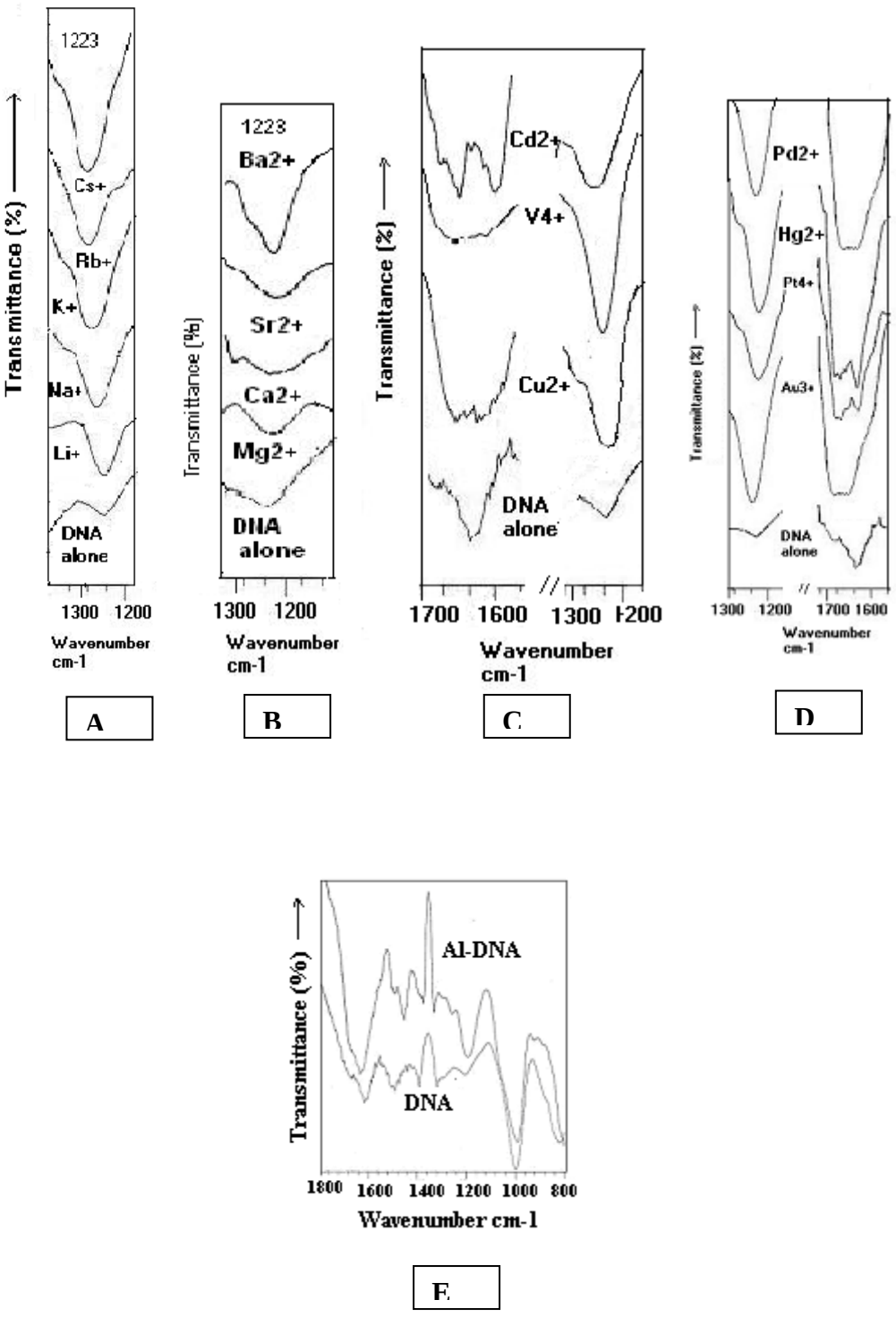

Fig.1: IR spectra of DNA in the presence of (A) Li^{+}, Na^{+}, K^{+}, Rb^{+} and Cs^{+} (0.5 M) (B) Mg^{2+}, Ca^{2+}, Sr^{2+} and Ba^{2+} (0.5M)(C) Cu^{2+}, Cd^{2+} and V^{4+} (0.725mM)(D) Hg^{2+}, Pd^{2+}, Au^{3+} and Pt^{4+} (0.2mM)(E) Al^{3+} (0.725mM)

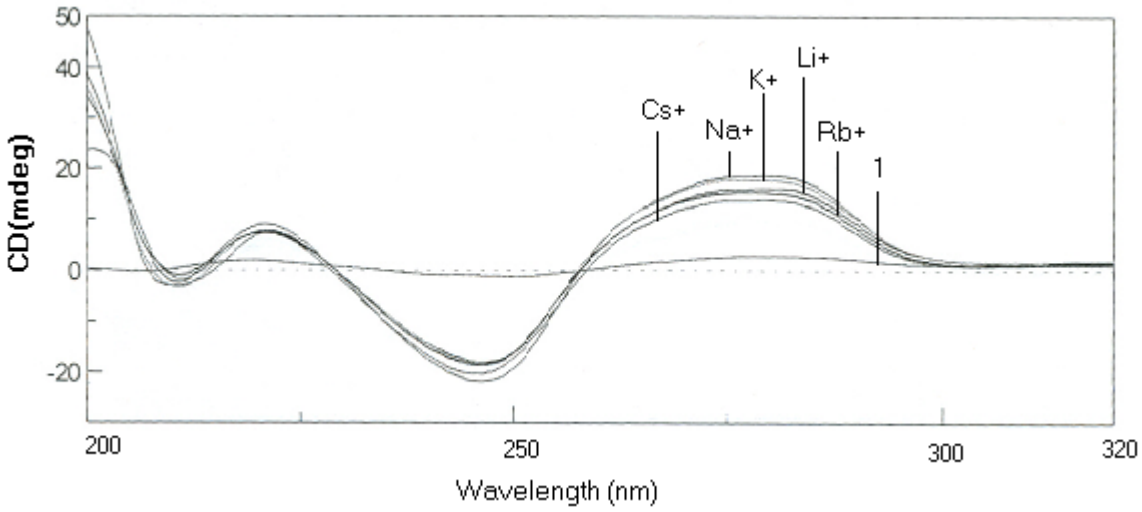

Fig.2. CD profile of DNA after addition of 0.5 M alkali metal ions (1- DNA alone)

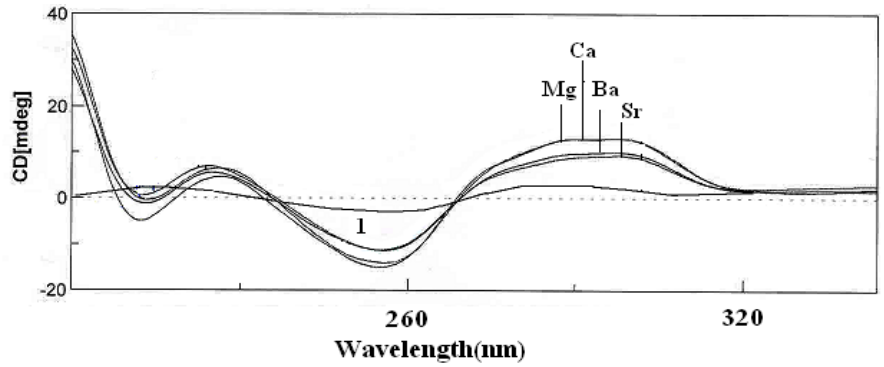

Fig.3. CD profile of DNA after addition of 0.5 M alkaline earth metal ions

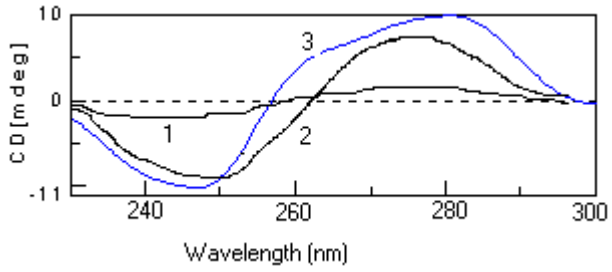

Fig.4. CD profile of V^{4+}-DNA system, 1-DNA alone, 2- V-DNA at low concentration (0.5mM), 3) V-DNA at high concentration (0.675mM).

Hydration of alkali and alkaline earth metal ions-Molecular Modeling Studies.

In order to study the phosphate…hydrated-metal ion interactions, it was also essential to study the hydrated structures of alkali and alkaline earth metal ions. Hence, the geometries of metal ions with different water molecules were optimized with B3LYP/6-31G(d) level of theory and the corresponding energies were used for interaction energy calculations, which are presented in Fig.5.

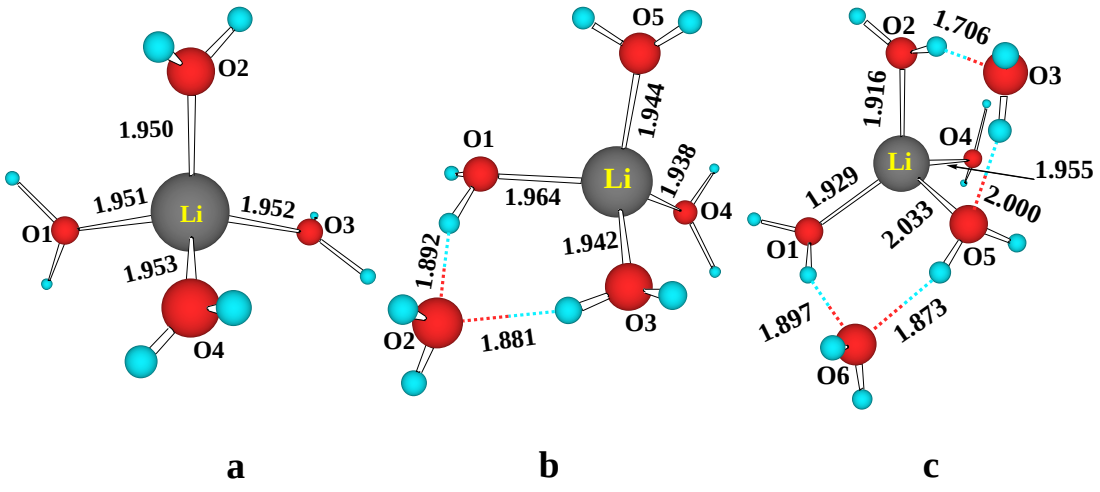

Fig.5. B3LYP level optimized geometries of hydrated lithium ion. (a) $Li(H_2O)_4$ (b) $Li(H_2O)_5$ and (c) $Li(H_2O)_6$. All bond lengths are in Å.

The optimized geometries of hydrated Li^+ in the presence of 4, 5 or 6 water molecules suggests (Fig.5) that Li^+ coordinates tetrahedrally to four water molecules, which is the primary solvation shell and the extra water molecules are hydrogen bonded to the water molecules in the primary solvation shell.

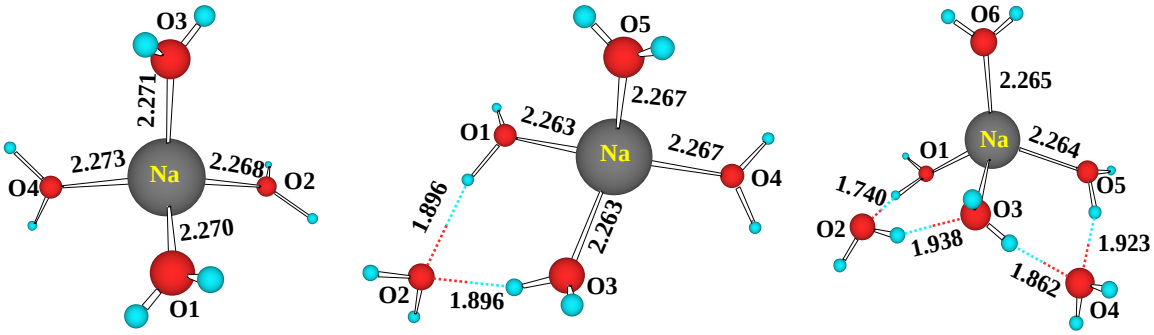

a **b** **c**

Fig.6. B3LYP level optimized geometries of hydrated sodium ion. (a) $Na(H_2O)_4$ (b) $Na(H_2O)_5$ and (c) $Na(H_2O)_6$. All bond lengths are in Å.

Like Li^+, Na^+ also affords a tetrahedral geometry with four water molecules, and the additional water molecules are hydrogen bonded to the water molecules in the primary solvation shell (Fig.6). Our results for Li^+ and Na^+ are in good agreement with the results obtained by Glendening et al.

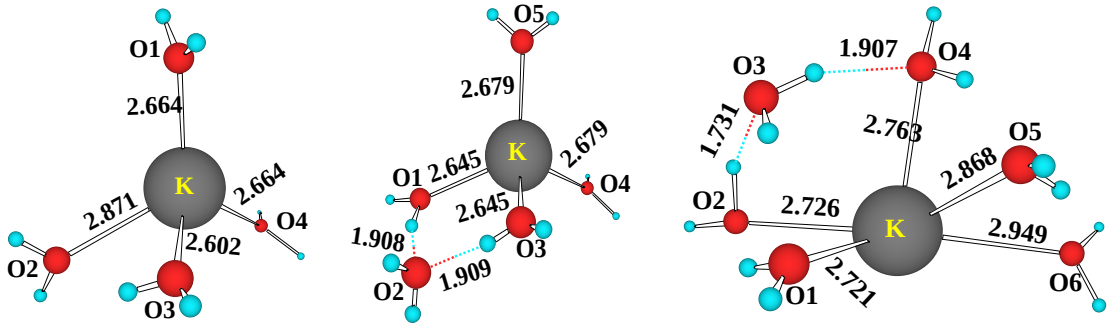

a **b** **c**

Fig.7. B3LYP level optimized geometries of hydrated sodium ion. (a) $K(H_2O)_4$ (b) $K(H_2O)_5$ and (c) $K(H_2O)_6$. All bond lengths are in Å.

In the case of K^+, with 4 and 5 water molecules, the primary solvation shell is found to be tetrahedral, while a sixth water molecule distorts this tetrahedral arrangement in such a way that the primary solvation shell appears as a distorted square pyramid containing five water molecules (See Fig.7). In this structure, the sixth one is interacting with two water molecules of the primary solvation shell. We

also optimized an octahedral geometry for the hexa hydration, but this was found to be 11.4 kcal/mol less stable than the square pyramidal structure.

Hydrated alkaline earth metal ions

With five water molecules, Mg^{2+} has a trigonal bipyramidal structure, while with the sixth water molecule it forms a regular octahedron.

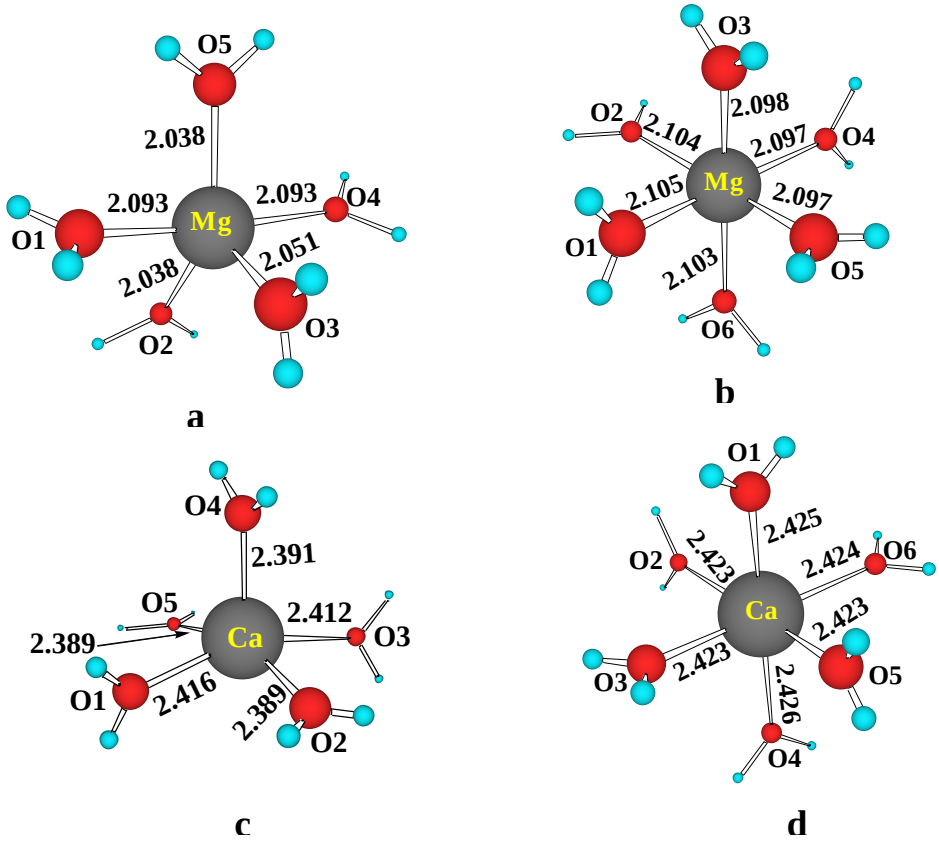

Fig.8. B3LYP level optimized geometries of hydrated magnesium and calcium dications. (a) $Mg(H_2O)_5$, (b) $Mg(H_2O)_6$, (c) $Ca(H_2O)_5$ and (d) $Ca(H_2O)_6$. All bond lengths are in Å.

On the other hand, with five water molecules, Ca^{2+} forms a square pyramidal structure and like Mg^{2+}, the hexahydrated Ca^{2+} has octahedral structure (See Fig.8). Energy data of all the B3LYP optimized level metal water systems are given in Table 1.

Table 1. Energies of the B3LYP level optimized metal-water systems

Metal ions	Metal 6H2O kcal/mol	Metal 5H2O kcal/mol	Metal 4H2O kcal/mol
Li^+	-466.01	-389.57	-313.13
Na^+	-620.45	-544.32	-467.88
K^+	-1058.36	-981.922	-905.48
Mg^{2+}	-658.26	-581.80	-
Ca^{2+}	-1135.76	-1059.30	-

Table 2. GC base pair hydrogen bond lengths in anion models for hydrated alkaline earth metals. All bond lengths are in Å.

Model System	Outer			Inner monodendate			Inner bidendate		
	N4(C)-O6(G)	N3(C)-N1(G)	O2(C)-N2(G)	N4(C)-O6(G)	N3(C)-N1(G)	O2(C)-N2(G)	N4(C)-O6(G)	N3(C)-N1(G)	O2(C)-N2(G)
Li^+	1.797	1.787	1.832	1.796	1.787	1.831	1.798	1.778	1.831
Na^+	1.809	1.779	1.820	1.809	1.777	1.819	1.808	1.779	1.822
K^+	-	-	-	1.807	1.781	1.822	1.808	1.778	1.823

Table 3. GC base pair hydrogen bond lengths in anion models for hydrated alkaline earth metals. All bond lengths are in Å.

Model system	Outer			Inner monodendate			Inner bidendate		
	N4(C)-O6(G)	N3(C)-N1(G)	O2(C)-N2(G)	N4(C)-O6(G)	N3(C)-N1(G)	O2(C)-N2(G)	N4(C)-O6(G)	N3(C)-N1(G)	O2(C)-N2(G)
Mg^{2+}	1.786	1.797	1.838	1.784	1.798	1.842	1.785	1.797	1.842
Ca^{2+}	1.822	1.782	1.807	1.810	1.777	1.822	-	-	-

Table 4. GC base pair hydrogen bond lengths in dianion models for hydrated alkali and alkaline earth metals. All bond lengths are in Å.

Model system	Outer			Inner monodendate			Inner bidendate		
	N4(C) - O6(G)	N3(C) - N1(G)	O2(C) - N2(G)	N4(C) - O6(G)	N3(C) - N1(G)	O2(C) - N2(G)	N4(C) - O6(G)	N3(C) - N1(G)	O2(C) - N2(G)
Li^+	-	-	-	1.784	1.801	1.852	1.785	1.801	1.854
Na^+	1.797	1.794	1.840	1.796	1.796	1.841	1.798	1.792	1.842
K^+	1.796	1.795	1.840	1.798	1.793	1.842	-	-	-
Mg^{2+}	1.824	1.810	1.870	1.830	1.814	1.886	1.826	1.814	1.890
Ca^{2+}	-	-	-	1.796	1.796	1.84	-	-	-

Table 5. Metal-oxygen bond lengths in anion and dianion models for hydrated alkali metals (Outer sphere). All bond lengths are in Å.

Model system	Outer (Anion)				Outer (Dianion)			
	O5	O6	O7	O8	O5	O6	O7	O8
Li^+	1.983	1.980	1.921	2.0	-	-	-	-
Na^+	2.466	2.238	2.207	2.241	1.838	1.738	1.820	1.947
K^+	-	-	-	-	2.715	2.762	2.806	2.722

Table 6. Metal-oxygen bond lengths in anion and dianion models for hydrated alkali metals (Inner sphere-monodentate). All bond lengths are in Å.

Model	Inner mono (Anion)				Inner mono (Dianion)			
system	O1	O5	O6	O7	O1	O5	O6	O7
Li^+	2.010	1.950	1.961	1.985	1.962	1.942	1.972	1.981
Na^+	2.335	2.305	2.296	2.272	2.303	2.251	2.296	2.313
K^+	2.711	2.643	2.701	2.719	2.672	2.642	2.657	2.686

Table 7. Metal-oxygen bond lengths in anion models for hydrated alkali metals (Inner sphere-bidentate). All bond lengths are in Å.

Model	Inner bi (Anion)				Inner bi (Dianion)			
system	O1	O2	O5	O6	O1	O2	O5	O6
Li^+	2.141	2.160	1.933	1.912	2.215	2.031	1.923	1.927
Na^+	2.439	2.364	2.256	2.238	2.439	2.364	2.256	2.238
K^+	2.770	2.728	2.616	2.649	-	-	-	-

Table 8. Metal-oxygen bond lengths in anion and dianion models for hydrated alkaline earth metals. All bond lengths are in Å.

Model	Outer (Anion)						Outer (Dianion)					
system	O5	O6	O7	O8	O9	O10	O5	O6	O7	O8	O9	O10
Mg^{2+}	2.095	2.127	2.117	2.108	2.067	2.084	-	-	-	-	-	-
Ca^{2+}	2.446	2.465	2.404	2.408	2.345	2.450	-	-	-	-	-	-

Table 9. Metal-oxygen bond lengths in anion and dianionmodels for hydrated alkaline earth metals. All bond lengths are in Å.

Model system	Inner mono (Anion)						Inner mono (Dianion)					
	O1	**O5**	**O6**	**O7**	**O8**	**O9**	**O1**	**O5**	**O6**	**O7**	**O8**	**O9**
Mg^{2+}	2.058	2.120	2.124	2.080	2.113	2.126	2.146	2.161	2.072	2.091	2.054	2.131
Ca^{2+}	2.356	2.469	2.432	2.428	2.390	2.436	1.945	2.426	2.394	2.413	2.447	2.407

Table 10. Metal-oxygen bond lengths for hydrated alkaline earth metals. All bond lengths are in Å.

Model System	Inner bi (Anion)						Inner bi (Dianion)					
	O1	**O2**	**O5**	**O6**	**O7**	**O8**	**O1**	**O2**	**O5**	**O6**	**O7**	**O8**
Mg^{2+}	2.165	2.173	2.135	2.092	2.040	2.103	2.234	2.239	2.207	2.045	2.050	2.041
Ca^{2+}	-	-	-	-	-	-	-	-	-	-	-	-